
**Relative ion intensities of *O*-alkyl-oligosaccharides in
ESI-IT-MS: A quantitative evaluation**

Von der Fakultät für Lebenswissenschaften
der Technischen Universität Carolo-Wilhelmina
zu Braunschweig
zur Erlangung des Grades
einer Doktorin der Naturwissenschaften

(Dr. rer. nat.)

genehmigte

D i s s e r t a t i o n

von Sheetal Gangula

aus Ramchandrapuram/Indien

1. Referentin: *

Professorin Dr. Petra Mischnick

2. Referent:

apl. Professor Dr. Ulrich Engelhardt

eingereicht am: 25.04.2016

mündliche Prüfung (Disputation) am: 30.06.2016

Druckjahr 2017

Vorveröffentlichungen der Dissertation

Teilergebnisse aus dieser Arbeit wurden mit Genehmigung der Fakultät für Lebenswissenschaften, vertreten durch die Mentorin der Arbeit, in folgenden Beiträgen vorab veröffentlicht:

Publikation

Gangula, S., Nimtz, M. & Mischnick, P. Relative ion intensities of maltooligosaccharide ethers in electrospray ionization ion trap mass spectrometry: A quantitative evaluation. *Int. J. Mass Spectrom.*, 402, 57-65 (2016).

Tagungsbeiträge

Gangula, S. & Mischnick, P.: Quantitative mass spectrometry by LC-ESI-IT-MS. (Poster). IGSM-Summer School of Metrology, Burg Warberg, Germany (2012).

Gangula, S. & Mischnick, P.: Quantitative mass spectrometry by LC-ESI-IT-MS. (Poster). Sixth International Symposium on the Separation and Characterization of Natural and Synthetic Macromolecules-SCM 6, Dresden, Germany (2013).

Gangula, S. & Mischnick, P.: Quantitative mass spectrometry by MS. (Poster). 27th International Carbohydrate Symposium-ICS 27, Bangalore, India (2014).

Gangula, S. & Mischnick, P.: Quantitative analysis of complex oligomeric mixtures by MS. (Vortrag). COST Action FP1105 meeting, Coimbra, Portugal (2014).

Gangula, S. & Mischnick, P.: Quantitative mass spectrometry by MS. (Poster). IGSM-Summer School of Metrology, Harz, Germany (2014).

Gangula, S. & Mischnick, P.: Quantitative aspects of ESI-IT-MS of oligosaccharide derivatives. (Poster). Seventh International Symposium on the Separation and Characterization of Natural and Synthetic Macromolecules-SCM 7, Amsterdam, Netherlands (2015).

Acknowledgement

I would like to thank Prof. Dr. Petra Mischnick for initiating an interesting project and mentoring me throughout the project with great care.

I appreciate the financial support from Braunschweig International Graduate School of Metrology (B-IGSM) and the DFG Research Training Group GrK1952/1 “Metrology for Complex Nanosystems”. I am thankful to Dr. Dezhen Li, former B-IGSM coordinator for helping me initially to start my work at TU Braunschweig.

I would also like to thank Prof. Dr. Ulrich Engelhardt for being my second mentor and Prof. Dr. Stephen Schulz for his hand in the disputation committee.

I appreciate financial support from COST action FP1105, which provided me an opportunity to visit KTH, Stockholm as a guest researcher. I would like to thank Dr. Manfred Nimtz and Mrs. Andrea Abrahamik at HZI, Braunschweig for helping me with nano-ESI-MS measurements.

Prof. Dr. Meinhard Schilling and Judith Krakowski organized metrology seminars, lectures, topical courses, summer schools, lab and industrial tours and always had an open ear to any information I needed regarding the metrology points. Dr. Bernd Güttler provided useful insights about metrology in chemistry and helped me with the calculation of uncertainty limits.

I had a wonderful time with my colleagues at Institute of food chemistry, especially with my working group ‘AK Mischnick’ during my PhD. It was nice of Dr. Inga Unterrieser, Dr. Kristin Voiges, Dr. Julia Cures and Marko Rother to initially help me with the experiments and Dr. Christian Bork for always helped me with IT problems. I am thankful to Silke Lehmann for always having an open ear to any problem I faced during my PhD. I would like to thank Qimeng Zhang for helping me with GC measurements and Payam Hashemi for helping me with the NMR data. Matthias Bol always helped me in difficult situations and to translate German documents to English.

During my PhD, my family always supported me especially my father (Narender Reddy), my mother (Pranitha Kumari) and my brother (Sidhartha Reddy). I would like to add a special note to my husband, Jeevan Kapaganti for always solving my problems even though he has no knowledge of chemistry.

Abbreviations

ABA	Aminobenzoic Acid
AC	Amplified Current
ACN	Acetonitrile
AGU	Anhydro Glucose Unit
ATR	Attenuated Total Reflection
BM	Binary Mixture
CD	Cyclodextrin
CM	Complex Mixture
DC	Direct Current
DMSO	Dimethylsulphoxide
DP	Degree of Polymerization
DS	Degree of Substitution
ECR	Effective Carbon Response
EI	Electron Impact
ESI	Electrospray Ionization
Et	Ethyl
FID	Flame Ionization Detector
GC	Gas Chromatography
HPLC	High Performance Liquid Chromatography
IR	Infrared Spectroscopy
IT	Ion Trap
MALDI	Matrix Assisted Laser Desorption Ionization
Me	Methyl
Me- <i>d</i> ₃	Deuteromethyl

MeOEt	Methoxyethyl
MC	Methylcellulose
MS	Mass Spectrometry
MR	Molar Ratio
NMR	Nuclear Magnetic Resonance
Pr	Propyl
Rel. Int.	Relative Intensity
RF	Radio Frequency
RP	Reverse Phase
TLC	Thin Layer Chromatography
TFA	Trifluoroacetic Acid
THF	Tetrahydrofuran
TM	Target Mass
ToF	Time of Flight
UV	Ultraviolet

INDEX

1. INTRODUCTION	1-1
1.1 ELECTROSPRAY IONIZATION (ESI)	1-1
1.2 ION TRAP (IT)	1-4
1.3 SAMPLE FLOW IN ESI-IT-MS	1-7
1.4 ANALYTE CHARACTER AND ESI RESPONSE	1-7
1.5 ANALYSIS OF OLIGOSACCHARIDES WITH ESI-IT-MS	1-8
1.5.1 PARAMETERS THAT INFLUENCE THE ION FORMATION	1-9
1.5.2 PARAMETERS THAT INFLUENCE ION TRANSPORT, ANALYSIS AND DETECTION	1-13
1.6 ANALYSIS OF CELLULOSE ETHERS	1-13
1.7 ROLE OF MASS SPECTROMETRY IN PATTERN EVALUATION	1-19
1.8 NANO-ESI-MS	1-19
2. SCOPE OF THE PROJECT	2-22
3. RESULTS AND DISCUSSION (REFERENCE DATA)	3-24
3.1 SELECTION OF MODEL COMPOUNDS	3-24
3.2 SYNTHESIS AND CHARACTERIZATION OF MODEL COMPOUNDS	3-27
3.3 CHARACTERIZATION OF THE MODEL COMPOUNDS	3-29
3.4 STRATEGY FOR PREPARATION OF DEFINED MIXTURES	3-35
3.5 PREPARATION OF DEFINED MIXTURES	3-36
3.5.1 PARTIAL HYDROLYSIS OF ALKYLATED CYCLODEXTRINS	3-37
3.5.2 PREPARATION OF COMPLEX MIXTURES WITH KNOWN COMPOSITION	3-38
3.5.3 MOLAR RATIO IN COMPLEX MIXTURES	3-40
3.5.4 MOLAR RATIO IN BINARY MIXTURES	3-45
4. RESULTS AND DISCUSSION (RELATIVE SENSITIVITIES)	4-51
4.1 <i>O</i> -METHYLATED AND <i>O</i> -DEUTEROMETHYLATED MALTOOLIGOMERS	4-51
4.1.1 DEPENDENCE OF RELATIVE SENSITIVITIES ON MOLAR RATIO OF ANALYTES	4-51
4.1.2 EFFECT OF TOTAL CONCENTRATION ON RELATIVE SENSITIVITIES	4-54
4.1.3 EFFECT OF INSTRUMENTAL PARAMETER 'TARGET MASS' ON RELATIVE SENSITIVITIES	4-59
4.1.4 EFFECT OF DP ON RELATIVE SENSITIVITY COEFFICIENTS OF ME AND ME- <i>D</i> ₃ OLIGOSACCHARIDES	4-64
4.1.5 NANO ESI-MS	4-64
4.1.6 ESI-IT-MS OF LABELED OLIGOSACCHARIDES	4-66
4.1.7 COMPARISON WITH MALDI-ToF-MS	4-67
4.2 ESI-MS STUDY OF MIXTURES OF <i>O</i> -METHYLATED AND <i>O</i> -ETHYLATED MALTOOLIGOMERS	4-69
4.2.1 DEPENDENCE OF RELATIVE SENSITIVITIES IN ESI-MS ON THE MR OF ME AND ET GLUCAN ANALYTES	4-69
4.2.2 COMPARISON OF CM AND BM	4-71
4.2.3 INFLUENCE OF TOTAL CONCENTRATION ON RELATIVE SENSITIVITY (I_{ET}/I_{ME})/MR	4-71
4.3 RELATIVE SENSITIVITIES OF ME- <i>D</i> ₃ AND ET GLUCAN ANALYTES IN ESI-MS	4-74
4.4 RELATIVE SENSITIVITY COEFFICIENTS OF ME AND ME- <i>D</i> ₃ AND ME AND ET WITH UNCERTAINTY	4-74

4.5	RELATIVE SENSITIVITIES OF HIGHER <i>O</i> -ALKYL- RELATED TO <i>O</i> -METHYL-MALTOOLIGOSACCHARIDES	4-77
4.6	RELATIVE SENSITIVITIES OF <i>O</i> -METHOXYETHYL RELATED TO <i>O</i> -ALKYL-MALTOOLIGOSACCHARIDES	4-80
4.7	COMPARISON OF RELATIVE SENSITIVITIES OF ALKYL OLIGOSACCHARIDES OBTAINED BY SYRINGE PUMP INFUSION OR LC/MS	4-82
4.8	EFFECT OF TOTAL CONCENTRATION	4-84
4.9	COMPARISON BETWEEN ESI AND NANO-ESI-MS	4-92
4.10	COMPARISON BETWEEN NON-LABELED AND LABELED COMPOUNDS	4-94
5.	APPLICATION OF ME-<i>D</i>₃/ME AND ET/ME SENSITIVITY COEFFICIENTS	5-95
6.	SUMMARY AND OUTLOOK	6-99
7.	MATERIALS AND METHODS	7-104
7.1	REAGENTS	7-104
7.2	MATERIALS	7-104
7.3	INSTRUMENTS AND METHODS	7-104
7.4	SYNTHESIS (PER- <i>O</i> -ALKYLATED β-CYCLODEXTRINS)	7-108
7.4.1	REACTION PROCEDURE (CIUCANU AND KEREK)	7-108
7.4.2	REACTION PROCEDURE (HAKOMORI)	7-108
7.4.3	SYNTHESIS OF HEPTAKIS[2,3,6-TRI- <i>O</i> -PROPYL]-β-CYCLODEXTRIN (PR-CD)	7-109
7.5	MONOMER ANALYSIS	7-110
7.6	PARTIAL HYDROLYSIS	7-112
7.7	REDUCTIVE AMINATION	7-112
7.8	PREPARATION OF MIXTURES	7-113
7.9	CALCULATION OF UNCERTAINTY LIMITS	7-113
8.	REFERENCES	8-115
9.	APPENDIX	9-122

1. Introduction

Early developments of ESI-IT-MS

Modern methods of mass spectrometry allow to ionize and analyze non-volatile compounds like carbohydrates or large biomolecules. In 1981 introduction of FAB¹ provided a convenient and rapid method for analyzing polar and thermally labile compounds. In late 1980's the introduction of ESI and MALDI made the analysis of large molecules easy by mass spectrometry. The phenomenon that a strong electric field can produce a fine spray of droplets goes back to more than 80 years prior to original research.²⁻⁴ The earliest successful efforts to combine electrospray with mass spectrometry were reported in 1968 by Malcolm Dole and coworkers.⁵⁻⁶ They demonstrated that polystyrene solutions with an average molecular weight of 51,000 u can be electrosprayed from a solution in benzene and acetone. The major work that was responsible for recognizing electrospray as ion source and an interface for LC/MS was done by John Fenn at Yale's.⁷⁻⁸ The earliest ESI sources were limited to a flow rate of few microliters per minute and were restrictive with respect to solvent composition. Pneumatically assisted⁹⁻¹³ electrospray made it possible to use a wider range of solvent flow rates, electrolyte concentrations and electric potentials. The 1990s were a period of growth and development in both, the instrumentation and application of electrospray ionization mass spectrometry. In 1990, Van Berkel et al.¹⁴ reported the combination of electrospray with an ion trap (ESI-IT-MS).

1.1 Electrospray ionization (ESI)

The electrospray is produced by passing the sample solution typically at a flow of 0.1-20 $\mu\text{L}/\text{min}$ through a capillary tube of diameter 0.1-0.2 mm into an atmospheric pressure chamber containing a high electric field.¹⁵ The electric field is obtained by applying a potential difference of 3-6 kV between the capillary tip and the counter electrode. The high electric field causes the formation of 'taylor cone' at the capillary tip. When the Coulomb

repulsion exceeds the solvent cohesive forces at Rayleigh's limit, a charged spherical droplet is expelled from the tip of the Taylor cone.¹⁶ These charged droplets further shrink due to solvent loss. The parent droplets further lose charge in subsequent fissions from which finally charged analytes are formed.¹⁷⁻¹⁹ Figure 1 shows the scheme of electrospray ionization, and Figure 2 shows the photograph of droplet formation obtained by Gomez and Tang²⁰ and Rayleigh's equation.²¹

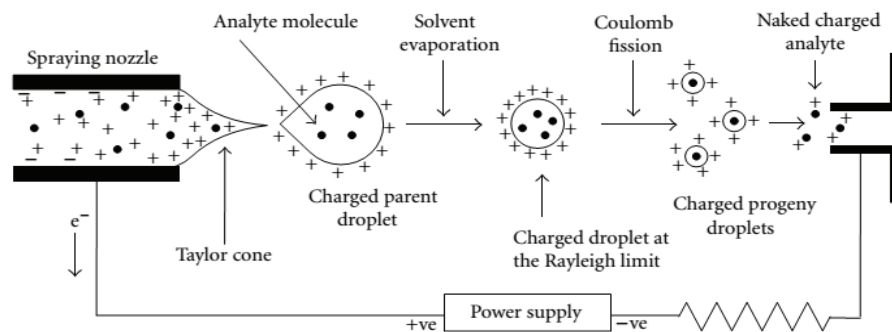
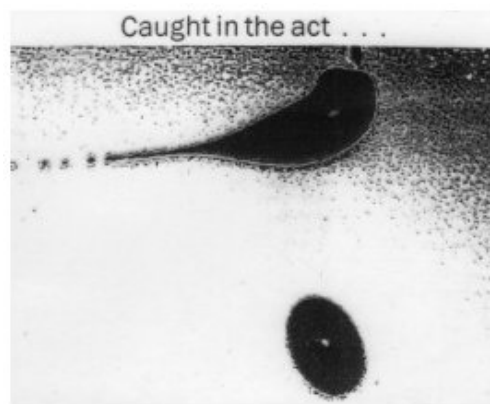


Figure 1. Mechanism of ionization in ESI-MS. Source: website-america.pink.²²



Rayleigh: $q^2 = 8\pi^2\epsilon_0\gamma D^3$

Figure 2. Photograph of droplet formation in electrospray source at Rayleigh's limit obtained by Gomez and Tang²⁰, where, q = charge, ϵ_0 = permittivity of the environment, γ = surface tension and D = diameter of a supposed spherical droplet at its Rayleigh limit. Reprinted by permission from AIP Publishing LLC.

An equation proposed by Smith²³ can be used to understand several aspects in the formation of charged droplet and the onset potential ' V_{on} ' required for the onset of ESI process.

$$V_{on} \approx 0.2\sqrt{r\gamma}\ln\left(\frac{4000d}{r}\right) \quad (1)$$

Here, r is the radius of the electrospray needle, γ is the surface tension of the solvent, and d is the distance between the needle tip and the counter electrode (vacuum orifice). The onset potential is highly dependent on the solvent. For example, using methanol as a solvent ($\gamma=0.0226$ N/m), a spray needle of radius 50 μm and a needle-counter electrode distance of 5 mm, the required onset potential is 1.27 kV, whereas, when water is used as a solvent ($\gamma=0.073$ N/m), the required onset potential increases to 2.29 kV. Decreasing the radius of the needle will reduce the onset potential (nano-ESI), as will be discussed in later sections (Sec 1.8).

Several theories have been proposed to explain the formation of gas phase ions from charged droplets, two main theories are widely accepted and experimentally proven for particular examples.

Charged Residue Model (CRM)

This model predicts that after the first fission from Taylor cone several subsequent fissions occur accompanied by shrinking of droplet due to solvent evaporation, until there is only one ion left in the droplet.²⁴⁻²⁵ Figure 3 illustrates the process.



Figure 3. Ion formation after desolvation in charge residue model.

Ion Evaporation model (IEM)

Figure 4 predicts that after the shrinkage of the droplet due to solvent evaporation, where, the droplet reaches a radius of less than 10 nm,²⁶⁻²⁷ the charge potential exceeds the surface tension of the droplet. The parent droplet becomes unstable and emits analyte ions.

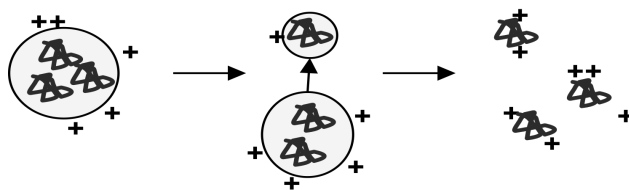


Figure 4. Ion formation after desolvation in ion emission model.

Both the theories did not achieve universal acceptance.²⁸⁻³⁰ It is argued that the mechanism of formation of ions differ from smaller analytes to larger analytes. Some experimental evidence show that smaller analytes are predominantly ionized by ‘IEM’ and larger analytes above 1000 u are ionized by ‘CRM’.³¹

Formation of ions takes place under atmospheric pressure, but ion analysis requires vacuum. Hence, the ions are gradually carried from atmospheric region to the vacuum region through a series of pumps, which assist in the production of vacuum. In the electrospray process not only ions, but also neutral species are released and cluster of ions with neutral species are formed. First challenge is to separate the ions from neutral species, which can be achieved by the aid of co-axial flow of ‘curtain gas’ usually dry nitrogen.³²⁻³⁴ This helps to drive neutral species away from mass spectrometric orifice, and series of skimmer and octopole voltages helps in desolvation and transport of ions to mass analyzer.

In a mass spectral analysis, not only the formation of ions but also the separation of ions according to their m/z and their subsequent detection is an important step. Ion trap is most commonly used with ESI since it is well suitable for continuous ion production as in ESI and can be easily coupled with chromatographic systems like HPLC.

1.2 Ion Trap (IT)

An ion trap is closely related to a quadrupole analyzer which therefore shall be explained first. A quadrupole analyzer³⁵ basically consists of four rods with circular or hyperbolic section. Ions enter at one end and exit at the other end. Ions will be driven by the difference in potential. Depending on the voltages applied, ions of a certain m/z can pass or collide with the

rods, whereat they will lose their charge. Hence the ions will travel under an electrical field which is created by applying a direct and an overlaying alternating potential to the opposite pairs of rods. As shown in Figure 5 ions travel in the direction of z-axis and they are ramped by alternating electric fields by the application of RF potential along x-axis and direct current along y-axis.³⁶ Scanning of these two voltages allows subsequent passing of ions. Thus the quadrupole acts as a mass filter.

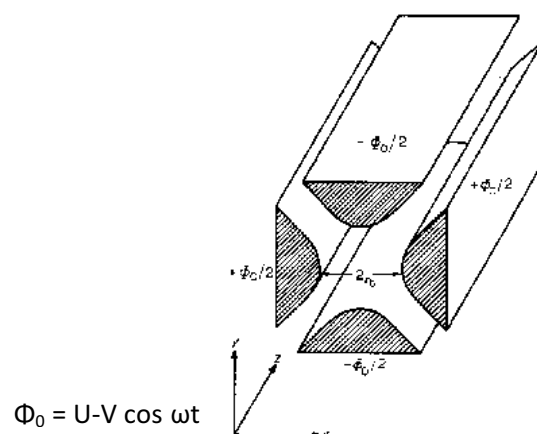


Figure 5. Basic principle of quadrupole mass analyzer. Where, Φ_0 is the potential applied to the rods, U is the direct potential, V is the ‘zero to peak amplitude’ of RF voltage and ω is the angular frequency. Ions travel along z-axis. Source: Reprinted from Paul and Steinwedel.³⁷ with permission of Z. Naturforsch.

By bending the rods of a quadrupole to a closed circle, ions can no longer pass but are trapped. That is the principle of an ion trap, introduced by Paul and Steinwedel³⁷ in 1954. The ion trap is made by circular electrodes with two spherical caps on the top and bottom of the ion trap (can be imagined as bent quadrupole rods). The design of the ion trap allows the overlapping of the alternating electric fields which creates a three dimensional quadrupole. Ions are trapped and oscillated in a ‘ ∞ ’ shaped trajectory³⁸ as shown in Figure 6 by applying RF to ring electrodes and AC potential to end caps.

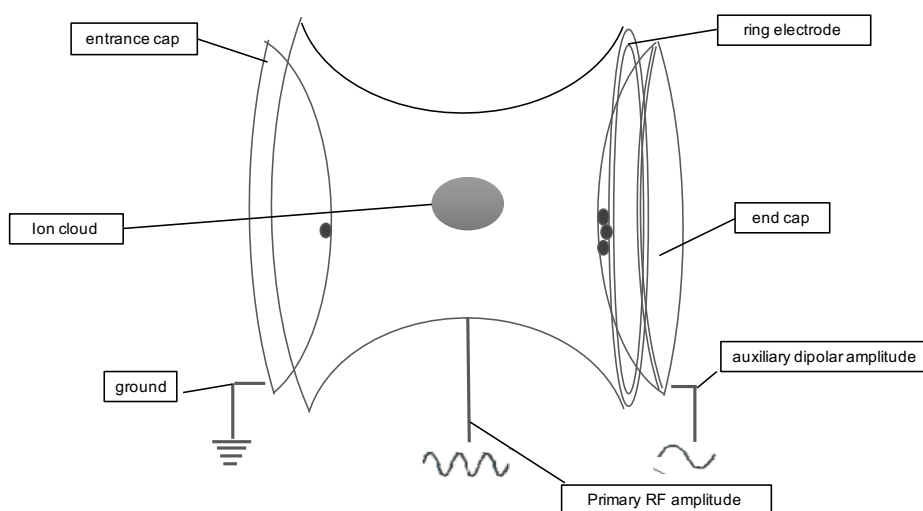


Figure 6. Ion trap design with trajectory as given in instrument guide line of HCT Ultra ETDII (Bruker Daltonics, Bremen, Germany).

Ions exit in the direction of z-axis. Figure 7 shows the ‘Mathieu stability’ diagram,³⁹ defining regions in which ions are stable in ion trap.

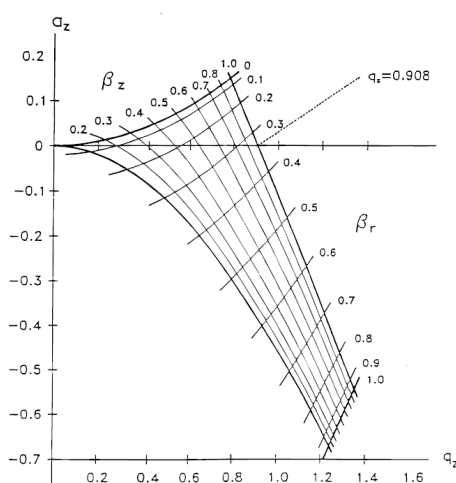


Figure 7. Mathieu stability diagram, showing the trajectory of ions and stability region. Source: Reprinted from March³⁹ with the permission of John Wiley and Sons.

Ions of a different m/z have individual oscillation frequencies, known as secular frequencies.⁴⁰

AC potential is applied to the endcaps. When this matches the secular frequency of ions they will be excited. Keeping the AC voltage constant at this point, if the RF frequency is continuously raised, it will cause the ions to take up the additional energy,⁴¹ and they are subsequently ejected in the direction of z-axis.

1.3 Sample flow in ESI-IT-MS

Figure 8, depicts the typical ESI-IT-MS setup, where, the sample is introduced through a capillary needle into the spray chamber which is maintained at atmospheric pressure and where ionization occurs. The ions generated in the spray chamber are later transported through the regions which gradually decrease in pressure. Skimmer and octopole voltages help in ion transportation and focusing. These ions are accumulated in ion trap (mass analyzer) where they are ejected according to m/z and later detected.

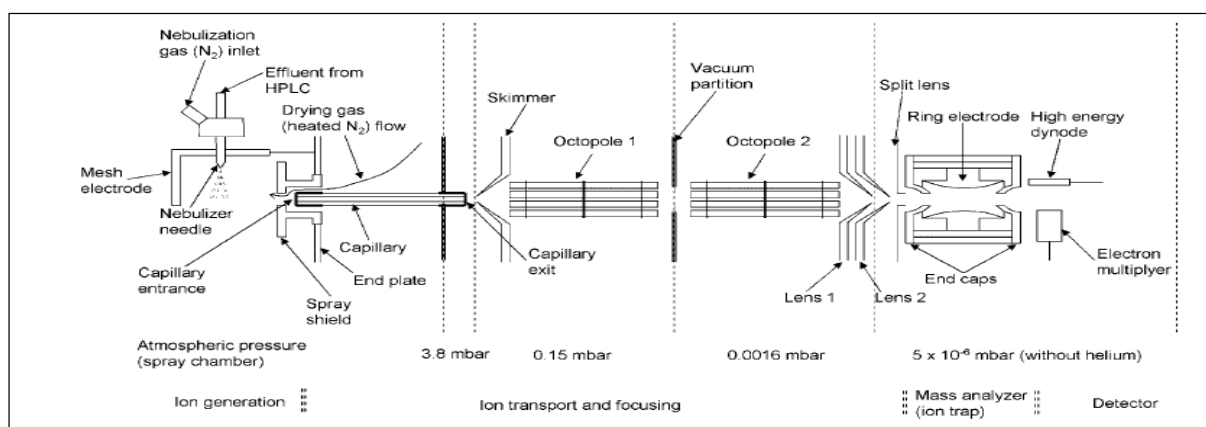


Figure 8. Flow of the sample in ESI-IT-MS, broadly dividing the setup into three parts; ion generation: spray chamber where ions are generated, ion transport and focusing region and mass analyzer: ion trap. Source: reprinted from Krueve et al⁴² with permission of John Wiley and Sons.

1.4 Analyte character and ESI response

Intensity of analytes in ESI is highly dependent on analyte character, for instance, Figure 9 shows an example of equimolar (10^{-6} M each) solution of cesium bromide (Cs^+) and decyltrimethylammonium bromide ($DTMA^+$),⁴³ which show unequal intensities. This difference arises because DTMA is more surface active compared to Cs ion. Therefore, to recognize such differences fundamental studies dealing with importance of analyte character in determining the ESI response is an area of interest for mass spectrometrists.

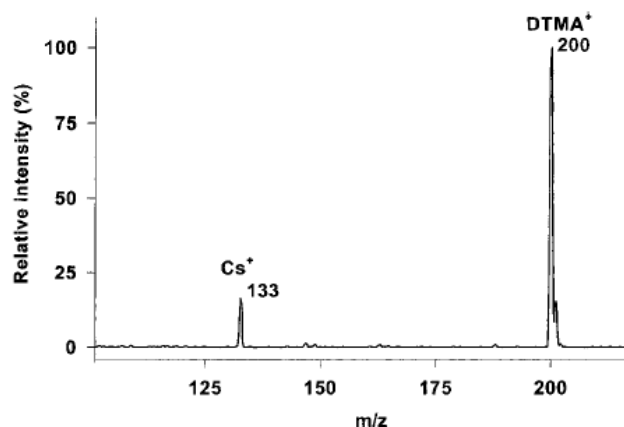


Figure 9. ESI mass spectrum of an equimolar (10^{-6} M each) mixture of Cs^+ and DTMA^+ in 50% methanol and 50% water solution. Source: Reprinted from Zhou & Cook⁴³ with permission of Elsevier.

1.5 Analysis of oligosaccharides with ESI-IT-MS

Ions can either already exist and are separated from their counter ions by the electrospraying process, or they are formed by adduct formation of neutral molecules with cations like protons, sodium ions etc.,. The first is the primary method of ionization for ions that already exists in solution (e.g. inorganic ions like sodium, cesium, quaternary ammonium compounds, protonated basic or deprotonated acidic compounds), gas phase ions are released after desolvation of the charged droplets. In the second case, polar analytes that do not have acidic or basic groups are charged by adduct formation with sodium, potassium, lithium ions, etc., in positive ion mode and mostly chloride adducts are seen in negative ion mode. Charging in gas phase generally occurs through gas-phase-proton-transfer reactions, where, molecules that were protonated in solution yield their protons to solvents or analytes with higher gas-phase basicity.⁴⁴⁻⁴⁶

Ion formation of oligosaccharides

Oligosaccharides are neutral molecules which have no basic group for protonation (in positive ion mode), except for amino sugars. Therefore, they are preferentially ionized by adduct formation, mostly seen as sodium adducts, since sodium is ubiquitously present in sufficient amounts in solution due to contact with glassware. Neutral oligosaccharides response in ESI

is primarily dependent on co-ordination with alkali metal ions like sodium, potassium, lithium, etc., depending on the availability, co-ordination is achieved by non-bonding electron pairs in oxygen. But absolute and relative ion intensities in ESI between two oligosaccharides with different chemistry and size do not only depend on equilibrium of sodium adducts in solution. They depend on many other parameters like surface activity of the analytes, concentration, desorption energies from the droplet, solvent, droplet size, instrument parameters, etc., which are explained in detail below.

1.5.1 Parameters that influence the ion formation

Parameters that influence the relative ion intensities in ESI-IT-MS can roughly be classified into two categories. Most parameters are described according to positive ion analysis.

Nebulization

To assist the electrospraying process when the sample solution is passed through the needle, a nebulizing gas, in most cases nitrogen, is mixed with the sample solution.⁴⁷ The flow of the nitrogen can be adjusted, and should be set to optimize the spray process, i. e. maintain pressure and stabilize spray.

Desolvation

During the spraying process a drying gas (nitrogen) is used to assist solvent evaporation and desolvation of the ions. The temperature (120 °C – 365 °C) and gas flow (1 L/min - 12 L/min) should be adjusted to maintain pressure and also care must be taken that the conditions do not cause the degradation of analytes, but are sufficient to assist solvent evaporation.⁴⁸ For example, when analyzing the same sample with syringe pump infusions and in combination with liquid chromatography (LC), higher temperature and flow rate of the drying gas are

required for infusion from LC effluent due to the increased flow rate (0.2 - 1 mL/min) in comparison to syringe pump infusions (150 – 300 μ L/h).

Solvent properties

Solvent properties belong to the most important parameters in ESI process. Surface tension, vapor pressure, conductivity and polarity are important in forming a stable spray (equation 1).⁴⁹ For example, if the solution becomes more aqueous the surface tension increases and it will be difficult to adjust the onset potential. Hence usually aqueous solutions are mixed with solvents of lower surface tension as methanol, acetonitrile, etc., for a lower onset potential. Furthermore, the solvent should not react with solute molecules and avoid solvent-solute adduct formation,⁵⁰ should not show strong dipole interactions and give less background interference.⁵¹⁻⁵²

Analyte properties

In Figure 10, the ESI mass spectrum of two chemically different oligosaccharide derivatives (*O*-methyl and *O*-ethyl), measured as their sodium adducts in positive mode, are shown. Their relative ion intensities (Rel. Int.) deviate from their molar ratio illustrated in the chromatogram of UV-labeled analytes of the same mixture. In Figure 10, a simple binary mixture is given to illustrate the problem, but in real time analysis more complicated mixtures as given in Figure 20 have to be analyzed which cannot be easily quantified only by HPLC. To overcome this problem of quantification from relative ion intensities and to get reliable quantitative results, it is of high interest to better understand how the chemical structure of the analyte influences the Rel. Int. in ESI-IT-MS.

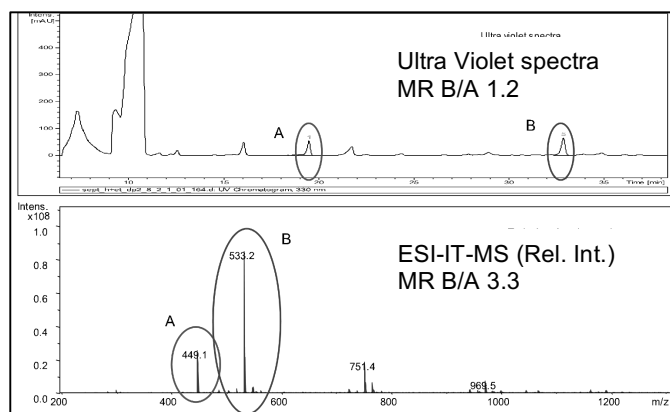


Figure 10. Comparison of relative signal or peak intensities obtained for a mixture of A (*O*-Methyl DP2) and B (*O*-Ethyl DP2) at a ratio of 1.2 measured in HPLC-UV, where, ESI-IT-MS measurement of the same mixture shows a molar ratio of 3,3. LC/UV, a part of the sample portion was labeled and measured at the absorption maximum of 330 nm to find out the exact molar ratio, while, in ESI-IT-MS the unlabeled mixture was measured in positive ion mode.

Surface activity

Surface activity plays a major role in the formation of ions from ES droplet. Analytes with higher surface activity have a higher chance of residing at the droplet surface and thus escaping the droplet surface and “surviving” the next fissions. These are finally detected with a higher sensitivity in MS. Tang and Smith⁵³ showed experimental evidence by photography of fluorescent compounds, with more surface active non-polar analytes dominating in subsequent fissions.

Sodium complexation ability or acidity/basicity

Ion yield of compounds which became charged either by protonation or deprotonation depend on their particular basic or acidic properties.⁵⁴ *O*-rich molecules like oligosaccharides, however, are ionized by adduct formation with alkali metals (Li^+ , Na^+ , K^+).⁵⁵ Because sodium is ubiquitous due to contact with glass of analyte solutions and solvents, sodium adducts are the preferentially observed pseudomolecular ions of carbohydrates. The ability or equilibrium constant for $[\text{M}+\text{Na}]^+$ formation depends on the sterical availability of electron density at these electron donating heteroatoms⁵⁶ and the number of electron density rich atoms present

in appropriate distance and orientation to allow n-fold coordination with energy minima for sodium adducts at $n=7-8$.⁵⁷

Electrophoretic mobility

Analytes reach from the inner bulk of the droplet to the droplet surface, driven by the potential difference.⁵⁸ Hence, the molecular weight of the analyte molecules can play a role, as higher mass molecules at a certain charge state exhibit lower electrophoretic mobility than the lighter molecules.⁵⁹

Concentration

Concentration has an important influence on absolute and relative ion intensities in ESI, as the dynamic linear range of ESI is limited both in lower and higher concentration ends.⁶⁰⁻⁶³ In a lower concentration range, the background noise interferes with analyte peaks' intensities even without the presence of any impurities in sample from solvent-solvent or solvent-ion clusters. At the higher end the absolute ion intensities of analyte molecules are close to constant since saturation effects occur at a concentration of approximately 10^{-5} M. Relative ion intensities of analytes which differ in surface activity are highly dependent on total concentration of the sample. They change with concentration until the absolute ion intensities becomes saturated, where, they remain constant.

Flow rate

With the increase in flow rate between syringe pump and LC-ESI-MS measurements, large droplets with larger diameter are produced in LC-ESI-MS.⁶⁴ At larger diameter of droplets and thus more bulk related to surface, the influence of surface activity and electrophoretic mobility on relative ion yields of competing analytes and thus discrimination become more pronounced.

1.5.2 Parameters that influence ion transport, analysis and detection

Ion formation is not the end of the story, voltages (skimmer and octopole, Figure 8) that support the transfer of these ions from the atmospheric region of the ion source to the mass analyzer also influence the absolute and hence relative ion intensities in MS.⁶⁵ Skimmer and octopole lens voltages help in ion focusing and reducing the background noise from solvent clusters.⁶⁶

Ion trap

As described in 1.2, ions entering the ion trap are oscillating in a ‘ ∞ ’ trajectory by applying DC and RF potentials to the ring. The main parameters that show direct effect on the absolute and relative intensities of ions are those subsumed under “target mass” (TM). When adjusting at higher target mass, the amplitude of octopole RF, octopole DC and trap drive are all automatically increased in a proper ratio which will aid in the energy take-up of subsequent masses and their ejection from IT and detection.⁶⁷

In summary, to determine the factors that affect sensitivity of oligosaccharides with different chemistry and the reason for differences in relative ion intensities of equimolar mixtures of oligosaccharide derivatives (as shown in Figure 10) in ESI-IT-MS, not only the analyte characteristics but also all the parameters mentioned in 1.5 need to be carefully considered.

1.6 Analysis of cellulose ethers

Cellulose

Cellulose is a high molecular weight linear chain polymer in which glucose units are linked by (1 \rightarrow 4)- β -D-glycosidic bonds (Figure 11).

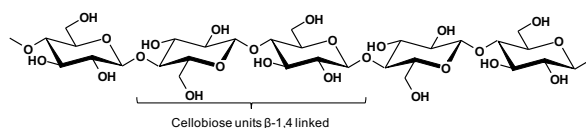


Figure 11. Fragment of a cellulose structure with glucose units (β -1-4 linked), due to the rotation of every second unit, cellobiose is considered as repeating unit.

The equatorial orientation of the β -1-4 linkage gives chains that have every other glucose residue rotated by 180° , providing a high propensity to form intra- and intermolecular hydrogen bonds⁶⁸ (Figure 12).

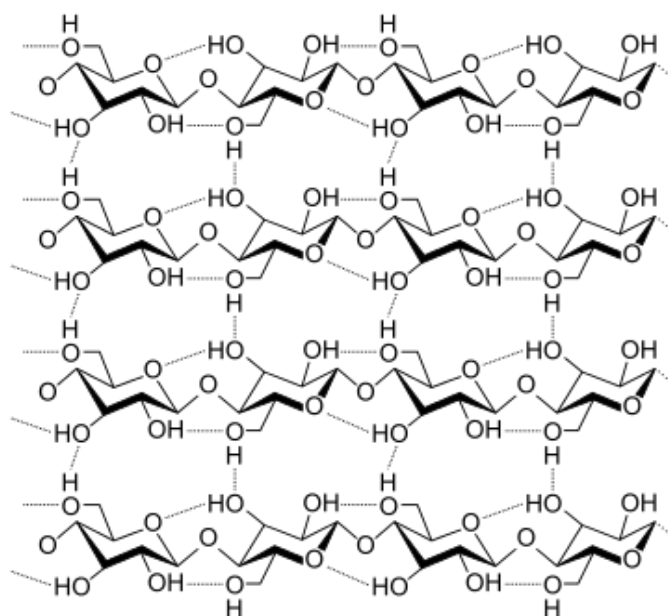


Figure 12. Intra-and intermolecular hydrogen bonding in cellulose. Source: website-chemwiki.ucdavis.edu.⁶⁹

As a result, large aggregates of parallel running chains are formed. These parallel chains in turn aggregate by further hydrogen bonding and van der Waals forces to produce three-dimensional microfibrils (Figure 13).

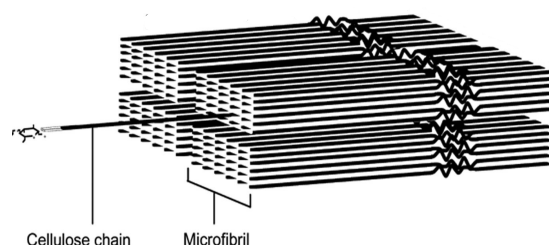


Figure 13. Structure of three-dimensional microfibrils in cellulose. Source: website-chemwiki.ucdavis.edu.⁶⁹

This intermolecular aggregation of highly associated cellulose chains gives a rigid fibrous structure which provides a strong matrix for plant cell walls.

Modification of cellulose: cellulose ethers

Naturally occurring cellulose is insoluble in common solvents and has to be modified along the polymer backbone to extent its application in various fields. First modification of cellulose was reported about 160 years ago.⁷⁰⁻⁷¹ Most common cellulose derivatives are cellulose esters and ethers of the free hydroxyl groups on position C-2, C-3 and C-6 as shown in Figure 14. The extent of derivatization is defined by the degree of substitution (DS), which is the average number of substituted hydroxyl groups per anhydro glucose units (AGU)

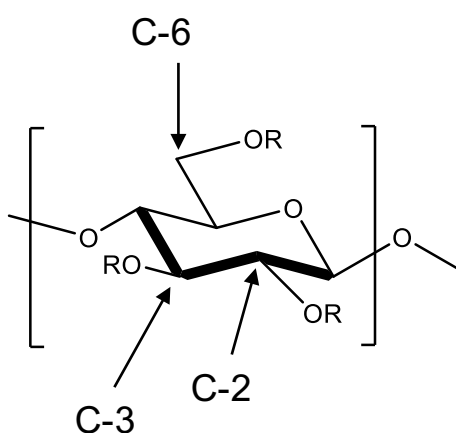


Figure 14. Glucosyl unit showing three 'OH' positions C-2, C-3 and C-6 at which cellulose modification can be performed.

Cellulose ethers, for example methyl cellulose, hydroxypropyl methylcellulose, ethyl cellulose, carboxymethyl cellulose, etc. have a wide range of industrial applications⁷²⁻⁷³ in textiles, pharmaceuticals (excipients), cosmetics, food (additives), oil, paper, coating materials, painting etc. Variations in the chemical structures of different cellulose ethers are shown in Figure 15.

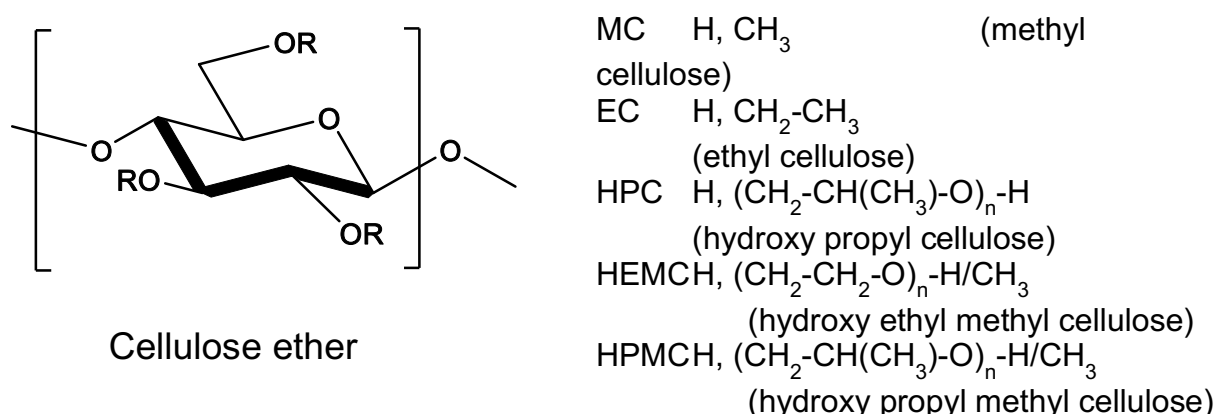


Figure 15. Various cellulose ethers produced commercially.

Determination of substitution pattern (oligomer analysis)

The physicochemical properties of modified cellulose like solubility, viscosity, thermoreversible gelation, flocculation, etc., do not only depend on the type or degree of substitution and molar mass distribution but also on the distribution of the substituents along the polymer chain,⁷⁴ because this will affect the interactions between chains. For example, methyl cellulose exhibits⁷⁵ thermoreversible gelation and phase separation at elevated temperatures⁷⁶ around 50-60 °C which has been attributed to aggregation of domains caused by hydrophobic interactions. Therefore, it is important to determine the DS and the substitution pattern over the polymer chains to influence and hopefully better understand the physicochemical properties of modified polymer and also to tailor-make products appropriate for a particular application.

Modified cellulose ethers are cleaved to smaller oligomers and the DS/DP pattern of these oligomers is analyzed. The DS profile within each DP reflects the distribution of substituents over the polymer chains.⁷⁷⁻⁷⁸ Depending on the reaction conditions the accessibility of glucosyl units is affected which in turn affects the substitution pattern over the chains. If all the glucose units are equally assessible according to Spurlin's model⁷⁹ a random substitution

(statistical distribution) over the cellulose chains is obtained. If certain areas are not accessible as some of the residual crystalline regions are not activated, a more heterogeneous distribution is obtained.⁸⁰ Examples of different types of substitution distributions over polymer chains are shown in Figure 16.

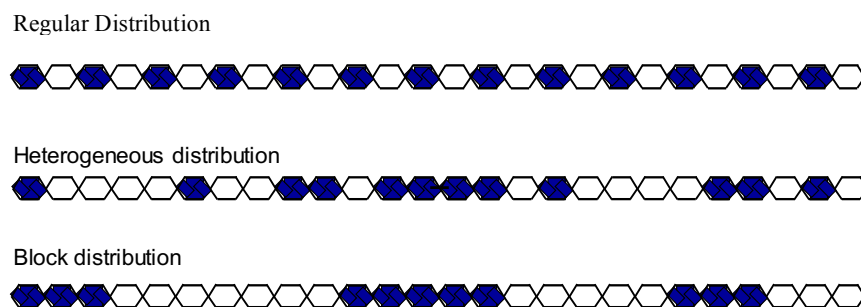


Figure 16. Homogeneous, heterogeneous and block like patterns in substituted cellulose ethers.

Different patterns of substitution have a direct effect on the physiochemical properties of modified cellulose, for example the higher presence of non-substituted regions due to heterogeneous distribution may cause an intramolecular aggregation of cellulose chains which may change the flow properties significantly.⁸¹ Hence not only the determination of DS and molar mass distribution but also the determination of substituent distribution is a critical step in the structural evaluation of modified cellulose.

A common approach of pattern evaluation is to degrade the cellulose ether by enzymatic hydrolysis by “cellulase” and measure the amount of glucose released which can be correlated to substitution pattern.⁸⁰ If the substituents are statistically distributed over cellulose the amount of glucose released will be less due to steric hindrance, whereas, in a heterogeneous distribution more glucose will be released.⁸²⁻⁸³ Enzymatic cleavage, however, is dependent on the enzyme specificity which is dependent on the type of substituent, DS and distribution pattern. Another approach to determine the substitution pattern is to randomly cleave the cellulose ether into oligomeric units by acid hydrolysis or methanolysis, into oligomeric units. The substitution pattern on these oligomeric units will represent the pattern on the cellulose

ether, but cleavage has to be random (statistical) and not dependent on the type of substituent, DS and distribution pattern.⁸⁴

Arisz et al. first reported⁸⁵ on the analysis of oligomers obtained from MC by hydrolysis and subsequent perdeuteromethylation. Mischnick and Kühn⁸⁶ perdeuteromethylated methyl amyloses prior to partial acid hydrolysis. Perdeuteromethylation should also level differences in the MS response. Analysis of the oligomeric fractions (DP 2-4) at that time was performed by mass spectrometric techniques (FAB-MS and MALDI-ToF-MS). To evaluate the methyl distribution from the mass spectrometric data, the relative intensities of signals representing different number of methyl groups for a certain DP were normalized and the average DS/DP was calculated. The average DS of the oligomers was in good agreement with the average DS (obtained by GLC-MS) of the constituents as mentioned above.⁸⁹ The distribution of methyl groups in each oligomer fraction is plotted as a graph and compared to the calculated random distribution of variously substituted glucosyl units⁹⁰ as exemplarily illustrated in Figure 17. Since then this method has been further developed and applied to various cellulose ethers⁹¹ using electrospray ionization mass spectrometry (ESI-MS) and LC-ESI-MS.

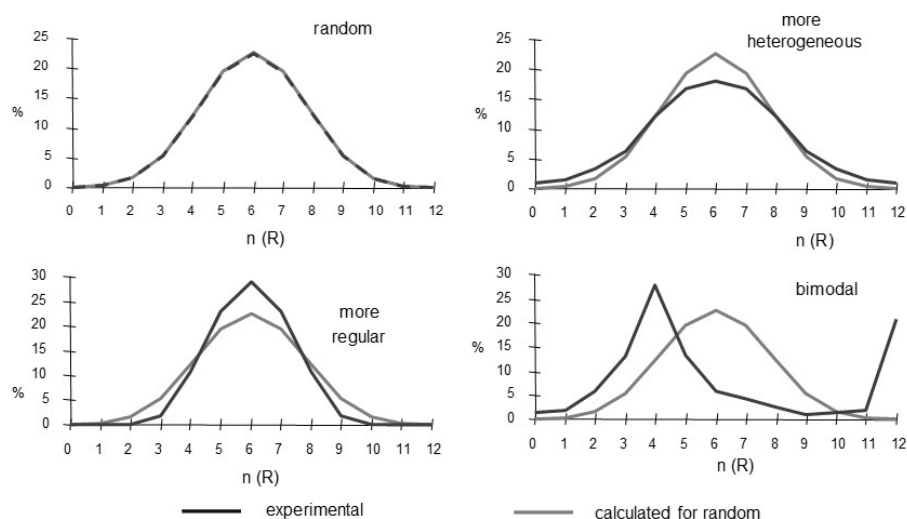


Figure 17. Comparison between experimental and calculated substitution pattern in DP4, to study the substitution pattern on cellulose chains. Source: Mischnick et al.⁹⁰

1.7 Role of mass spectrometry in pattern evaluation

As mentioned above, methyl cellulose ethers are further derivatized with deuterated methyl iodide to gain chemically more uniform material for further analytical steps. In the mass spectrum the signals of individual oligomer units with different m/z are separated with a good resolution, hence it would be easy to obtain the quantitative data of molar composition from the relative ion intensities in mass spectrum. Correct quantification requires equal ion yield of all constituents belonging to a certain DP. While this can be expected for chemically uniform *O*-methyl-*O*-methyl- d_3 -glucooligomers, it can, however, not be implied for chemically more diverse oligosaccharides (as shown in Figure 10), for instance *O*-methyl-*O*-methoxyethyl ethers. Whether the results are representative or suffer from discrimination in MS can be checked by the average DS of each oligomer which should be in accordance with the average DS of the material. While for MC, constant DS values are found, this is not the case for combinations of methyl with higher alkyl, methoxyalkyl, or methoxycarbonyl groups.⁹²⁻⁹³ The discrimination due to differences in chemistry has been up to a certain DS and DP overcome by labeling strategies. For a better understanding and maybe theoretical correction of relative ion yields, it should be studied, how the chemistry and the molar mass, increasing with DP and DS, influence relative ion yield in mass spectrometry and how this is depending on solvent, concentration, measurement parameters etc. Therefore, fundamental studies with oligosaccharide mixtures with different chemistry are required to understand the pattern these compounds follow in ESI-IT-MS.

1.8 Nano-ESI-MS

Nano-ESI is the modification of ESI, where the size of the capillary is reduced to 1-2 μm and the flow rate is reduced to $<1 \mu\text{L}/\text{min}$, hence the droplets produced in nano-ESI are less than 200 nm, which is 1000 times smaller than normal ESI.⁹⁴⁻⁹⁵ It is assumed that since the droplet size is reduced, the surface and electrophoretic effects are less relevant as illustrated in

Figure 18⁹⁶, which will result in higher response of the analytes with poor response in ESI. This phenomenon was demonstrated by Bahr et al.,⁹⁷ by analyzing a mixture of insulin and maltopentose (molar ratio 1:1) both in ESI and nano-ESI. In Figure 19 it can be seen that the relative response of maltopentose increased in nano-ESI.

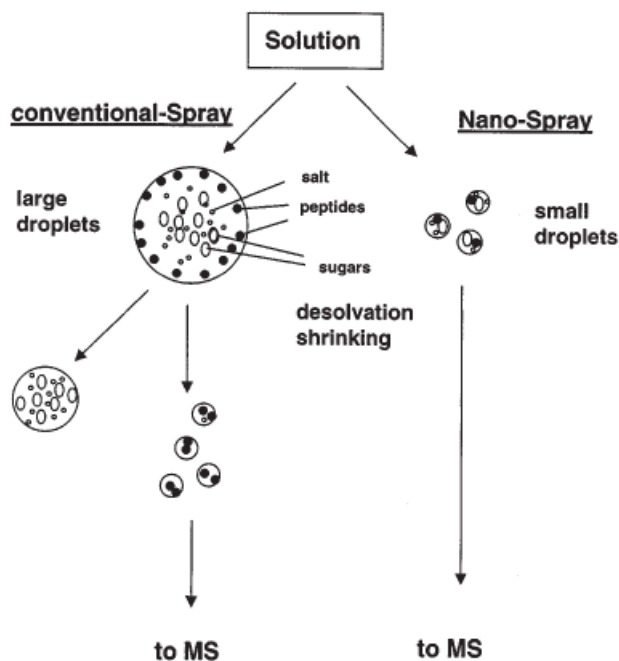


Figure 18. Mechanism of ion formation: comparison of ESI to nano-ESI, source: Reprinted from Karas et al.⁹⁶ with the permission of Springer.

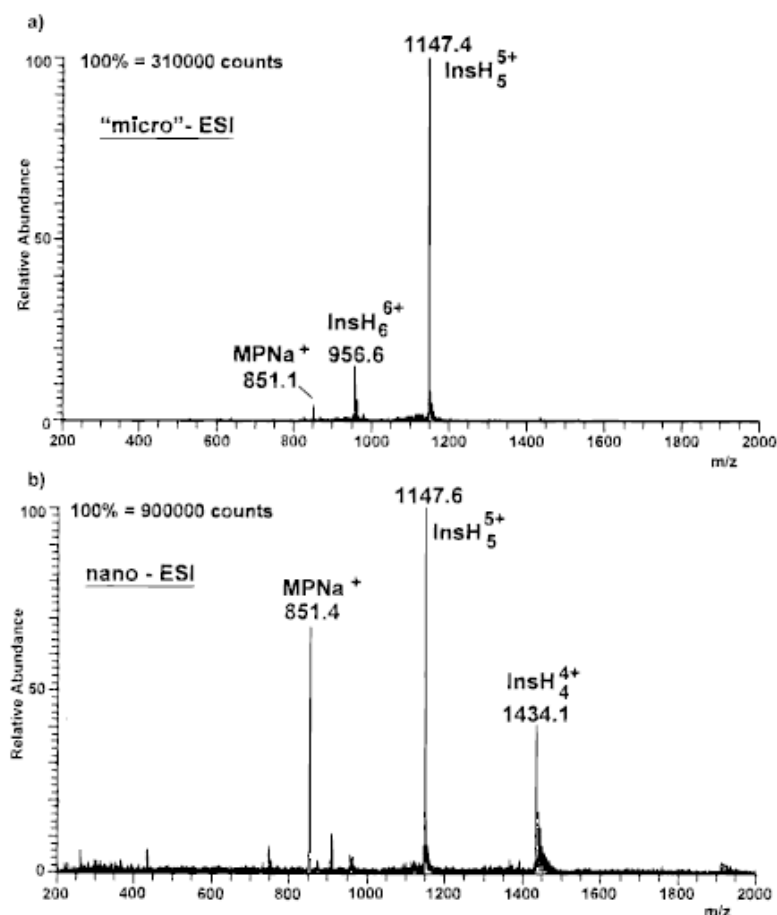


Figure 19. Comparison of the analysis of insulin and maltopentose mixture in ESI to nano-ESI at a concentration of 10^{-5} M and 10^{-6} M respectively; a) In ESI-MS maltopentose (MP) is detected with much lower intensity than insulin (Ins), b) The same solution in nano-ESI shows a higher intensity of MP. Source: Reprinted from Bahr et al.⁹⁷ with permission of American chemical society.

Similar, results can also be obtained for oligosaccharide mixtures which differ in chemistry (as in Figure 10), hence studies have to be performed to compare the relative sensitivities between ESI-MS and nano-ESI-MS, to see if equal intensities can be obtained for an equimolar oligosaccharide mixture differing with respect to chemistry.

2. Scope of the project

As described in the introduction of this thesis, the molar composition of oligosaccharide derivatives determined from the relative ion intensities in ESI-IT-MS is a critical information for substituent pattern evaluation of modified polysaccharides. Due to the complexity of parameters that influence absolute and relative ion intensities of oligosaccharides with different chemistry and size, it is not possible to predict the Rel. Int. merely from the knowledge of chemical structure of analytes in combination with other parameters like concentration, instrumental voltages etc.. The availability of standards for each type of oligosaccharide is also rare. Hence for the quantitative analysis of oligosaccharides with ESI-IT-MS, it is important to understand the basic rules these compounds follow in ESI.

Therefore, the behavior of defined oligosaccharide derivative mixtures in MS, especially ESI-IT-MS, should be experimentally studied to find out whether systematic relations can be found. To perform such studies, model compounds should be prepared from α -1,4-linked β -cyclodextrin (β -CD) instead of a polysaccharide to limit the number of DPs produced by partial hydrolysis. Various alkylated β -cyclodextrins should be synthesized and characterized to confirm the purity and a DS of 3. From these compounds, defined mixtures should be prepared and analyzed in ESI-IT-MS and nano-ESI-MS, and in selected cases also by MALDI-Tof-MS. Reference data of exact composition can be obtained by HPLC/UV after reductive amination. Initially, the influence of measurement parameters on Rel. Int. should be studied with the well-known system of methylated and deuteromethylated oligosaccharides of DP 2-6 to understand the parameters of influence like concentration, molar ratio, target mass, flow rate (comparison between syringe pump and LC infusions and comparison between ESI-IT-MS and nano-ESI-MS). For comparison some mixtures should be labeled with a negatively charged tag and measurement in negative mode to exclude the influence of sodium complexation ability on ion yield.

Subsequently, the study should be extended to defined mixtures of *O*-methyl derivatives with higher alkylated homologs and thus higher difference in chemistry. Methoxyethyl derivatives with an additional oxygen, amplifying the coordinating properties and presenting an important type of cellulose ethers, should also be included. These mixtures should be analyzed in a similar way. Finally, instead of binary mixtures of fully methylated or otherwise alkylated maltooligomers, presenting the extreme cases in polysaccharide analysis, a random sample should be synthesized, which contains oligosaccharides with two types of *O*-alkyl glucosyl units (methyl and deuteromethylated or methylated and ethylated) as in cases of modified and derivatized polysaccharide. Upon partial hydrolysis, these compounds would yield a similar pattern to that of corresponding polysaccharide ethers. These samples should be studied in comparison to the extreme cases. The scope of the project is to summarize all these influences and provide a better understanding of quantitative analysis of various oligosaccharide ethers with ESI-IT-MS. It is also aimed to find out whether the relative sensitivity factors can be used as correction factors to determine the molar composition in oligomeric mixtures.

3. Results and discussion (reference data)

3.1 Selection of model compounds

Methyl ethers are most commonly used in analytical method development as they are chemically stable, small and neutral, and also the isotope-label version is easily available. Several basic studies have therefore been performed on methyl ethers of cellulose to develop an analytical method for polymer structure analysis with mass spectrometry.⁹⁸⁻¹⁰⁰ Cellulose methyl ethers are important commercial products which are used as adhesives and thickeners. Other cellulose ethers as described in sec. 1.6, EC, HPC, HPMC, etc., are applied in pharmaceuticals, construction and packing areas. As described in the introduction the analysis of the substitution pattern of cellulose ethers is important for better understanding of the properties of the modified polymer. In case of hydroxyalkyl or higher alkyl glucan ethers, permethylation with MeI or MeI- d_3 can only partly level the chemical diversity of the oligomers obtained after partial hydrolysis.⁹¹⁻⁹³ And this difference in chemistry (ethyl/methyl, hydroxyalkyl/methyl, etc.,) and probably also the wider m/z range covered by the individual constituents of a certain oligomer, causes the difference in sensitivities in ESI-MS, which results in distortion of DS/DP patterns calculated. Figure 20, shows the oligomer pattern after permethylation, partial hydrolysis and ESI-MS analysis of ethyl-methyl cellulose (EMC), the enlarged section showing the oligomeric pattern in DP2, where, two ‘extreme cases’ of only *O*-methylated and only *O*-ethylated oligosaccharides (circled) are visible. The difference in relative ion sensitivities between these two ‘extreme cases’ has to be investigated in order to evaluate the molar composition from relative ion intensities in ESI-MS. Another application of quantitative ESI-MS is the calculation of the average block length of chemically synthesized block co-polymers.¹⁰¹⁻¹⁰² Figure 21 shows an example of oligomeric pattern in partially hydrolyzed block co-polymer synthesized by cationic ring-opening polymerization (CROP),¹⁰³ from heptakis[2,3,6-tri-*O*-methyl]- β -cyclodextrin (A_7) and heptakis[2,3,6-tri-*O*-deuteromethyl]- β -cyclodextrin (B_7). From the ratio of ion

intensities detected for AA, AB+BA and BB dimers the average block length of DP 2 can be calculated. Hence relative sensitivity coefficients of oligomers ('extreme cases' circled in Figure 21) with different chemistry must be known for quantification.

Initial step in developing a quantitative method for such oligomeric pattern analysis is the determination of the difference in sensitivity between the 'extreme cases' in each DP and to find out whether all the other oligomers with patterns in between, from Me_n over Me_{n-1}Et , $\text{Me}_{n-2}\text{Et}_2$, ... to Et_n , behave proportional to the number of Et groups. To study this question cyclodextrins instead of polymers were chosen as substrates, as partial hydrolysis gives no higher oligosaccharides than DP 7 and 4-*O*-alkylation can be avoided. Thus, defined fully alkylated derivatives can be synthesized and purity can be checked by NMR. Upon hydrolysis oligomers belonging to DP 1 – DP 7 including those who represent the uniform "extreme cases", are obtained. Hence defined oligomeric mixtures can be synthesized which can be systematically analyzed in ESI-MS. Cyclodextrin are enzymatically derived from starch hence they are α -linked, not β -linked as in cellulose, but it is assumed that this has no influence on relative ion intensities.

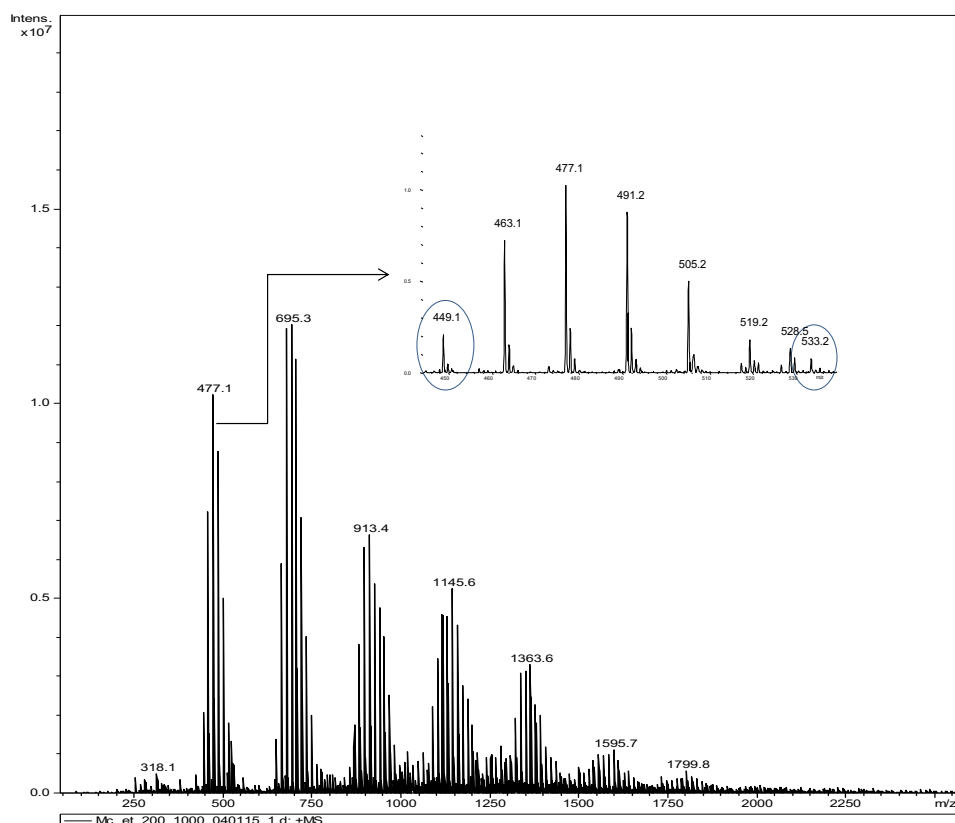


Figure 20. Oligomeric pattern in partially hydrolyzed perethylated MC, measured in positive ion mode at a concentration of 10^{-5} M under defined conditions (*sec 7.3*). Enlarged section shows the oligomeric pattern in DP2 with the two extreme cases of $(M+Na)^+$ of Me (m/z 449) and Et (m/z 533) circled.

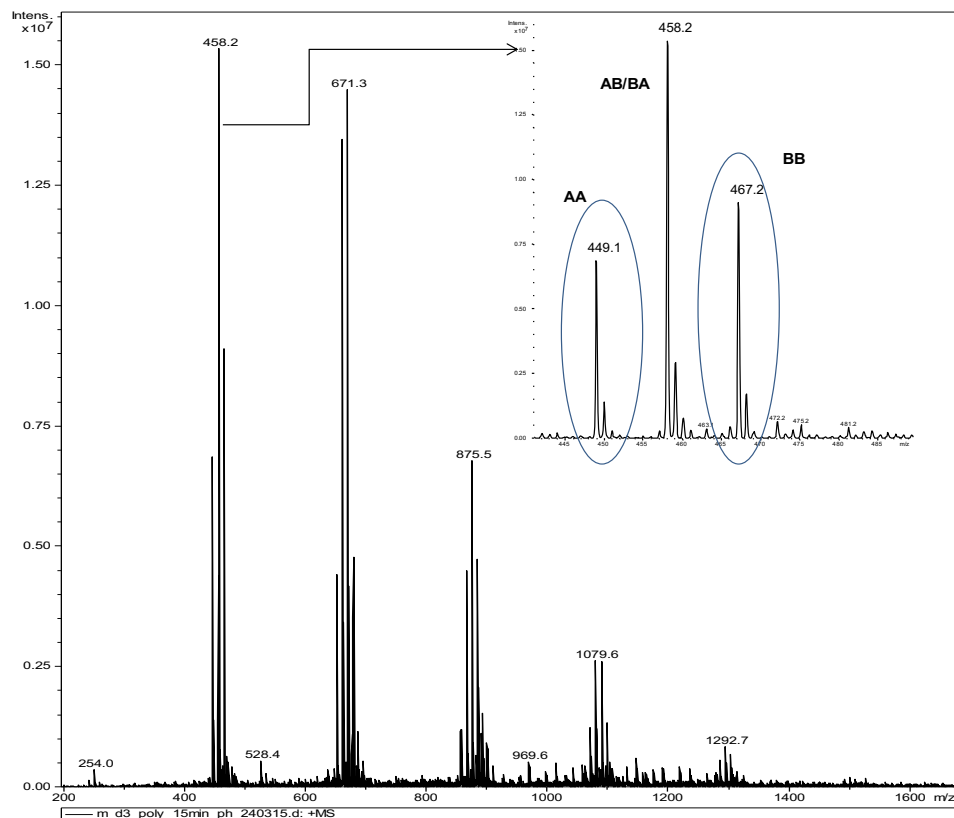


Figure 21. Oligomeric pattern in partially hydrolyzed block co-polymer synthesized by CROP (Me and Me- d_3 CDs), measured in positive ion mode at a concentration of 10^{-5} M under defined conditions (*sec 7.3*). Enlarged section shows the oligomeric pattern in DP 2 with the two extreme cases of Me₆ and (Me- d_3)₆ circled.

3.2 Synthesis and characterization of model compounds

Substrate

β -CD was chosen as a substrate to synthesize model compounds. β -CD contains seven glucose units in a ring, where each glucose unit is linked through α -1-4 glycosidic linkage as described above.

Alkylated β -CD's

As described in *sec 3.1* in the analysis of cellulose derivatives methyl, ethyl and hydroxyethyl/methoxyethyl ethers (MC, EC, HEC, HEMC, etc.) are of particular interest.^{89, 91-93} Methoxyethylated carbohydrates are detected with much higher intensity compared to alkylated counterparts, probably due to the increased sodium complexation ability.¹⁰⁴ Further propyl was chosen to extend the series of homologs methyl and ethyl to three members.

Alkylation of β -CD

Methylated β -CD (Me-CD), deuteromethylated β -CD (Med_3 -CD), ethylated β -CD (Et-CD), propylated β -CD (Pr-CD), and in addition methoxyethylated β -CD (MeOEt-CD) were synthesized, structures of which are shown in Figure 22. All the compounds were synthesized according to Ciucanu and Kerek,¹⁰⁵ with few exceptions (explained later in *chapter 7*). The reaction is performed using freshly pulverized NaOH as base in a polar aprotic organic solvent (DMSO).

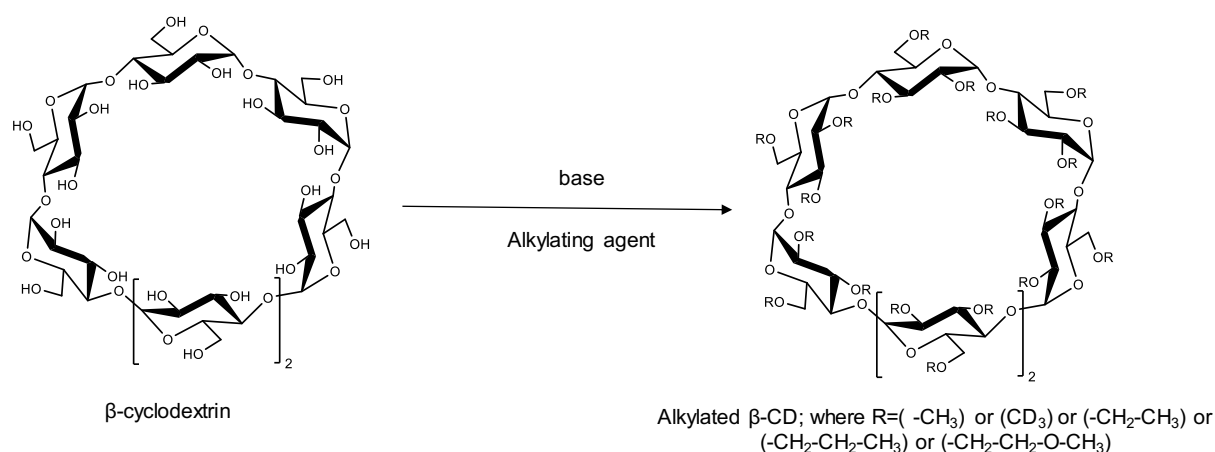


Figure 22. Types of *O*-alkylated β -cyclodextrins synthesized; R = Me, Me-*d*₃, Et, Pr and MeOEt cyclodextrins.

The reaction includes deprotonation of CD-hydroxyl groups by base (2) followed by subsequent reactions with alkylating agent (3), an alkyl halide or an oxirane, until it is complete (4). Equation (5) shows the competing consumption of the alkylating agent by the base:

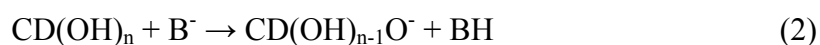


Table 1 gives the list of all the alkylated β -cyclodextrins synthesized along with the product yield and the type of alkylating agent used for the synthesis. Me-CD and Me-*d*₃-CD were obtained as white crystalline powder. These products were purified by re-crystallization from acetone. Et-CD and Pr-CD were obtained as clear to light yellow viscous material, and MeOEt-CD as light yellow oil. These products were purified by column chromatography on silica with acetone/ hexane (2:1, v/v) as eluent.

Table 1

List of β -cyclodextrins derivatives and the respective alkylating agents used along with product yield

Compound	Abbreviation	Alkylating agent	Raw product [g]	Yield [%]	Purified product [g]	Isolated Yield [%]
Heptakis [2,3,6-tri- <i>O</i> -methyl] β -cyclodextrin	Me-CD	Me-I	1.32	104	0.97	77
Heptakis [2,3,6-tri- <i>O</i> -deuteromethyl] β -cyclodextrin	Me- <i>d</i> ₃ -CD	Me- <i>d</i> ₃ -I	1.28	100	1.05	82
Heptakis [2,3,6-tri- <i>O</i> -ethyl] β -cyclodextrin	Et-CD	Et-I	1.27	103	1.14	93
Heptakis [2,3,6-tri- <i>O</i> -propyl] β -cyclodextrin	Pr-CD	Pr-Br	2.72	77	----	----
Heptakis [2,3,6-tri- <i>O</i> -methoxyethyl] β -cyclodextrin	MeOEt-CD	MeOEt-Br	2.11	92	1.98	88
Heptakis [2,3,6-tri- <i>O</i> -methyl] β -cyclodextrin	Me-CD (2)	Me-I	1.13	89	0.82	65

3.3 Characterization of the model compounds

All the compounds in Table 1 are checked for purity and completeness of alkylation. Completeness of alkylation was checked by the absence of OH-absorption $> 3000\text{ cm}^{-1}$ by ATR-IR spectroscopy, Figure 23 shows an IR spectrum of MeOEt-CD. IR spectra of all other CD-derivatives look similar. In the enlarged section slight residual absorption is visible which is due to a DS of 2.98. If the compound is completely alkylated, all glucosyl units and thus all H-1 should be chemically and magnetically identical. Therefore, ^1H -NMR spectra should show only a single doublet for H-1 confirming the uniformity, Figure 24 shows an example of MeOEt-CD all the other compounds also showed a similar spectrum and were in accordance with the literature.¹⁰⁶ Portions of Me-CD, Me-*d*₃-CD, Et-CD and MeOEt-CD were hydrolyzed and transformed in *O*-alkyl-glucitol acetates to determine the DS by GLC. Completeness of alkylation in Pr-CD was only checked with IR and ESI-MS analysis. ESI-MS spectra of Me-CD, Me-*d*₃-CD, Et-CD, Pr-CD and MeOEt-CD are shown in Figure 25.

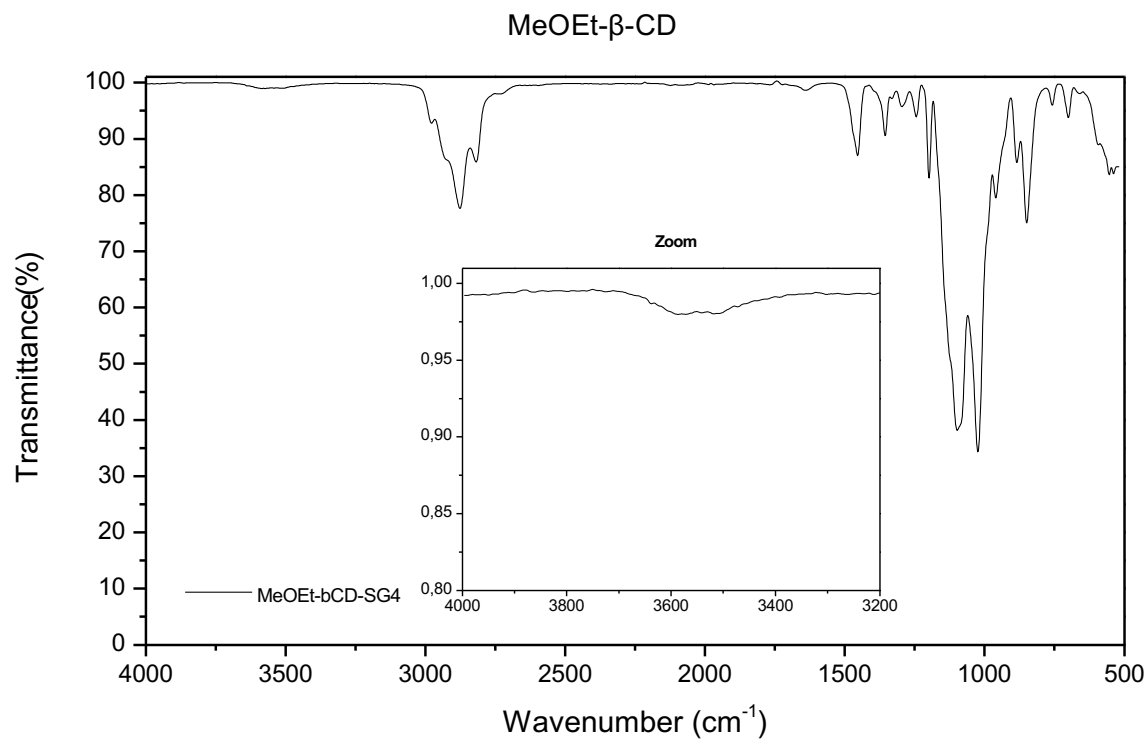


Figure 23. IR spectrum of MeOEt- β -CD, enlarged section shows the region of OH-absorption, where a residual absorption is seen, probably due to a DS of 2.98.

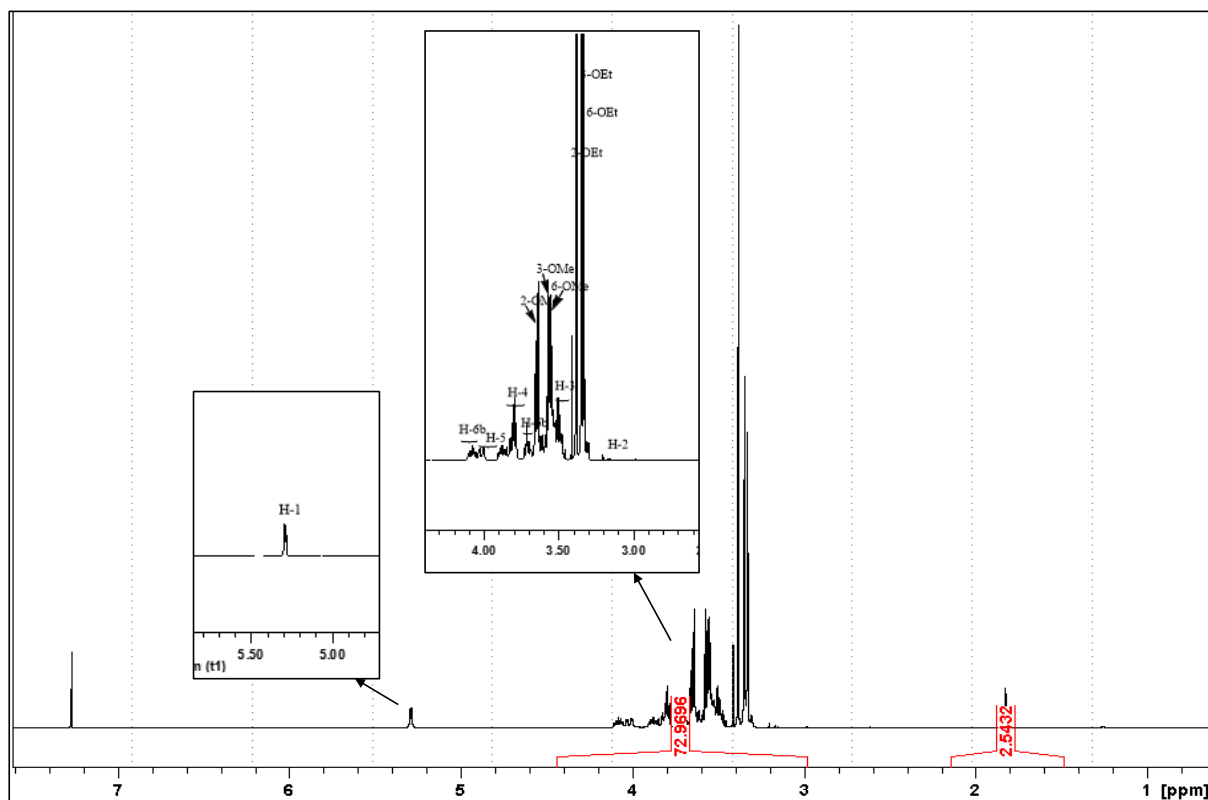


Figure 24. ^1H -NMR spectrum of MeOEt- β -CD, sample measured in CDCl_3 at MHz 399.93.

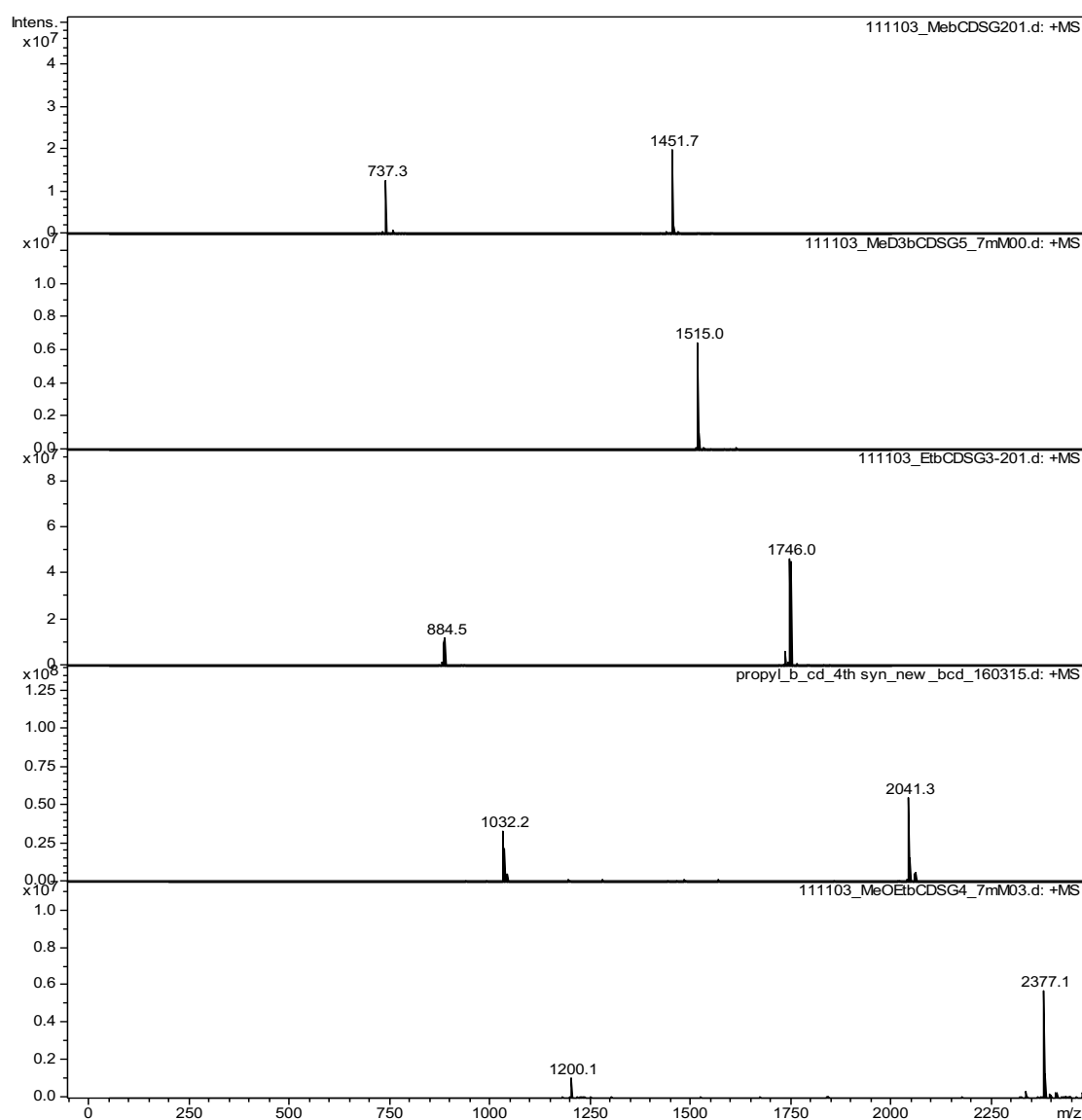


Figure 25. ESI-MS spectra of Me-CD (1451.7), Me-*d*₃-CD (1515.0), Et-CD (1746.0), Pr-CD (2041.3) and MeOEt-CD (2377.1) from top to down showing [M+Na]⁺. First peak in all the spectra is from [M+2Na]²⁺, samples were measured in methanol at a concentration of 0.02 mg/mL

Determination of DS

Degree of substitution was determined by completely degrading the alkylated cyclodextrins into their monomer constituents and subsequently derivatizing these for GLC analysis. Two techniques were used for the determination of DS: i) compounds were submitted to methanolysis¹⁰⁷ and then trimethylsilylated (Figure 26). ii) Alditol acetate method:¹⁰⁸ Compounds were hydrolyzed and reduced to glucitols to avoid α - and β -diastereoisomers, then acetylated and analyzed by GLC (Figure 27).

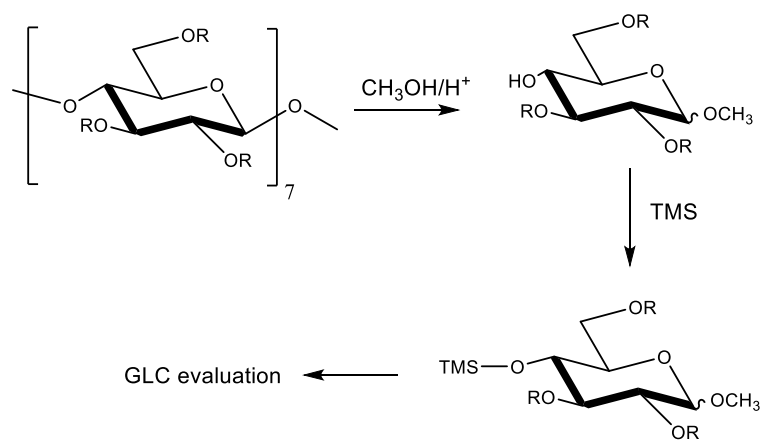


Figure 26. Preparation of methyl *O*-alkyl-*O*-TMS-glucosides by methanolysis followed by trimethylsilylation of CD derivatives

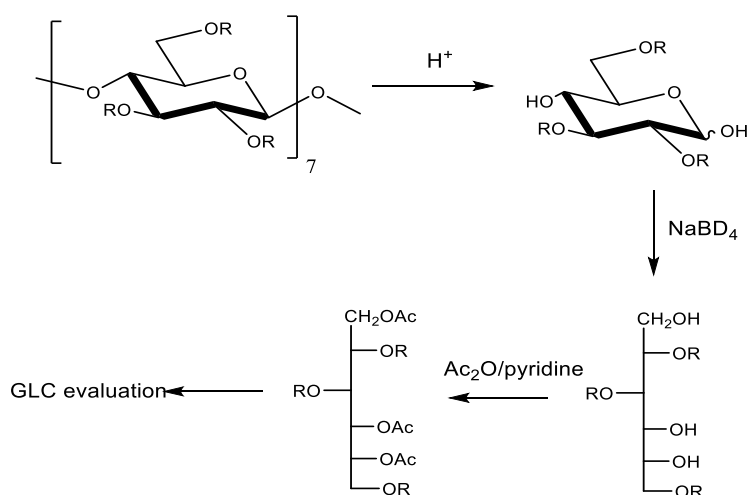


Figure 27. Preparation of *O*-alkyl-glucitol acetates by hydrolysis and subsequent reduction, followed by acetylation

Tiny peaks of underalkylated glucosyl units could be assigned by GLC/MS, as shown in Figures 28-31 for Me-CD, Me-*d*₃-CD, Et-CD and MeOEt-CD, respectively. After correcting the peak area according to the effective-carbon-response concept,⁸⁴ the DS was calculated to be 2.98 (both for methyl glucosides and glucitol acetates) for Me-CD and Me-*d*₃-CD, and 2.98 for MeOEt-CD (glucitol acetates), and 2.94 for Et-CD (glucitol acetates).

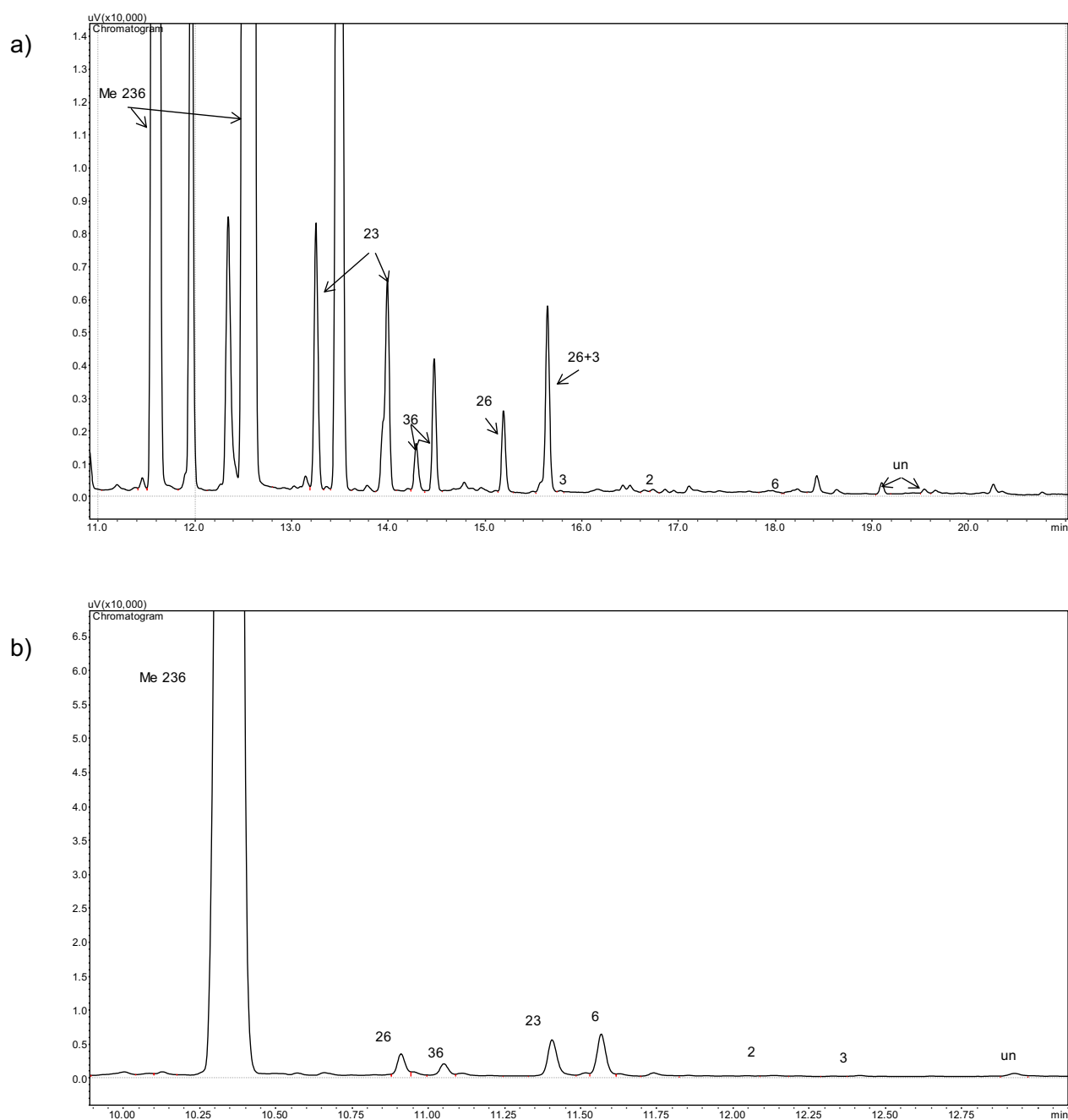


Figure 28. GLC peak assignment of monomers obtained from Me-CD a) methyl *O*-alkyl-*O*-TMS- α,β -glucosides, b) *O*-alkyl-glucitol acetates. Additional unassigned peaks in methyl glucosides were eluting in GC-MS column and they were not interfering with main peaks.

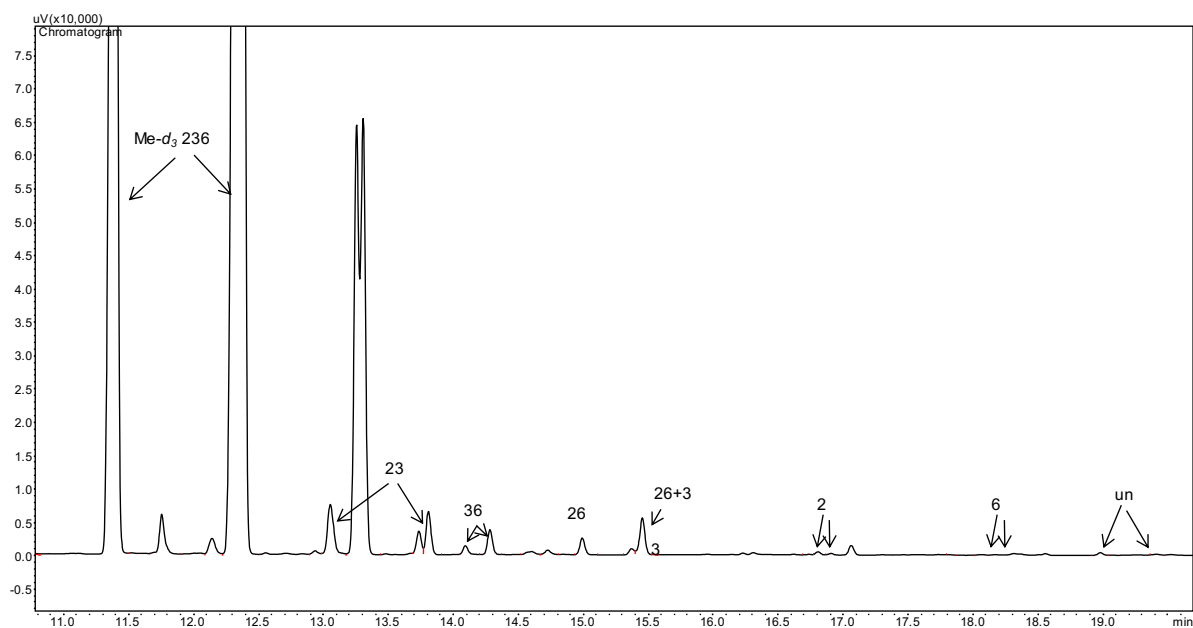


Figure 29. GLC peak assignment of monomers with different substitution in Me-*d*₃-CD, deuteromethyl *O*-alkyl-*O*-TMS- α,β -glucosides. Additional unassigned peaks were eluting in GC-MS column and they were not interfering with main peaks.

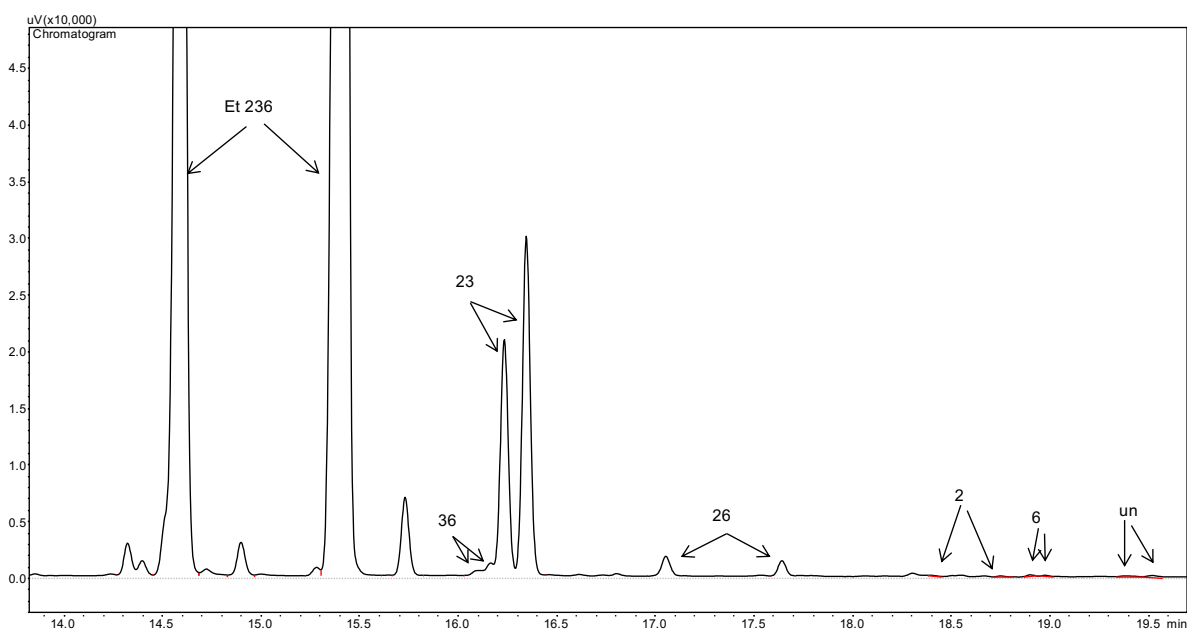


Figure 30. GLC peak assignment of monomers with different substitution in Et-CD, ethyl *O*-alkyl-*O*-TMS- α,β -glucosides. Additional unassigned peaks were eluting in GC-MS column and they were not interfering with main peaks.

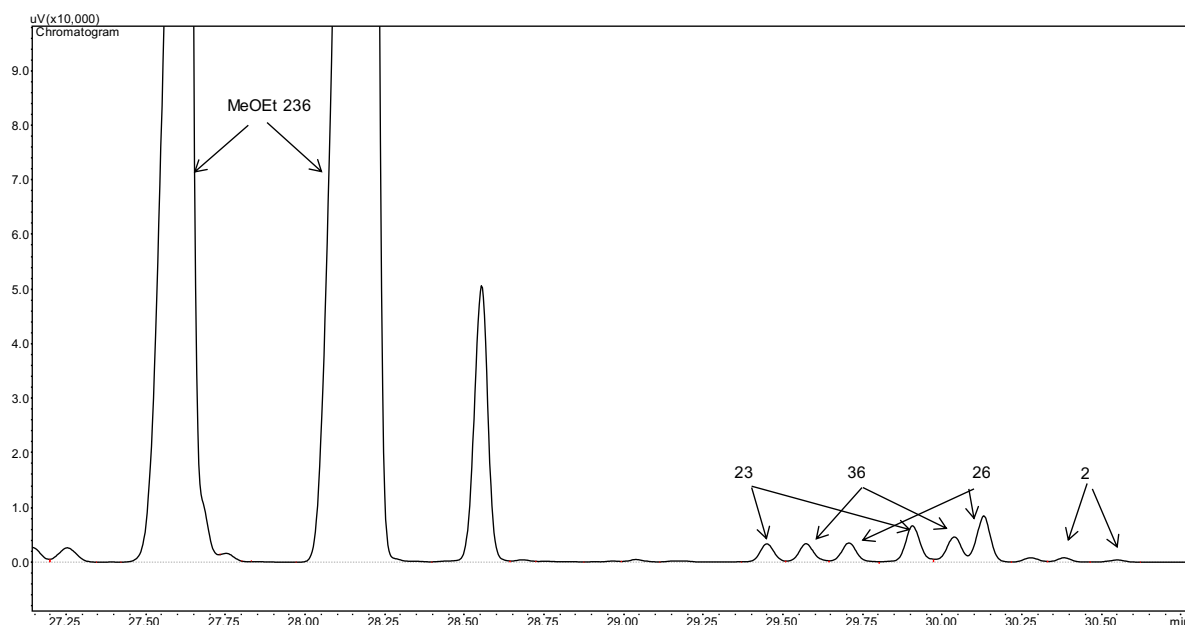
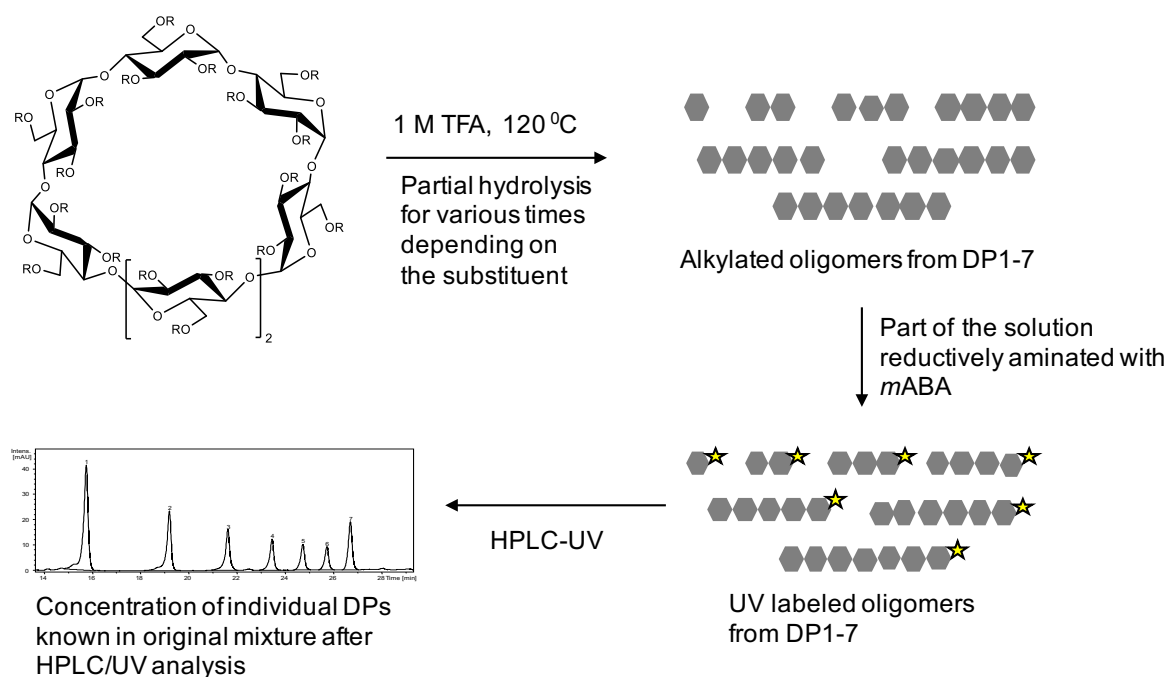


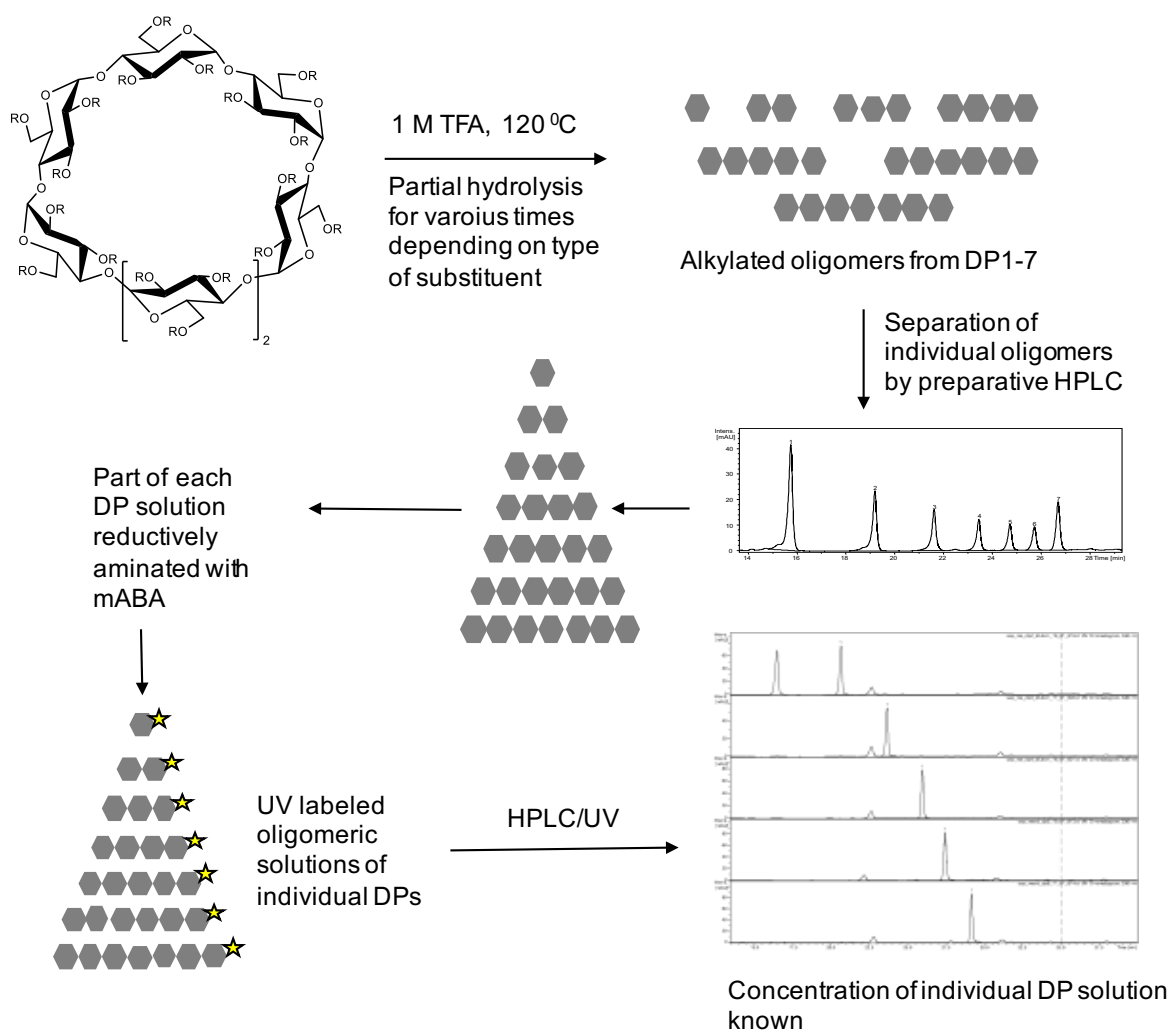
Figure 31. GLC peak assignment of monomers with different substitution in MeOEt-CD, methoxyethyl *O*-alkyl-*O*-TMS- α,β -glucosides. Additional unassigned peaks were eluting in GC-MS column and they were not interfering with main peaks.

3.4 Strategy for preparation of defined mixtures

The main aim to synthesize these pure *O*-alkylated-CDs is to obtain uniformly substituted ω -4-OH maltooligosaccharides for the preparation of defined standard mixtures with known molar ratio of the components. These glucooligomers, although α -linked, resemble the extreme cases in fully alkylated and partially hydrolyzed glucan ethers. Scheme 1 and 2 depict the general outline for preparing these standard mixtures. Details are explained in *sec. 3.5*. Two types of standard mixtures were prepared, complex mixtures and binary mixtures. Complex mixtures (Scheme 1) were prepared by mixing oligomers (DP 1-7), obtained by independent partial hydrolysis of two *O*-alkylated-CDs, for example Me-CD (A) and Et-CD (B). Hence each complex mixture contains 14 various oligosaccharides, two types, each of DP 1-7. In addition, pure oligosaccharides were isolated by preparative HPLC from the partially hydrolyzed CDs to prepare binary mixtures, containing only two chemically different oligosaccharides of the same DP (Scheme 2).



Scheme 1. General outline for preparation of **complex mixtures** with known molar ratio.



Scheme 2. General outline for preparation of **binary mixtures** with known molar ratio.

3.5 Preparation of defined mixtures

3.5.1 Partial hydrolysis of alkylated cyclodextrins

Cyclodextrins undergo hydrolysis in aqueous acid, pioneer work in this area was done by French¹⁰⁹ and Freudenberg.¹¹⁰ They reported that the hydrolysis of the first glycosidic linkage in the ring proceeds five times slower than cleavage of the linear chain. Hence, hydrolysis proceeds at two different rates: k_1 for the ring-opening step, and k_2 for the subsequent hydrolysis of linear oligosaccharide. As the ring opening is slower compared to the open chain hydrolysis, concentration of DP 7 is higher than expected from theory. Apart from this, the kinetics of hydrolysis also depends on the type of substituent on the glucose ring. Therefore, it is important to study the time course hydrolysis profile of the prepared alkylated β -cyclodextrins to find out appropriate conditions. Me- d_3 -CD, Et-CD and MeOEt-CD were partially hydrolyzed with 1M TFA for different time periods.

Maltooligosaccharides obtained after partial hydrolysis are not UV active,¹¹¹ hence to determine the concentration of each DP in the sample they are labeled,¹¹² as shown in Scheme 1 and 2. The response in UV is determined by the label that is attached to the oligomer unit, and does not depend on the type of oligomer. This has been previously proved by Cuers.⁸⁹ After labeling the composition of the hydrolyzates was determined by HPLC-UV. In partial hydrolysis of Me- d_3 -CD, at the beginning (3 min), only DP 7 and a very low amount of DP 1 is detected. When hydrolysis proceeds, the concentration of DP 7 remains always higher than that of DP 5 and DP 6, but a distribution suitable for the study was obtained after 15 min and 20 min. In case of Et-CD hydrolysis was not significantly detectable until 5 min, where a very low amount of DP 1, DP 6 and DP 7 were observed. The increase in non-polar nature decreased the rate of hydrolysis in water. Even after 10 min only DP 1, DP 5, DP 6 and DP 7 were visible. As hydrolysis proceeds the molar concentration of DP 1 increased (due to the increasing possibility to form DP 1) relative to DP 2-6. To decrease the concentration of DP 7 and obtain appropriate amounts of the oligosaccharides of interest, a partial hydrolysis

time of 30 min was chosen to prepare a stock solution for the preparation of 'complex mixtures'. Partial hydrolysis of MeOEt-CD proceeded at a much faster rate compared to all the other alkylated CDs. Due to the additional O in the alkoxy residue, water solubility is improved. After 3 min, DP 7 and a very low concentration of DP 1 was obtained. All the other DPs became already visible after 5 min of hydrolysis. After 25 min hydrolysis of MeOEt-CD was almost complete. Only DP 1 and very low amounts of DP 2 and DP 3 were obtained.

After the partial hydrolysis study, 10-20 mg of Me-CD, Me- d_3 -CD, Et-CD, Pr-CD and MeOEt-CD were independently subjected to partial hydrolysis with 1M TFA at 120 °C for 15-25, 15&20, 30, 60 and 15 min, respectively. The distribution of oligosaccharides of methyl (Me, 20 min), deuteromethyl (Me- d_3 , 15 min), ethyl (Et, 30 min), propyl (Pr, 60 min) and methoxyethyl (MeOEt, 15 min) are shown in Figure 32. Data from DP 7 (linear) is not included in the graphs, there is also a residual amount unopened alkylated cyclodextrin ring present in each hydrolysis solution which is not detected since it cannot be labeled. These partial hydrolysis conditions were used to obtain oligosaccharides for stock solutions for the preparation of “complex mixtures”.

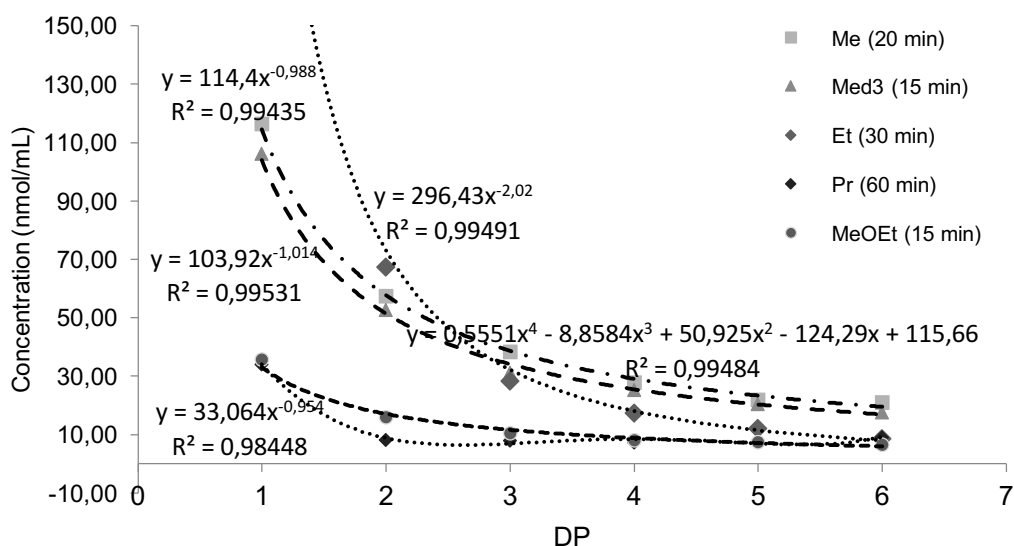


Figure 32. Distribution of DP 1-6 obtained after partial hydrolysis (time of hydrolysis for each compound shown in legend), labeling with *m*ABA and HPLC-UV analysis of maltooligosaccharides obtained from Me-CD (1041.1 nmol, AGU), Me- d_3 -CD (1112.3 nmol, AGU), Et-CD (951.0 nmol, AGU), Pr-CD (951.1 nmol, AGU), and MeOEt-CD (1189.4 nmol, AGU). HPLC-UV analysis was performed at 330 nm with RP-C₁₈ according to Cuers et al.⁸⁹

3.5.2 Preparation of complex mixtures with known composition

As described in Scheme 1, stock solutions (2 mg/mL) from two different alkylated oligomers were mixed in certain proportion to give a complex mixture. Tables 2 and 3 give the concentration of DP 1-7 in stock solutions of Me-CD, Me-*d*₃-CD, Et-CD, Pr-CD, and MeOEt-CD respectively.

Table 2

Concentration (nmol/mL) of DP 1-7 in individual stock solutions in methanol of Me and Me-*d*₃ maltooligomers given with uncertainty

DP	Me-S1	Me-S2	Me-S3	Me- <i>d</i> ₃ -S1	Me- <i>d</i> ₃ -S2
1	279.09±0.001	22.16±0.012	116.42±0.007	156.68±0.015	107.03±0.012
2	100.10±0.008	14.89±0.013	57.53±0.017	65.29±0.058	53.11±0.013
3	49.65±0.012	11.57±0.022	38.50±0.009	36.47±0.006	31.82±0.027
4	31.34±0.093	10.08±0.046	28.00±0.023	24.39±0.001	25.66±0.020
5	19.87±0.023	10.30±0.039	22.02±0.011	17.67±0.075	20.64±0.011
6	13.73±0.029	12.33±0.020	21.20±0.006	14.32±0.025	17.83±0.017
7	15.37±0.012	69.34±0.004	40.38±0.025	20.68±0.001	36.80±0.016

each data point is an average from two independent determinations.

*S1, S2, S3 are three independent stock solutions prepared from three independent partial hydrolysis experiments, Me-S1(1100.3 nmol, AGU), S2 (1050.8 nmol, AGU) and S3(1014.1 nmol, AGU) were hydrolyzed for 25, 15 and 20 min respectively and Me-*d*₃S1(1112.3 nmol, AGU) and S2(1112.3 nmol, AGU) for 20 and 15 min.*

Table 3

Concentration (nmol/mL) of DP1-7 in individual stock solutions in methanol of Et, Pr and MeOEt maltooligomers given with uncertainty

DP	Et-S1	Et-S2	Pr-S	MeOEt-S
1	320.66±0.076	328.24±0.018	34.10±0.020	35.85±0.033
2	65.35±0.021	67.44±0.047	8.25±0.034	16.05±0.026
3	19.23±0.034	28.34±0.052	7.98±0.029	10.67±0.018
4	12.89±0.065	17.34±0.038	7.39±0.015	8.23±0.006
5	10.20±0.162	12.09±0.056	7.50±0.029	7.42±0.044
6	6.11±0.088	8.70±0.038	9.09±0.033	6.55±0.009
7	7.53±0.017	7.63±0.011	44.83±0.035	16.06±0.019

each data point is average from two independent determinations for Et and nine determinations for Pr and MeOEt. Et-S1(892.2 nmol, AGU) and Et-S2 (951.0 nmol, AGU) were hydrolyzed for 30 min, Pr-S (951.1 nmol, AGU) for 60 min and MeOEt-S (1189.4 nmol, AGU) for 15 min.

3.5.3 Molar ratio in complex mixtures

From the above stock solutions complex mixtures with different molar ratio (MR) were prepared. To begin with mixtures with almost equal chemistry, i.e., methyl and its ‘isotopomer’ deuteromethyl, methylated and deuteromethylated oligomeric mixtures (Me- d_3 and Me **CM**) were prepared. Later, to study the change in relative ion intensities as the difference in chemistry between the two types of alkylated oligomers in the mixture increases, mixtures with increasing chemical difference such as Et and Me **CM**, Et and Me- d_3 **CM**, Pr and Me **CM**, as well as MeOEt and Me **CM** were prepared. Furthermore, Pr and Et **CM**, MeOEt and Et **CM**, and MeOEt and Pr **CM** were included. For each type of complex mixture, several mixtures with different molar ratios of the two types of derivatives were prepared. The proportions were calculated to achieve an equimolar mixture with respect to DP 2, DP 3, or DP 4, respectively.

Determination of actual molar ratio in CM

Although, the concentration of each DP in stock solutions is known from HPLC/UV analysis (see Tables 2 and 3), there might be manual error or error in pipette’s delivering volume which might cause an error in delivering the exact calculated proportion when mixing two solutions in certain calculated proportions. Hence, it is important to exactly determine the actual MR in these mixtures, since these serve as reference data for the ESI-MS studies. Therefore, again a part of these mixtures was labeled and analyzed by HPLC-UV. Figure 33 shows an example of HPLC-UV chromatogram of MeOEt and Me oligomer solutions, where, DP 1-7 are well separated. But when these two solutions are mixed due to similarity in HPLC retention, not all of the 14 oligomers were separated, even when different gradients were applied (Figure 34). Hence, to calculate the actual MR in CM, the MR of one DP pair is determined, the MR of all the other DPS can be calculated by using the internal MR of various DPS of the same derivative type. To increase the reliability of the reference data not

only one gradient system was applied, but as shown in Figure 34, different gradient systems were used to resolve peaks of different DPs, average difference is used to calculate actual MR. Additionally, care must be taken to completely labeling of all the components in the mixture. Completeness can be checked by performing the ESI-MS analysis of labeled sample in positive ion mode; if the labeling is complete no peaks from the unlabeled oligomers should be visible.

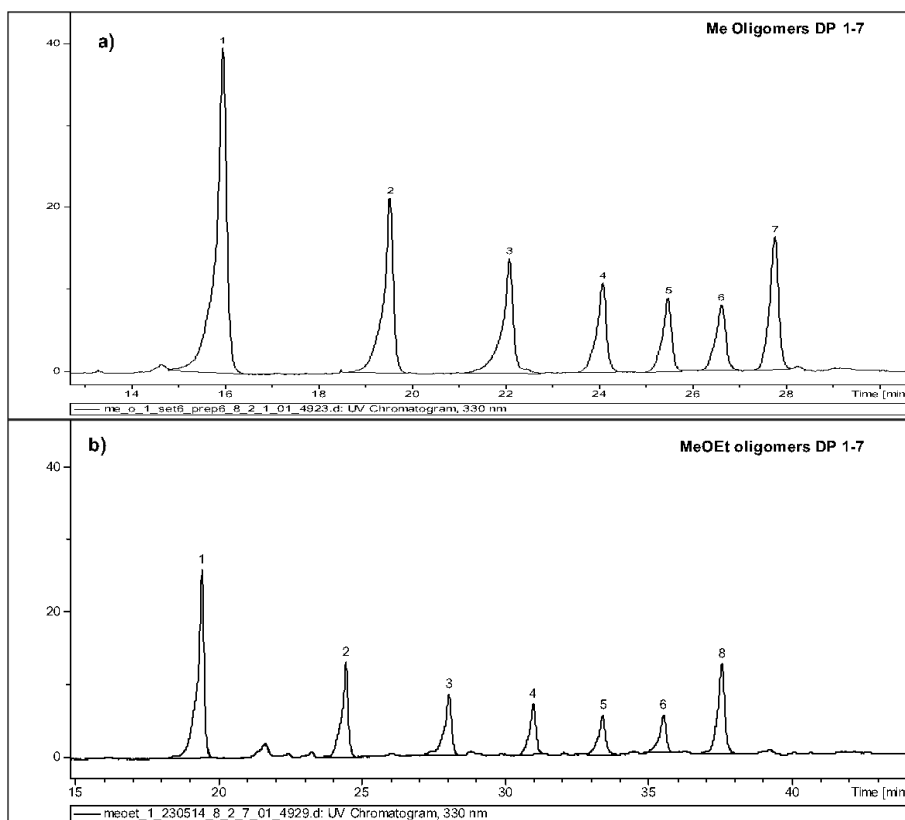


Figure 33. HPLC-UV chromatogram showing DP 1-7 of (a) Me oligomers and (b) MeOEt oligomers, both measured with a linear gradient water/acetonitrile, 80/20 at 0 min to 100% acetonitrile at 50 min. Sample were measured at a total concentration of 0.2 mg/mL. HPLC-UV analysis was performed at 330 nm with RP-C₁₈ according to Cuers.⁸⁹

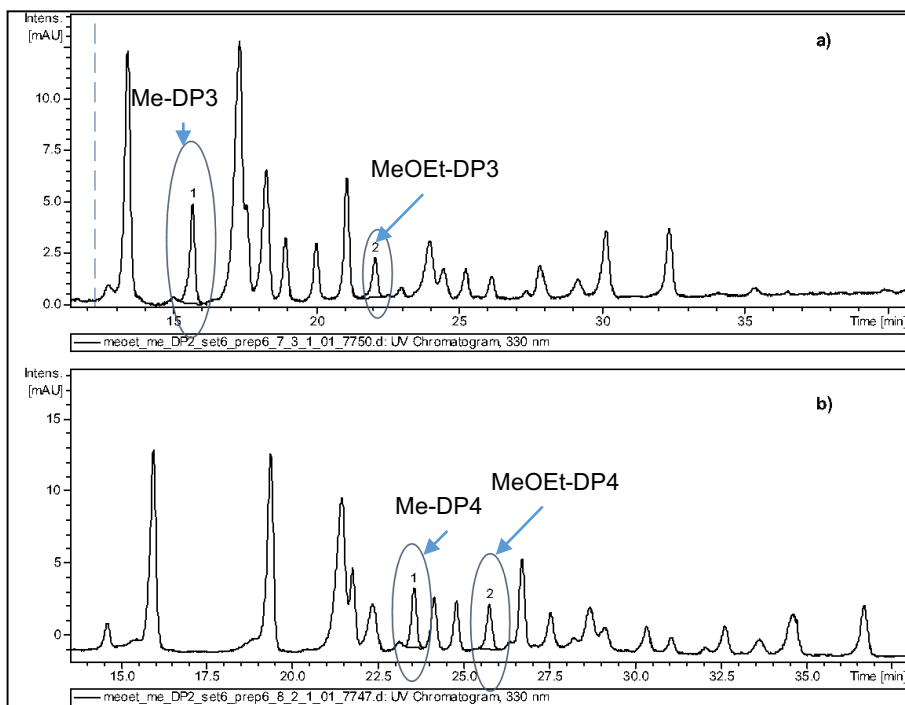


Figure 34. HPLC-UV chromatogram of MeOEt and Me CM mixture, (a) showing the separation of DP 3 of MeOEt and Me (circled) with linear gradient water/acetonitrile, 70/30 at 0 min to 100% acetonitrile at 50 min, (b) showing the separation of DP 4 MeOEt and Me (circled) with linear gradient water/acetonitrile, 90/10 at 0 min to 100% acetonitrile at 50 min. Sample were measured at a total concentration of 0.2 mg/mL, HPLC-UV analysis was performed at 330 nm with RP-C₁₈ according to Cuers.⁸⁹

Molar ratios of maltooligosaccharides in all types of complex mixtures were calculated in a similar way. Results of DP 2-6 are given in Table 4-11 for Me- d_3 and Me CM, Et and Me CM, Et and Me- d_3 CM, Pr and Me CM, Pr and Et CM, MeOEt and Me CM, MeOEt and Et CM and MeOEt and Pr CM, respectively, with uncertainties (obtained by determination of molar ratio composition in triplicates).

Table 4

Molar ratios of maltooligosaccharides ([Me- d_3]/[Me]) in individual CM of ***O*-methylated** maltooligosaccharides, determined by HPLC-UV after reductive amination (n=3)

CM	DP2	DP3	DP4	DP5	DP6
1	0.94±0.004	0.72±0.003	0.67±0.002	0.53±0.002	0.38±0.001
2	1.09±0.015	1.22±0.027	1.30±0.028	1.48±0.020	1.74±0.024
3	1.21±0.001	1.36±0.001	1.44±0.001	1.65±0.001	1.93±0.001
4	1.22±0.014	1.37±0.026	1.46±0.027	1.66±0.020	1.95±0.023
5	1.37±0.029	1.06±0.015	0.98±0.014	0.77±0.011	0.55±0.018
6	1.37±0.019	1.54±0.010	1.63±0.011	1.87±0.012	2.19±0.014
7	1.54±0.017	1.19±0.015	1.10±0.005	0.87±0.004	0.63±0.003
8	1.57±0.014	1.77±0.026	1.87±0.027	2.14±0.029	2.51±0.022
9	1.78±0.032	2.00±0.046	2.12±0.048	2.43±0.044	2.85±0.051

CM 2, 3, 4, 6, 8 and 9 were prepared from Me-S1 and Me- d_3 -S1, CM 1, 5 and 7 were prepared from Me-S2 and Me- d_3 -S2 (*sec.* 3.5.2)

Table 5

Molar ratio of maltooligosaccharides ([Et]/[Me]) in individual CM of ***O*-methylated and ethylated** maltooligosaccharides, determined by HPLC-UV after reductive amination (n=3)

CM	DP2	DP3	DP4	DP5	DP6
1	0.78±0.010	0.46±0.006	0.49±0.006	0.61±0.008	0.53±0.007
2	1.33±0.006	0.79±0.003	0.84±0.003	1.05±0.004	0.91±0.004
3	1.61±0.213	0.95±0.023	1.01±0.087	1.26±0.052	1.10±0.040
4	1.00±0.013	0.63±0.008	0.53±0.007	0.47±0.006	0.35±0.005
5	1.63±0.007	1.03±0.005	0.86±0.004	0.77±0.003	0.57±0.003
6	1.99±0.104	1.25±0.065	1.05±0.055	0.93±0.048	0.70±0.036

CM 1, 2 and 3 were prepared from Me-S1 and Et-S1, and CM 4, 5 and 6 were prepared from Me-S3 and Et-S2 (*sec.* 3.5.2).

Table 6

Molar ratio of maltooligosaccharides ([Et]/[Me- d_3]) in individual CM of **O-deuteromethylated and ethylated** maltooligosaccharides, determined by HPLC-UV after reductive amination (n=3)

CM	DP2	DP3	DP4	DP5	DP6
1	1.06±0.005	0.68±0.003	0.57±0.003	0.49±0.002	0.40±0.002
2	1.53±0.010	0.98±0.007	0.82±0.005	0.71±0.005	0.57±0.004
3	2.06±0.005	1.32±0.003	1.10±0.003	0.96±0.002	0.77±0.002

CM 1, 2 and 3 were prepared from Me- d_3 -S2 and Et-S2 stock solutions of individual oligomer solution of Me- d_3 and Et.

Table 7

Molar ratio of maltooligosaccharides ([Pr]/[Me]) in individual CM of **O-methylated and propylated** maltooligosaccharides, determined by HPLC-UV after reductive amination (n=3)

CM	DP2	DP3	DP4	DP5	DP6
1	0.81±0.003	1.17±0.004	1.49±0.006	1.92±0.007	2.42±0.009
2	0.95±0.012	1.38±0.017	1.76±0.022	2.27±0.029	2.85±0.036
3	0.77±0.003	1.11±0.005	1.41±0.006	1.82±0.008	2.30±0.010

CM 1, 2 and 3 were prepared from Me-S3 and Pr-S stock solutions.

Table 8

Molar ratio of maltooligosaccharides ([Pr]/[Et]) in individual CM of **O-ethylated and propylated** maltooligosaccharides, determined by HPLC-UV after reductive amination (n=3)

CM	DP2	DP3	DP4	DP5	DP6
1	1.12±0.006	2.57±0.013	3.89±0.020	5.67±0.030	9.55±0.050
2	0.52±0.002	1.19±0.005	1.81±0.007	2.63±0.011	4.43±0.018
3	0.32±0.000	0.73±0.000	1.10±0.001	1.60±0.001	2.70±0.001

CM 1, 2 and 3 were prepared from Et-S2 and Pr-S stock solutions of individual oligomer solution of Et and Pr.

Table 9

Molar ratio of maltooligosaccharides ([MeOEt]/[Me]) in individual CM of **O-methylated and methoxyethylated** maltooligosaccharides, determined by HPLC-UV after reductive amination (n=3)

CM	DP2	DP3	DP4	DP5	DP6
1	0.48±0.001	0.48±0.001	0.50±0.001	0.57±0.001	0.53±0.001
2	0.53±0.003	0.53±0.003	0.55±0.003	0.63±0.004	0.58±0.004
3	0.44±0.003	0.44±0.003	0.46±0.004	0.52±0.004	0.48±0.004
4	0.47±0.004	0.47±0.004	0.49±0.005	0.56±0.005	0.52±0.005
5	1.16±0.008	1.15±0.008	1.22±0.008	1.40±0.009	1.28±0.009

CM 1, 2 and 3 were prepared from Me-S3 and MeOEt-S stock solutions.

Table 10

Molar ratio of maltooligosaccharides ([MeOEt]/[Et]) in individual CM of **O-ethylated and methoxyethylated** maltooligosaccharides, determined by HPLC-UV after reductive amination (n=3)

CM	DP2	DP3	DP4	DP5	DP6
1	0.36±0.007	0.57±0.011	0.70±0.013	0.91±0.017	1.12±0.021
2	0.24±0.001	0.38±0.002	0.47±0.003	0.60±0.004	0.75±0.004
3	0.18±0.040	0.28±0.040	0.35±0.019	0.45±0.030	0.56±0.029
4	0.21±0.002	0.34±0.003	0.42±0.004	0.55±0.005	0.67±0.006
5	0.61±0.011	0.96±0.017	1.21±0.022	1.56±0.028	1.91±0.044

CM 1- 5 were prepared from Et-S2 and MeOEt-S stock solutions.

Table 11

Molar ratio of maltooligosaccharides ([MeOEt]/[Pr]) in individual CM of **O-methoxyethylated and propylated** maltooligosaccharides, determined by HPLC-UV after reductive amination (n=3)

CM	DP2	DP3	DP4	DP5	DP6
1	1.39±0.004	0.96±0.003	0.78±0.002	0.69±0.002	0.51±0.002
2	1.31±0.005	0.90±0.004	0.74±0.003	0.65±0.003	0.48±0.002
3	2.18±0.012	1.50±0.009	1.23±0.007	1.09±0.006	0.80±0.005

CM 1- 5 were prepared from Pr-S and MeOEt-S stock solutions

3.5.4 Molar ratio in binary mixtures

The stock solutions described in *sec. 3.5.2* contain oligomers from DP 1-7, but for this study also stock solutions with only one DP which are separated from the other oligomers are also required (as described in *sec. 3.3*). Separation of these oligomers was achieved by preparative HPLC, using RP-C₁₈-column. LC-MS grade acetonitrile and freshly filtered nanopure water were used as eluents. The separation technique was similar to HPLC-UV analysis of labeled compounds (*sec. 7.3*). But, as non-labeled compounds are not UV active, the eluent from the column was collected every one minute in separate tubes. Fractions were checked by TLC, as samples were collected each minute, there were some tubes which contained two DPs. The samples from these tubes were not used in the binary mixture preparation. Only the samples from the tubes containing individual oligosaccharides of same DP were combined. Identity and purity was proved by syringe pump infusion in ESI-IT-MS. The particular concentration (nmol/mL) of an oligosaccharide of certain DP in a stock solution was determined by

HPLC/UV of labeled oligosaccharides as described in *sec. 3.5.2*. For example, chromatogram of the separated and labeled Me-DP 2 and Et-DP 2 oligomers is depicted in Figure 35.

Table 12

Concentration (nmol/mL) of isolated Me, Me- d_3 and Et oligomers (DP 2-DP 6) in methanol stock solutions

DP (nmol/mL)	2	3	4	5	6	7
Me	661.55	469.61	629.05	716.89	660.35	838.73
Me- d_3	806.13	573.31	290.80	215.70	298.00	3243.80
Et	752.51	538.52	740.97	342.76	251.24	---

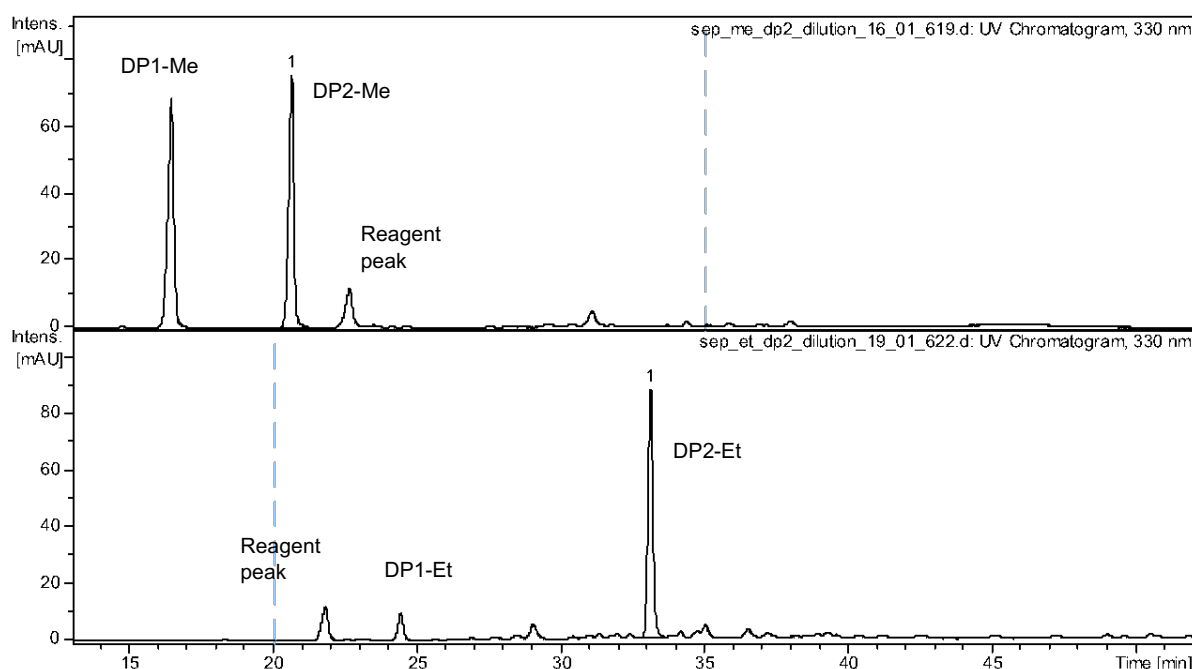


Figure 35. HPLC-UV chromatogram of *mABA*-labeled maltooligosaccharide derivatives from individual stock solutions of DP 2 Me and Et, obtained by isolation by preparative HPLC. Samples were measured with a linear gradient of water/acetonitrile, 80/20 at 0 min to 100% acetonitrile at 50 min. HPLC-UV analysis was performed at 330 nm with RP-C₁₈ according to Cuers.⁸⁹

Two types of mixtures were prepared from these individual oligosaccharide ethers: binary mixtures of methylated and deuteromethylated oligomers (Me- d_3 and Me **BM**), and of methylated and ethylated oligomers (Et and Me **BM**). Initially, oligomers of different sizes were selected. Binary mixtures of DP2 and DP5 with increasing molar ratio of [Me- d_3]/[Me] were prepared, compositions of which are given in Table 13. Later, two independent sets of binary mixtures DP 2-6 of Me- d_3 and Me were prepared with different molar ratios given in

Table 14. Similarly, two independent sets of methylated and ethylated binary mixtures of DP 2-6 were prepared, duplicated results of which are given in Table 15. Determination of the exact molar ratio in these mixtures is easier compared to complex mixtures, as there are only two DPs of interest. Figure 36 shows a HPLC-UV chromatogram of DP 2-6 Et/Me BM, where the two peaks are separated with good resolution in all the binary mixtures.

Table 13

Molar ratio in individual BM of DP2 and DP5 of **O-methylated** maltooligosaccharides with increasing $[\text{Me-d}_3]/[\text{Me}]$, determined by HPLC-UV after reductive amination

BM								
DP2	0.18	0.29	0.44	1.02	2.28	2.77	4.00	6.22
DP5	0.27	0.35	0.58	1.03	2.37			

Molar ratio of the mixtures was only determined once

Table 14

Molar ratio of oligomers ($[\text{Me-d}_3]/[\text{Me}]$) in individual BM, determined by HPLC-UV (n=3)

MR	BM	DP 2	DP 3	DP 4	DP 5	DP 6
$[\text{Me-d}_3]/[\text{Me}]$	1	0.77±0.002	0.84±0.001	1.05±0.003	1.28±0.002	1.06±0.001
$[\text{Me-d}_3]/[\text{Me}]$	2	1.01±0.007	0.80±0.001	2.44±0.001	1.21±0.001	1.05±0.003

Table 15

Molar ratio of oligomers ($[\text{Et}]/[\text{Me}]$) in individual BM, determined by HPLC-UV (n=3)

MR	BM	DP 2	DP 3	DP 4	DP 5	DP 6
$[\text{Et}]/[\text{Me}]$	1	1.00	0.95	0.97	1.10	1.12
$[\text{Et}]/[\text{Me}]$	2	1.00±0.002	1.10±0.001	1.05±0.003	1.14±0.002	1.13±0.001

BM 1 molar ratio was only determined once

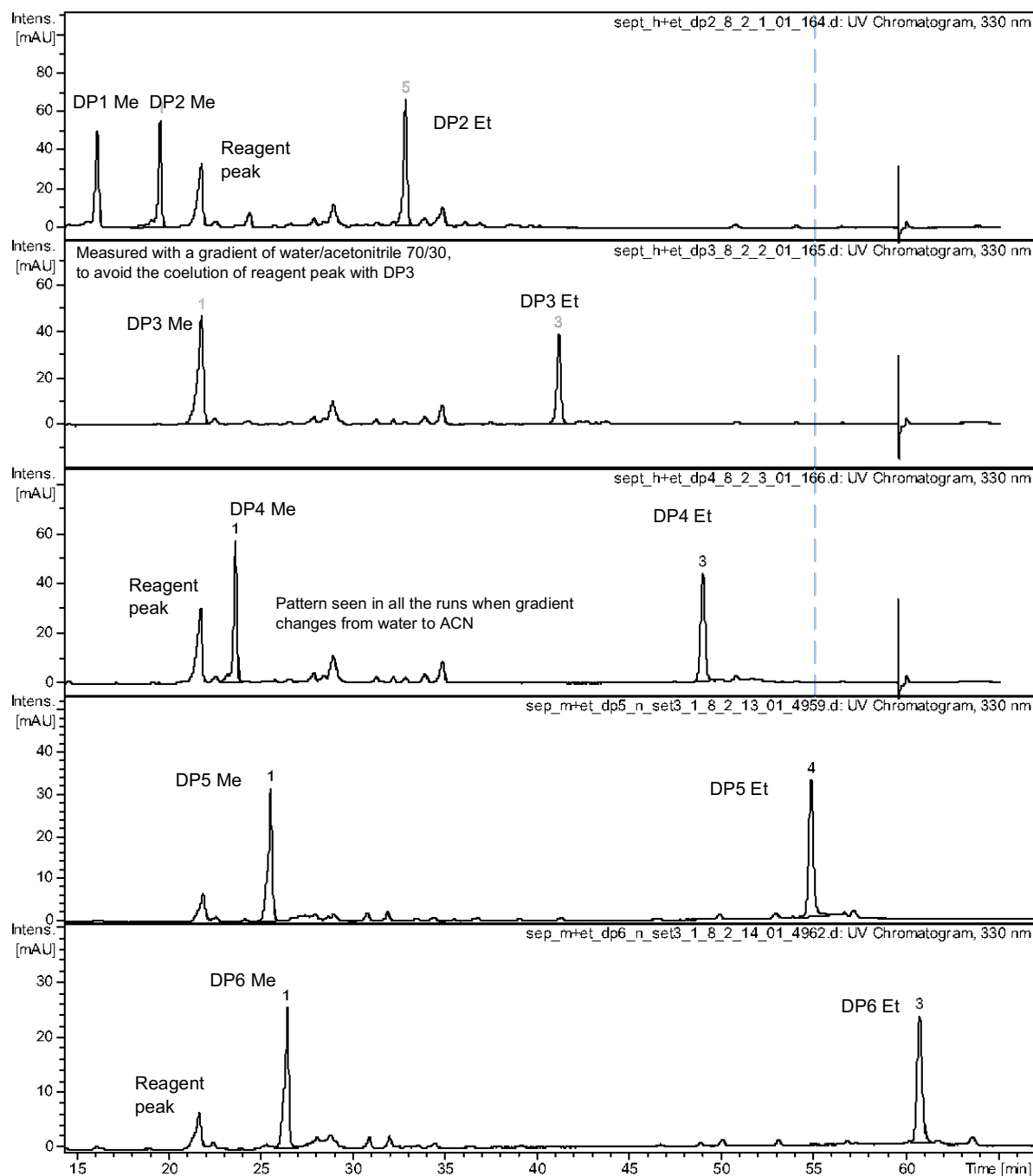


Figure 36. HPLC-UV chromatograms of BM1 of Et and Me oligomers given in Table 18, samples were measured with a linear gradient of water/acetonitrile, 80/20 at 0 min to 100% acetonitrile at 50 min, except for DP3 mixture which was measured with a linear gradient of water/acetonitrile, 70/30 at 0 min to 100% acetonitrile at 50 min to avoid coelution with reagent peak, which elutes much earlier than 15 min at this gradient (not shown in chromatogram). All the chromatograms were carefully evaluated with extracted ion chromatograms in ESI-MS to check no other peaks are coeluting with the desired DP.

List of peaks seen as sodium adducts from DP 2-7 of Me, Me- d_3 , Et, Pr and MeOEt are given in Table 16. Figure 37 and 38 gives an example of ESI mass spectra of Me- d_3 /Me and Et/Me to show the difference between CM and BM.

Table 16*m/z* of oligomeric sodium adducts seen in mass spectra of Me, Me-*d*₃, Et, Pr and MeOEt

DP	Me	Me- <i>d</i> ₃	Et	Pr	MeOEt
2	449.2	467.3	533.2	617.3	713.4
3	653.3	680.5	779.5	905.6	1049.6
4	857.5	893.6	1025.6	1193.8	1385.7
5	1061.6	1106.8	1271.8	1482.0	1721.9
6	1265.7	1319.9	1517.9	1770.2	2059.0
7	1469.7	1533.2	1764.0	2058.1	2395.1

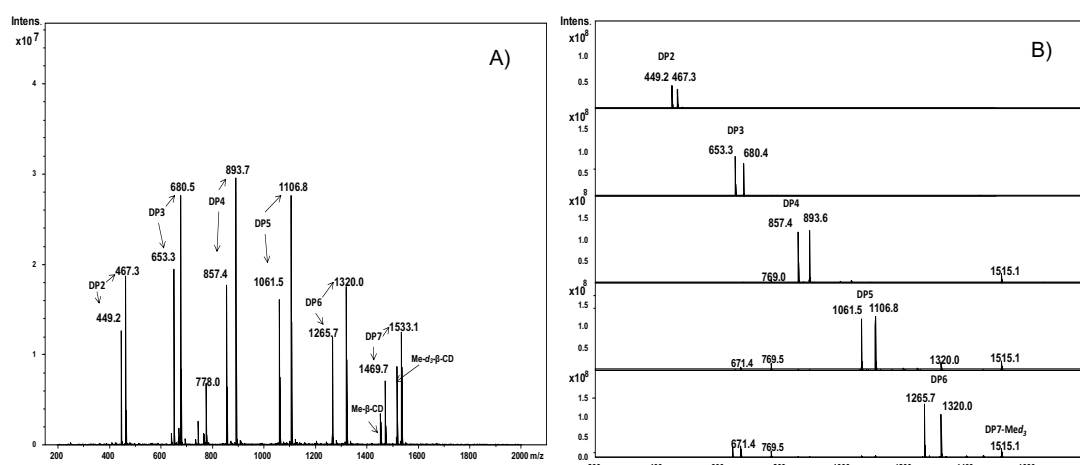


Figure 37. ESI-IT mass spectra of oligomeric mixtures prepared from partially hydrolyzed Me- β -CD and Me-*d*₃- β -CD in MeOH; showing $[M+Na]^+$ signals in positive ion mode. At each DP first signal is from Me oligomer and second signal is from Me-*d*₃ oligomer; (a) **complex mixture (CM)** including DP 2-7; (b) **binary mixtures (BM)** of DP 2-6 of methylated and deuteromethylated maltooligosaccharides. Additional signals are from doubly charged sodium adducts of DP 6 and DP 7 oligomers. Mass spectra are from syringe pump infusions measured under conditions given under 7.3. (Molar ratios of corresponding oligosaccharides are different.)

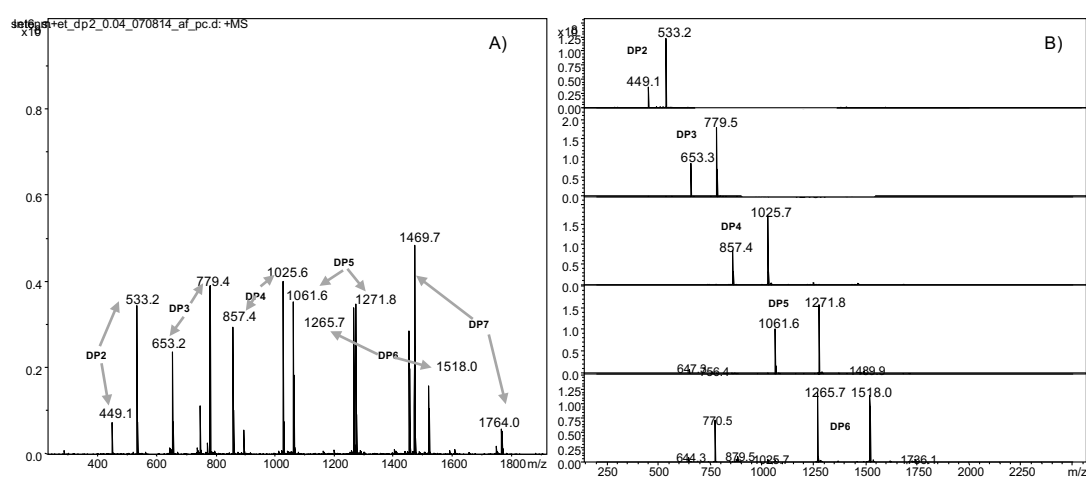


Figure 38. ESI-IT mass spectra of oligomeric mixtures prepared from partially hydrolyzed Me- β -CD and Et- β -CD in MeOH; showing $[M+Na]^+$ signals in positive ion mode. At each DP first signal is from Me oligomer and second signal is from Et oligomer; (a) **complex mixture (CM)** including DP 2-7; (b) **binary mixtures (BM)** of DP 2-6 of methylated and ethylated maltooligosaccharides. Additional signals are from doubly charged sodium adducts of DP 6 and DP 7 oligomers. Mass spectra are from syringe pump infusions measured under conditions given under 7.3. (Molar ratios of corresponding oligosaccharides are different.)

Normalization of data

As discussed in *chapter 3*, the molar ratio MR of two differently alkylated oligosaccharides A and B of a particular DP is known with its uncertainty for all the mixtures used in this study. The intensities measured by ESI-IT-MS were always referred to the candidate with the lower mass, usually methyl. For comparison Rel. Int. (I_B/I_A) obtained from ESI-IT-MS measurements of mixtures with different MR (B/A) are normalized to equimolar concentrations (MR = 1) for each individual DP. Normalized Rel. Int. which represent the relative sensitivities of B/A will be denoted as $(I_B/I_A)/MR$. For a robust quantitative ESI-IT-MS method, relative sensitivities $(I_B/I_A)/MR$ should be constant under the instrumental conditions and within the range of sample concentrations applied.

Conditions for mass spectral analysis

All the samples were measured under similar conditions. These are addressed as ‘defined condition’ in materials and methods (7.3). Unless otherwise specified in the text or the figures the same conditions were used for all the measurements.

Data processing

All the data from the mass spectra were analyzed by Bruker Daltonics Data Analysis software except the mass spectra from nano-ESI-MS. These were analyzed by Thermo Scientific Xcalibur. Intensity of peak heights in mass spectra were analyzed by adding the relative intensity of the 1st to 5th calculated isotopic signal to the main peak.

4. Results and Discussion (Relative sensitivities)

4.1 *O*-Methylated and *O*-deuteromethylated maltooligomers

Complex and binary mixtures of *O*-methyl and *O*-deuteromethyl maltooligosaccharides, described in Tables 4, 13 and 14, have been measured by ESI-IT-MS in methanol solution. The influence of various sample (molar ratio, total concentration, DP and labeling) and instrumental parameters (target mass) on relative sensitivity coefficients was studied. In addition, comparative study between relative sensitivity coefficients in ESI and nano-ESI-MS, syringe pump infusions and LC-MS analysis has been performed.

4.1.1 Dependence of relative sensitivities on molar ratio of analytes

A prerequisite for quantification of MR of two analytes is a linear relationship between MR ($[\text{Me-}d_3]/[\text{Me}]$) of the sample and the ratio of signal intensities ($I_{\text{Me-}d_3}/I_{\text{Me}}$). This is fulfilled if both analytes show linear response, but in principle also if both behave in the same way, even if not linear. In ‘oligomer analysis’ of polysaccharide derivatives (see chapter 1), MR of analytes of a certain DP with different substituents, present in different proportions must be determined.¹¹³ Therefore, we proved that relative sensitivity increased linearly with the increase of the MR ($[\text{Me-}d_3]/[\text{Me}]$) of the analytes in the sample solution. According to the literature,⁶⁰ the surface of the droplet formed in the electrospray process is usually saturated at common sample concentrations. Consequently, there is a competition between various ionized analytes for places on this surface from where they finally – after subsequent Coloumb explosions – can be evaporated and desolvated to form gas phase ions (according to the ion evaporation model). This competition between analyte ions can affect the ionizing efficiency of different analyte molecules which will in turn influence the Rel. Int. in ESI-MS. Therefore, we performed a study with increasing MR of the samples, at a total concentration of 10^{-6} to 10^{-5} M, the critical range for surface saturation.⁹⁵

We started our study with binary mixtures (BM) containing only one DP of each type, and later extended the study to complex mixtures containing all DPs of interest (CM). Initially, BM of DP 2 and DP 5 were prepared with increasing MR (Table 13) to check linearity and to investigate whether the relative sensitivity varies with increasing DP. Figure 39a shows that both oligomers display linearity with increase of MR ($[Me-d_3]/[Me]$) in this range of concentration. Results for all the BM listed in Table 14 are averaged in Figure 39b. A decrease of the relative sensitivity with increasing DP was observed. With 1.01 ± 0.04 for $(I_{Me-d_3}/I_{Me})/MR$ of DP2, ion yield of both analytes was shown to be equal as expected for these chemically very similar compounds (isotopomers). With increasing molar mass, however, $(I_{Me-d_3}/I_{Me})/MR$ decreased and was found to be only 0.78 ± 0.02 for DP 6. To extend these studies to more complex mixtures, all CMs shown in Table 4 were analyzed at a total concentration of 10^{-6} M. to study the effect of saturation due to competition from other DPs. It is observed from Figure 40 that the relative sensitivity for a particular DP is not influenced by the presence of other oligomers and is linearly proportional to increasing MR ($[Me-d_3]/[Me]$). From the various slopes of the graphs in Figure 40, dependence of relative intensities on DP in CM is visible at a total concentration of the sample 10^{-6} M. With 1.09 ± 0.04 for DP 2 it is slightly higher than the expected 1.0 observed in BM. Later these were analyzed in a concentration window of 10^{-5} to 10^{-6} M at three different total concentrations. Summarized relative sensitivities of CM and BM are given in Table 17.

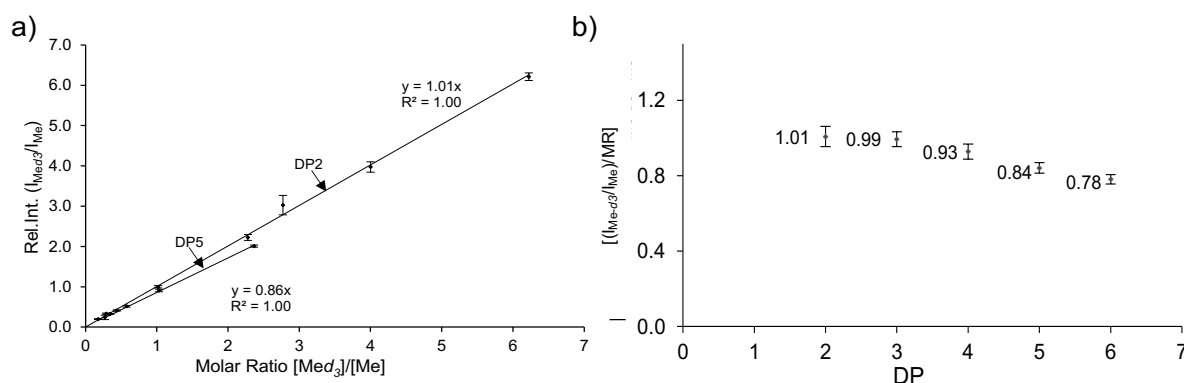


Figure 39. a) Measured relative ion intensities with increasing MR ($[\text{Me-d}_3]/[\text{Me}]$) in BM of DP 2 and DP 5 (Table 13); each data point is an average of three measurements. The slope gives the relative sensitivity. b) Average of all measurements of relative sensitivities $[(I_{\text{Me-d}_3}/I_{\text{Me}})/\text{MR}]$ of BM 1 and BM 2 (Table 14); each DP in BM 1 and BM 2 was measured 10 times; error bars show the uncertainty limits with 95% confidence (4.1.2, Table 17). Samples were measured in positive ion mode ESI-MS, at a total concentration range of the sample from 10^{-6} to 10^{-5} M in methanol. Reprinted from Gangula et al¹¹⁴ with permission of Elsevier.

Tang and Kebarle¹¹⁵ used the relationship (equation 6) between relative ion intensities (I_A/I_B), relative sensitivity coefficients (k_A/k_B), and molar ratio of components ($[A]/[B]$) for a two-component system with the presence of electrolytes.

$$\frac{I_A}{I_B} = \frac{k_A[A]}{k_B[B]} \quad (6)$$

In Figures 39 and 40 it can be observed that relative ion intensities increase linearly with molar ratio for all DPs in BM and CM, while the relative sensitivity is decreasing with DP (investigated in later sections). These results imply that molar ratio of methylated and perdeuteromethylated carbohydrates can be calculated from relative ion intensities as long as the relative sensitivity coefficient of the components is known. Robustness of relative sensitivities (k_A/k_B) was further studied with regard to the influence of total concentration of the sample, while keeping the MR constant (4.1.2).

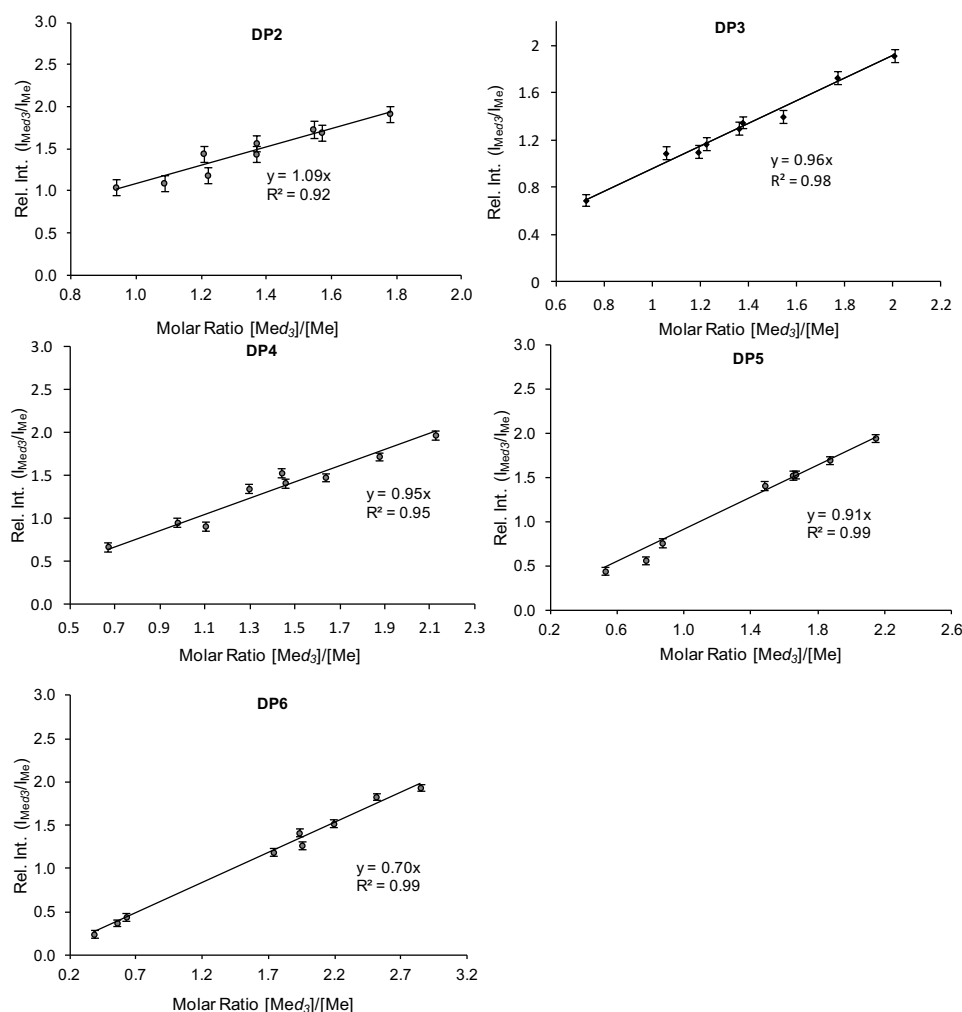


Figure 40. Relative ion intensities with increase in MR ($[Me-d_3]/[Me]$) for various DPs in CM (Table 4) for DP 2-6. Samples were measured in positive ion mode; each data point is an average of three syringe pump infusion measurements with ESI-MS at a total concentration of 10^{-6} M in methanol. The slopes represent the relative sensitivities. Reprinted from Gangula et al¹¹⁴ with permission of Elsevier.

4.1.2 Effect of total concentration on relative sensitivities

Tang and Kebarle (1993)¹¹⁵ and Kebarle and Verkerk (2009)¹¹⁶ reported on relative sensitivity coefficients (as given in equation 6) of two components with similar, slightly different, and very different relative sensitivities in ESI-MS over a wide range of total concentration (10^{-8} to 10^{-2} M), while keeping the molar ratio of the components equal ($[A]=[B]$). Up to a total concentration of about 10^{-6} M, they observed a linear increase of the ion intensities. At higher total concentration, absolute intensities did not increase further, in addition, the ratio of sensitivity coefficients changed and remained constant above 10^{-5} M. This behavior was explained by saturation of the droplet surface and a continuous re-supply from the bulk of the

droplet after the depletion of ions at the surface. Analytes with lower ionizing efficiency have a lower chance to reach the surface and to “survive” the subsequent fission. In contrast, at lower concentration all analyte molecules have a chance to find a place at the surface and finally to escape from the droplet and form gas phase ions. This phenomenon leads to a change of observed relative sensitivity coefficients with concentration. Tang and Kebarle¹¹⁵ reported that Rel. Int. of two analytes with different chemistry represent their corresponding sensitivity coefficients in ESI when competing for the droplet surface at higher concentration; at lower concentrations these may approach 1. Before, studies had been performed with alkali ions, quaternary ammonium ions and alkaloids. In our typical application, the analysis of oligosaccharide derivatives obtained from corresponding polysaccharides, we are confronted with a complex mixture with varying MRs with respect to DP and to chemistry within an individual DP.⁹⁸ Hence, the dependence of Rel. Int. on total concentration and MRs of components has to be studied in detail.

Initially, DP 2 and DP 5 of BM 1 (Table 14) were gradually diluted from a concentration of 10^{-5} to 10^{-9} M. In addition, CM 9 (Table 4) was gradually diluted from 10^{-5} to 10^{-8} M. Results of ESI-MS of BM and CM are shown in Figure 41 and 42, respectively. From these Figures, it can be observed that the absolute ion intensities of Me and Me-*d*₃-maltooligosaccharides in BM and CM exhibit a flattening effect above 10^{-6} M. This effect is more pronounced in CM compared to BM as expected due to competition from other oligomers in CM. Nevertheless, the decreasing trend of relative sensitivities with increasing DP is maintained irrespective of total concentration in both BM and CM.

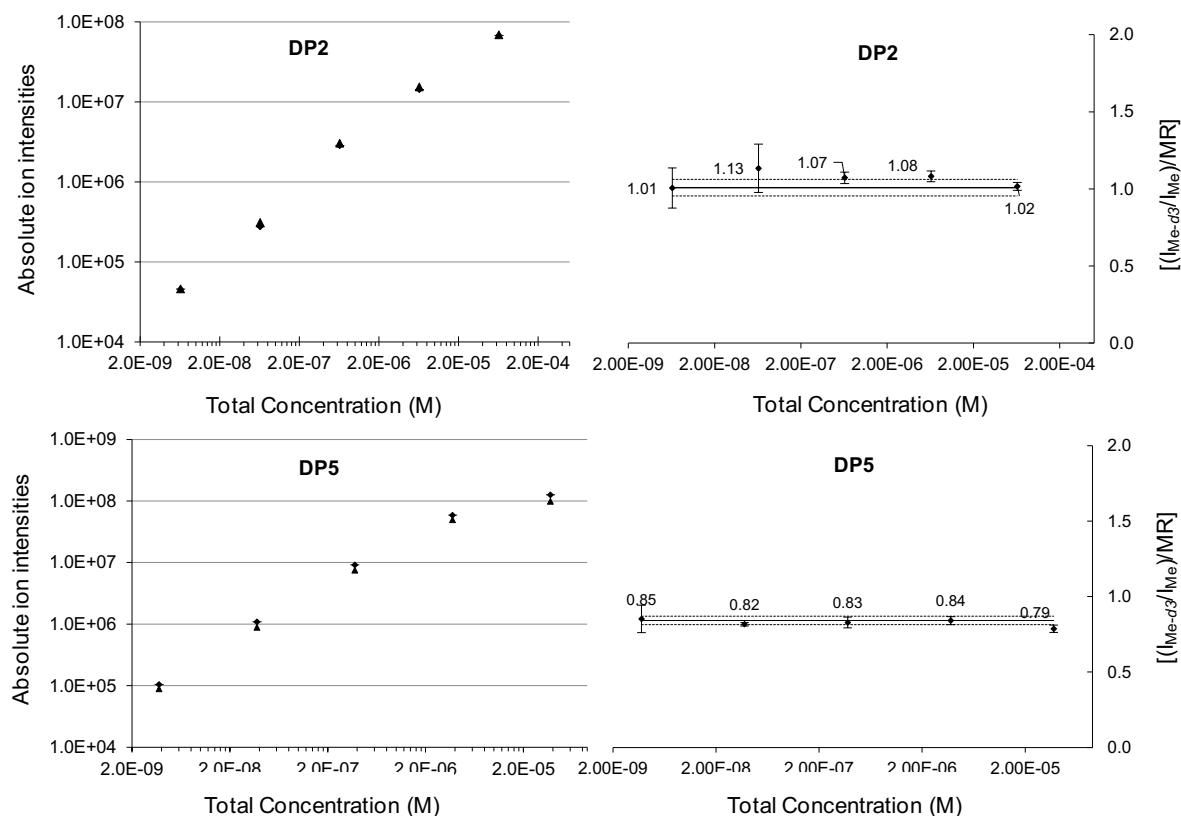


Figure 41. BM 1 (Table 14) of DP2 and DP5; measured at varying total concentration of BM while keeping the MR constant; conditions see (*sec. 7.3*); left: absolute ion intensities (normalized to an equimolar ratio); right: relative sensitivities $[Me-d3]/[Me]$, at different total concentrations; given with the average values shown in Figure 39b and uncertainty limits (4.1.2, Table 17), each data point shows the standard deviation for $n=3$ (each solution measured three times). Reprinted from Gangula et al¹¹⁴ with permission of Elsevier.

4 Results and discussion (Relative sensitivities)

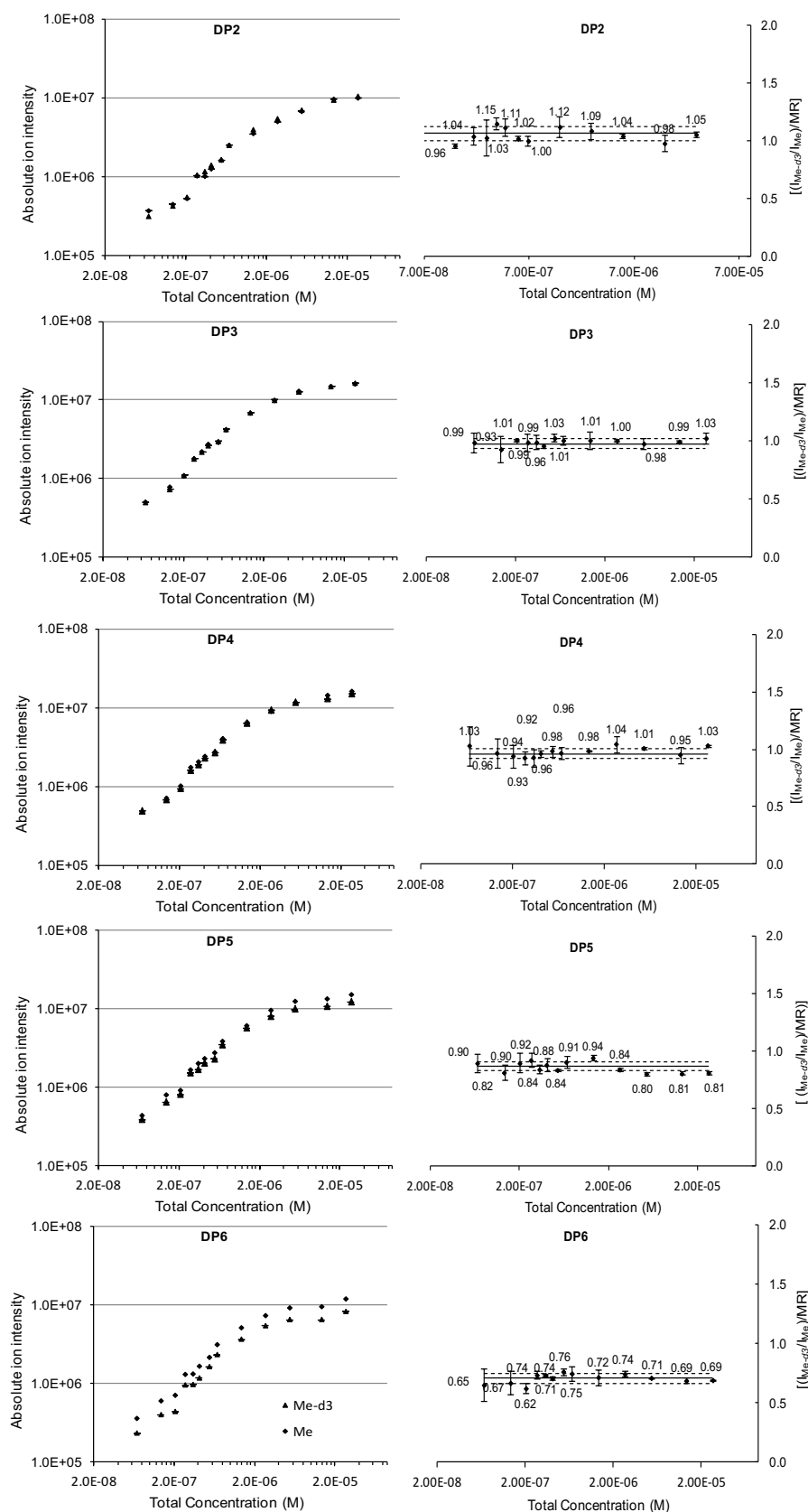


Figure 42. CM 9 (for composition see Table 4); Left: Absolute ion intensities (normalized to an equimolar ratio), of oligomers of different DP measured at varying total concentration in methanol, while the MR of the components is kept constant; Right: relative sensitivity of each DP; conditions see (*sec. 7.3*); given with the average relative sensitivities and U limits for 95% confidence (*4.1.2*, Table 17), each data point shows the standard deviation for $n=3$ (each solution measured three times). Reprinted from Gangula et al¹¹⁴ with permission of Elsevier.

At lower concentration and increasing S/N ratio, the standard deviation of the measurement increases as expected, but the relative sensitivities of these very similar analytes are not concentration dependent in this range, but are constant. This confirms that the ESI-IT-MS method can be applied for the quantification of MR in complex mixtures of *O*-Me/*O*-Me-*d*₃ oligosaccharides, typical for the analysis of substituent patterns in polysaccharide derivatives. The deviation from the expected equal ion yield and the drop of relative sensitivity coefficients ($k_{\text{Me-d3}}/k_{\text{Me}}$) with increasing DP was, however, unexpected. No such discrimination effect is observed for the randomly substituted *O*-Me/*O*-Me-*d*₃-oligosaccharides obtained from partial hydrolysis of methyl cellulose. In contrast to our model compounds with the extreme cases of fully *O*-methylated and fully *O*-deuteromethylated oligosaccharides, oligosaccharides obtained from deuteromethylated methyl cellulose contain all possible patterns, e.g. in case of DP 3 from Me₉/(Me-*d*₃)₀ over Me₈/(Me-*d*₃)₁, Me₇/(Me-*d*₃)₂ etc. up to Me₀/(Me-*d*₃)₉. With increasing DP these profiles become narrower, and thus the analytes being compared become more similar in mass and polarity. Thus, the drop of relative sensitivity coefficients ($k_{\text{Me-d3}}/k_{\text{Me}}$) with increasing DP is probably of low relevance for randomly substituted polymer derivatives,⁸⁹ but have to be considered in case of block like structures.¹⁰³ Average values for all DPs of BM (n=20 for each DP) and CM (n=106 for each DP) given in Table 17, measured at three different total concentrations of the sample in the range 10⁻⁶ to 10⁻⁵ M, are given in Figure 43.

Table 17

Relative sensitivities [$(I_{\text{Me-d3}}/I_{\text{Me}})/\text{MR}$] of BM (Figure 39) and CM (Figure 43f) given with U limits (4.4, 95% confidence)

$(I_{\text{Me-d3}}/I_{\text{Me}})/\text{MR}$	DP 2	DP 3	DP 4	DP 5	DP 6
BM	1.01±0.04	0.99±0.03	0.93±0.03	0.84±0.02	0.78±0.02
CM	1.06±0.09	0.98±0.06	0.96±0.06	0.87±0.05	0.71±0.05

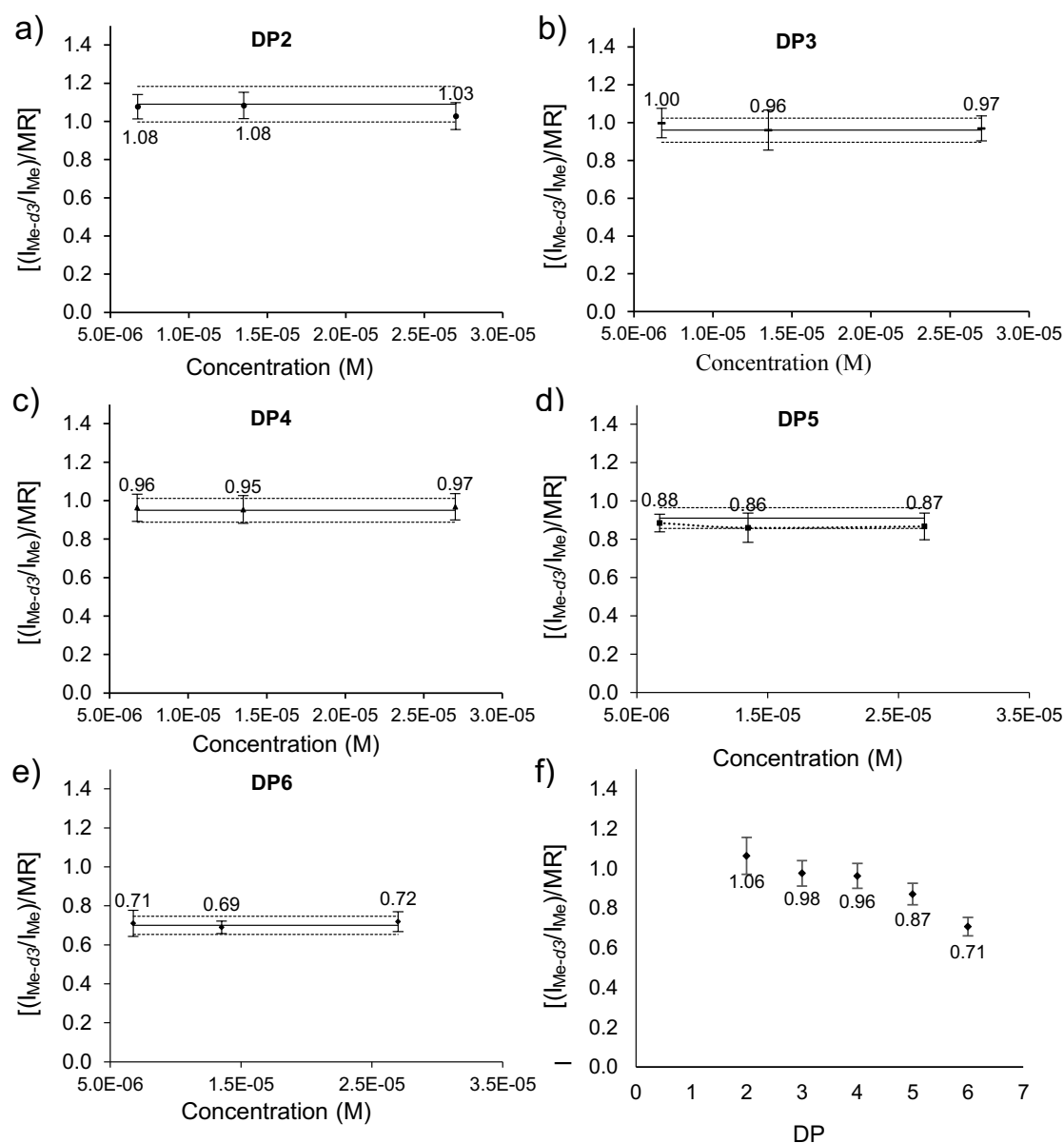


Figure 43. Relative sensitivities for all CM given in Table 4 measured by ESI-MS at three different total concentrations (10^{-6} to 10^{-5} M) in methanol while keeping the MR of the components constant. Graphs a - e show the averaged values for DP 2-6, respectively measured by syringe pump infusion under conditions given in *materials and methods* (sec 7.3), given with the average relative sensitivity; each data point shows the standard deviation of $n=3$. Graph f shows the summarized values of relative sensitivity coefficients of DP 2-6 from all CM measurements ($n=106$); U limits with 95% confidence (Table 17) in all graphs.

4.1.3 Effect of instrumental parameter ‘target mass’ on relative sensitivities

Beside the electrospray ionization process there is a set of instrumental voltages that can be changed by the operator in the ‘instrument expert parameter setting’ which helps in ion transporting and focusing (cap exit, skimmer and octapole DC) to ion trap (IT) analyzer. There another set of voltages (octapole [DC and RF], lens and trap drive level) controls ion

ejection (Figure 8) and detection according to their m/z .¹¹⁷ Not only the sample parameters but also these instrumental settings will affect the Rel. Int. in ESI-IT-MS and thus the quantification of molar ratio from Rel. Int. The first set of voltages determines the ion transport efficiency and noise from the background from entering the ion trap. The main parameter that shows direct effect on the absolute and relative intensities of ions is ‘target mass’ (TM). With the increase of the instrumental parameter TM, the amplitude of octapole RF, octapole DC and trap drive are increased which will aid in the energy take-up of subsequent masses and their ejection from IT and detection.¹¹⁸ In an ion trap, trapped ions have their own oscillation frequency known as ‘secular frequency’.⁴⁰ If the AC potential matches the secular frequency of ions they will be excited. If the AC potential is kept constant at this point and RF is increased, ions will exit in the direction of z-axis according to their m/z . Figure 44 depicts an example of how trapped ions are excited and ejected. It also explains how ejection can be delayed by varying the phase correlation between AC and RF potentials.

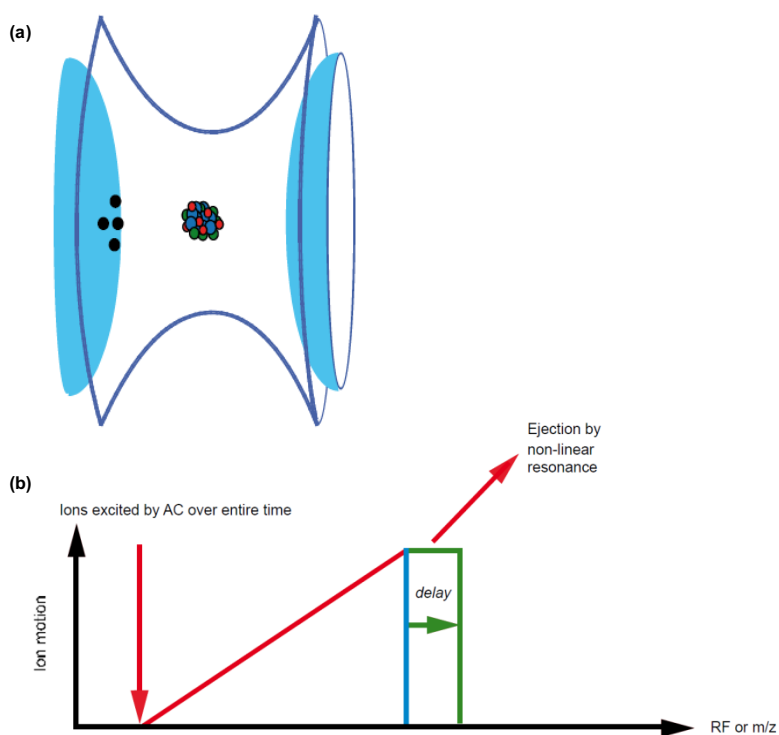


Figure 44. (a) Trapped ions in spherical ion trap; (b) Ions are resonantly excited (red line) and ion motion increases for a given phase correlation between the resonance ac and the main RF, ions would be ejected quickly (blue line). At a different more optimal phase correlation between the resonance ac and the main RF ion ejection is delayed allowing ions to spend more time in the RF at higher orbit and a lower space charge conditions. Source: figure taken from Bruker Daltonics technical note.

Hence it can be understood that TM is an important parameter and individual ions may be ejected differently which will finally influence relative sensitivities in ESI-IT-MS. Our aim was to see whether the change of TM at otherwise constant conditions affects the relative sensitivities in MS, and whether it is a source of bias for the analysis of our oligosaccharide derivatives, where the mass difference increases with each additional glucosyl unit ($\Delta m = 3 \cdot (m_{\text{Me-d3}} - m_{\text{Me}}) \cdot \text{DP}$). Two types of studies were performed with BM 2 (Table 14): direct infusion by syringe pump where both the components in the sample are injected together and thus competing (Figure 45), and by LC/ESI-MS where the components of the sample are separated before entering the ion source (Figure 46). Target mass for syringe pump infusions was set at 300, 500, 1000, and 1500, while in LC/ESI-IT-MS all the DPs of BM were measured at TM 1000 and for DP 2-5 also at TM corresponding to the average m/z value of the oligosaccharides of interest (e.g. for DP 3 $(653+680)/2 = 666$). For DP 6 where the mass difference between two oligomers is already 54, the sample was measured at TM 1000 and at TM corresponding to $[M+\text{Na}]^+$ of DP 6 Me (m/z 1265) and DP 6 Me- d_3 (m/z 1319). From Figure 46 it can be observed that the decreasing trend of relative sensitivity of Me- d_3 /Me oligomers is observed for all TM, but the individual values are influenced by TM. At low TM (300, 500) $(I_{\text{Me-d3}}/I_{\text{Me}})/\text{MR}$ is <1 for all DPs which means that always the larger analyte is discriminated, even for DP2, where the difference in m/z is only 18, while the decrease of $(I_{\text{Me-d3}}/I_{\text{Me}})/\text{MR}$ for DP 5 and DP 6 was less pronounced at TM 1500. From Table 18 it can be seen that absolute ion intensities of Me and Me- d_3 oligomers from DP 5-6 at target mass 1500 are decreased, compared to the absolute ion intensities at TM 1000. As determined earlier,¹¹⁹ at TM 1000 the best and most robust results can be obtained as the discrimination effects for lower and higher target masses can be kept to a minimum here.

Table 18Absolute ion intensities (Abs. Int.) of Me and Me-d₃ DP 2-6 at different TM

	Me	Me-d ₃	Me	Me-d ₃	Me	Me-d ₃	Me	Me-d ₃	Me	Me-d ₃
TM	DP 2	DP 2	DP 3	DP 3	DP 4	DP 4	DP 5	DP 5	DP 6	DP 6
300	1.3E+08	1.1E+08	4.7E+07	2.8E+07	9.1E+06	1.6E+07	7.1E+06	5.4E+06	3.2E+06	2.2E+06
500	1.2E+08	1.2E+08	1.8E+08	1.4E+08	7.6E+07	1.3E+08	4.7E+07	3.5E+07	2.3E+07	1.8E+07
1000	8.0E+07	8.1E+07	1.2E+08	9.9E+07	7.1E+07	1.6E+08	1.5E+08	1.4E+08	1.4E+08	1.2E+08
1500	5.5E+07	7.3E+07	8.5E+07	6.7E+07	4.4E+07	9.4E+07	7.9E+07	8.2E+07	9.8E+07	8.9E+07

Note: the values are from Abs. Int. which have not been normalized to MR, the measurements are of BM 2 Table 14.

From Figure 46 it can be concluded that results obtained for BM after LC-separation are comparable to those of syringe pump infusion. Thus, the pre-separation of the analytes and thus avoidance of the competition in the ionization process does not change the relative ion yields in the concentration range applied. Relative sensitivity was comparable at both, TM 1000 and TM close to m/z of the DP of interest.¹¹⁹ Thus, the two analytes from same DP independently show different ionization behavior and ion yield which might be due to sodium complexation ability, surface activity, desolvation energy and/or electrophoretic mobility as discussed above. As found earlier, reliable quantitative results are obtained when TM is around or above the m/z of interest. That effect of TM is not the reason for the less sensitive detection of the deuteromethylated oligomers of higher DP is proved from the labeling experiments described in 4.1.6, where the chemistry is changed, while the mass difference is maintained, but nearly no discrimination is observed at TM 1000. Thus it can be concluded that the discrimination with increase in DP is due to analytes and not due to bias from instrumental parameters when TM is carefully considered.

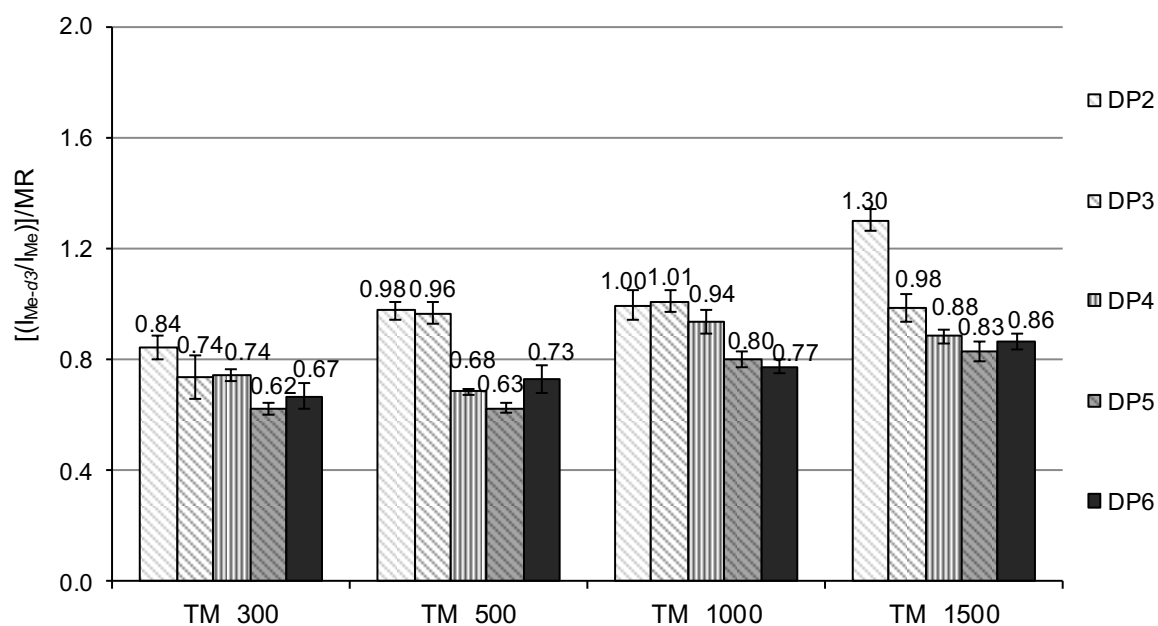


Figure 45. Relative sensitivities of BM 2 given in Table 14, measured by syringe pump infusion in ESI-MS under conditions given in 7.3 except that target mass is varied while keeping all the other parameters constant. Samples were dissolved in methanol at a total concentration of approximately 10^{-5} M, error bars show the standard deviation for $n=3$ (each sample solution measured three times).

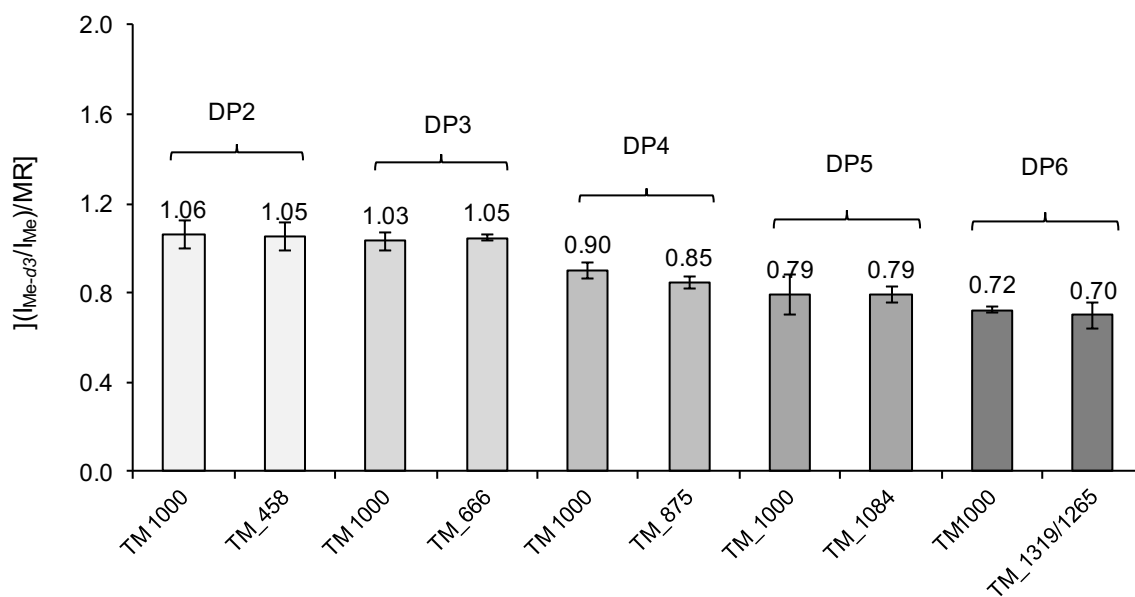


Figure 46. BM 2 (Table 14) measured by LC-ESI-IT-MS under conditions given under 7.3 in positive ion mode at varied target mass (TM); comparison of relative sensitivity of each DP at TM 1000 and TM according to the average DPs of interest. Samples were dissolved in methanol at a total concentration of approximately 10^{-5} M, error bars show the standard deviation $n=3$ (each sample solution measured three times). LC-ESI-IT-MS run was programmed to measure Me DP6 at TM 1265 and Me- d_3 DP6 at TM 1319

4.1.4 Effect of DP on relative sensitivity coefficients of Me and Me- d_3 oligosaccharides

It can be inferred from Figures 39-46 that relative sensitivities $[(I_{\text{Me-}d_3}/I_{\text{Me}})/\text{MR}]$ are decreasing with DP. As DP increases, the chemical character of the homolog oligosaccharide ethers in principle remains the same, but the absolute size and mass difference between two corresponding oligomers of Me- and Me- d_3 -series increases. The probability of an analyte to be located on the droplet surface of the droplets formed by electrospraying the analyte solution, is assumed to depend on its surface activity and electrophoretic mobility. Compared to CH_3 , the CD_3 group is more hydrophobic, more volatile and probably more easily desolvated in MeOH. These properties favor a higher ionization rate and thus a relative sensitivity $[(I_{\text{Me-}d_3}/I_{\text{Me}})/\text{MR}] > 1$. This is indeed observed in CM for DP 2, where the value is slightly above an equal intensity. Already at DP 3, however, $(I_{\text{Me-}d_3}/I_{\text{Me}})/\text{MR}$ drops below 1.00 and further decreases to about 0.87 for DP 5 and even 0.71 for DP 6 (see Table 17). Obviously, another effect begins to dominate. The deuteromethyl group is bulkier and higher in mass than methyl and this mass difference increases by 9 Da/glucosyl unit. Consequently, the differences in electrophoretic mobility – at same charge – will increase with DP in favor of the smaller Me oligomers. Literature for this phenomenon in ESI is rare. A Monte Carlo simulation study has been performed which predicts that ‘analytes with higher molecular weight and larger size have lower ionizing efficiency than smaller molecules.’⁵⁹ Therefore, the initial droplet size generated in the electrospray ionization process should also influence the relative ion intensities. To investigate this effect, we applied nano-ESI-MS for comparison.

4.1.5 Nano ESI-MS

As described in section 1.8, nano-ESI-MS is known to reduce discrimination in the ionization process. Due to a diameter of 1-2 μm of the spraying capillary, initial droplet size is reduced which means more surface and less bulk, fewer generations of Coulomb explosions and thus less discrimination of the less surface active and slower migrating compounds. This

phenomenon was impressively demonstrated for a mixture of maltopentaose and the protein insulin by Bahr et al.⁹⁷ At a very low diameter of the spray capillary and thus droplet size < 200 nm, i.e., 100-1000 times smaller than normal ESI, discrimination due to different chemical behavior and size can be suppressed.⁹⁷ To establish whether this effect can be observed for Me/Me- d_3 mixtures, binary mixtures (BM 2, Table 14) were measured in nano-ESI-IT-MS and nano-ESI-Orbitrap-MS under the conditions reported in *Materials and Methods* (sec. 7.3). Orbitrap¹²⁰ is the modified version of ion trap which can analyze up to m/z of 6000, has a mass resolution up to 150,000 and a mass accuracy of 2-5 ppm. Hence, no difference in the relative sensitivities were expected between ion trap and orbitrap. Figure 47 depicts the results obtained from nano-ESI measurements of both, ion trap and orbitrap-MS. Indeed, no decrease of relative sensitivities with an increase in DP is observed, indicating that the differences in surface activity and electrophoretic mobility may no longer play a role. Rel. Int. for O-Me- d_3 /O-Me-maltooligomers scatter around 1.0 without any trend and an average value of 1.01 for all DPs; with normal ESI-IT-MS they decrease from 1.01 at DP 2 to 0.78 at DP 6 for BM as shown above. There is no systematic difference between the results obtained by nano-ESI-IT-MS and nano-ESI-Orbitrap-MS.

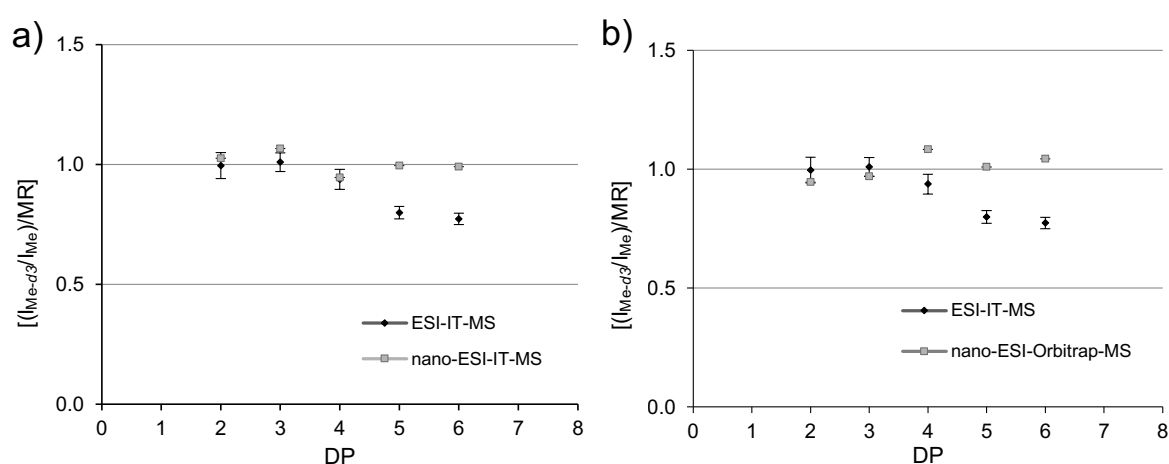


Figure 47. a) Comparison of relative sensitivities of BM 2 from Table 14 measured in ESI-IT-MS and nano-ESI-IT-MS. b) Comparison of relative sensitivities of BM 2 from Table 14 measured in ESI-IT-MS and nano-ESI-Orbitrap-MS. Samples were dissolved in methanol at a total concentration of ca. 10^{-6} M, measured under the conditions given in (sec. 7.3) for ESI-MS and nano-ESI-MS, respectively. Reprinted from Gangula et al¹¹⁴ with permission of Elsevier.

4.1.6 ESI-IT-MS of labeled oligosaccharides

Differences in ionization efficiency of analytes of different chemistry and size can also be overcome by labeling.¹²¹ The introduction of a charged tag, amino benzoic acid for negative ion mode, and Girard's T for positive ion mode,¹¹⁹ can level off differences in sodium complexation ability and at the same time influence surface activity. *m*ABA-labeled *O*-Me/*O*-Me-*d*₃ cellooligosaccharides have been analyzed by LC-ESI-IT-MS up to DP 10 by Cuers.⁸⁹ In the analysis of such 'real samples' (i.e. from technical MCs), analytes can cover the whole range of partially *O*-Me/*O*-Me-*d*₃ carbohydrates. In more or less randomly substituted polysaccharides small or – with increasing DP – no amounts of the extreme cases of fully methylated and fully deuteromethylated oligosaccharides are present, but should also be quantifiable in case of unusual, e.g. bimodal or blocky patterns. Therefore, we tested whether labeling can level the decrease in relative sensitivity observed with the normal ESI-MS for oligomers of higher DP. Reductively aminated BM (*m*ABA) were measured in negative ion mode under the conditions mentioned in *materials and methods* (Sec. 7.3). Quantitative evaluation (Figure 48) shows that the differences observed for corresponding higher Me and Me-*d*₃ oligomers can also be leveled by this tag, and thus the range for quantitative evaluation in the analysis of the substitution patterns of polysaccharide derivatives is extended. This result also confirms that it is not the difference in mass in combination with TM which is responsible for the decrease of the relative ion intensities with increasing DP (see Table 17).

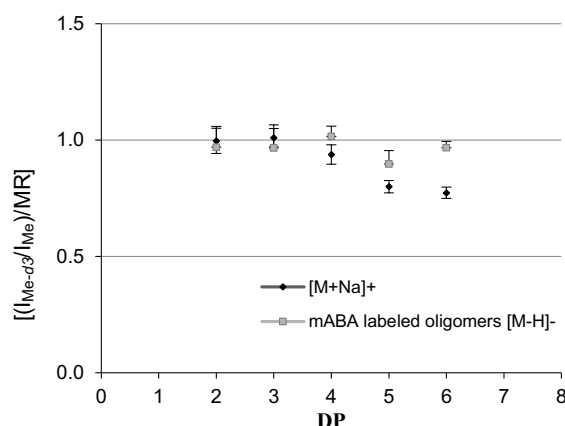


Figure 48. Comparison of relative sensitivities of BM 2 from Table 14; $[M+Na]^+$ measured in positive ion mode and $[M-H]^-$ of labeled oligosaccharides (reductively aminated with *m*ABA) measured in negative ion mode. Samples were dissolved in methanol at a total concentration of approximately 10^{-5} M, measured under the conditions reported under *sec.* 7.3; error bars show the standard deviation, $n=3$ (each sample solution measured three times); target mass was 1000 in both cases. Reprinted from Gangula et al¹¹⁴ with permission of Elsevier.

4.1.7 Comparison with MALDI-ToF-MS

ESI-IT-MS has an advantage of ease of automation, but MALDI-ToF-MS has shown better results with respect to analysis of molar ratios of similar compounds for quantitative analysis of polysaccharide and oligosaccharide mixtures.¹²²⁻¹²³ Hence to compare the relative sensitivities of Me and Me-*d*₃ oligosaccharides in ESI to MALDI-ToF-MS, CM 2, 3 and 8 of Table 4 were measured in MALDI-ToF-MS at KTH, Stockholm. Three different matrices were tested: 2,5-dihydroxybenzoic acid (sDHB), α -cyano-4-hydroxycinnamic acid (CHCA) and 2-(4-hydroxyphenylazo) benzoic acid (HABA). Mass spectra of Me and Me-*d*₃ oligomers with different matrices at the laser power optimized for the particular matrix are shown in Figure 49. It can be seen that sDHB is the most suitable matrix for the analysis of these compounds. Different matrix:sample- ratio, 10:1, 20:1 and 40:1 (weight ratio), were tested, and 10:1 was found to be most appropriate causing no interference of matrix and sample signals. For sDHB matrix laser power of 45% was optimal. Results from laser power just higher than the threshold at 40 % were of low intensity and without clear trends, while laser power of 50% already caused increasing noise in the mass spectrum. However, optimum laser power to record the spectra changes by time and depends on the state of the laser. Average

values of the relative sensitivities of DP 2-6 with sDHB matrix and a matrix:sample-10:1 (weight ratio) recorded at a laser power of 45% are 1.03, 0.97, 0.99, 0.94 and 0.89 respectively with a SD of 0.6, 1.8, 0.6, 1.7 and 2.6% for $n = 3$ (from three different samples). It is obvious that, compared to ESI-IT-MS (Table 17), same samples showed less discrimination of the *O*-deuteromethylated oligomers referred to the *O*-methylated ones with increasing DP. Up to DP 4 the response is equal within experimental error and from DP5 there is a slight decrease in relative sensitivity, the reason for the discrimination from DP5 cannot be determined at this time.¹²⁴

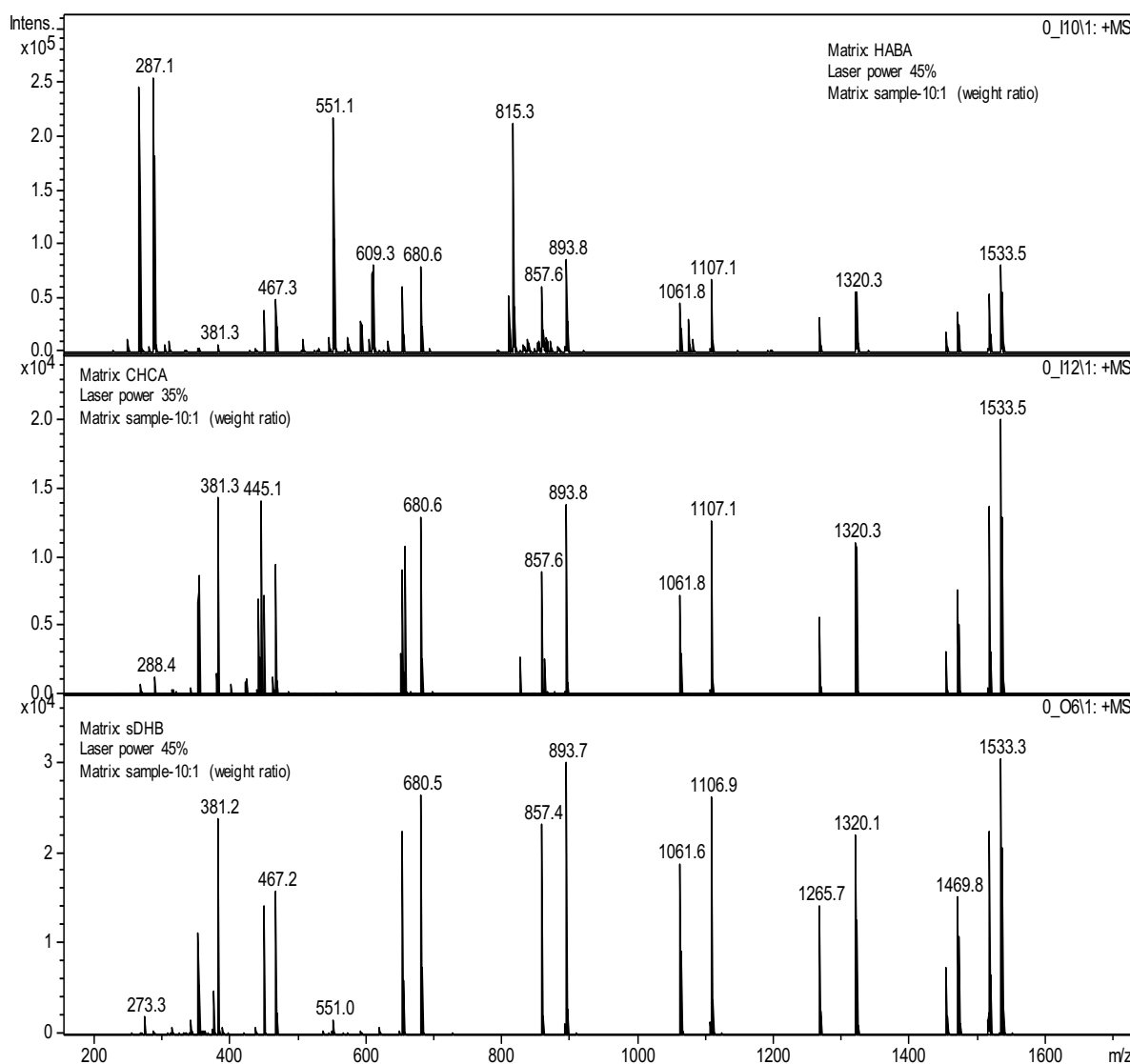


Figure 49. MALDI-ToF-MS spectra of Me and Me- d_3 maltooligomers of CM 2 from Table 4 measured with different matrices, conditions see *materials and methods* (Sec. 7.3). Samples were measured in positive ion mode, and oligomers are seen as $[M+Na]^+$; for peak assignment see Table 16 and Figure 37, all the additional signals are from the respective matrices.

4.2 ESI-MS study of mixtures of *O*-methylated and *O*-ethylated maltooligomers

Ethyl cellulose (EC) is manufactured on industrial scale¹²⁵ and has many applications for instance in the field of thermoplastics, as flexible coatings for paper or as electrical insulant. Beside DS, the relevant properties of EC also depend on the distribution of ethyl substituents over the cellulose chains. The relative composition of mixed oligosaccharide ethers (DS distribution/DP) obtained from peralkylated EC is the basis of this analysis and is determined from the relative ion intensities in ESI-MS. In contrast to Me-*d*₃/Me, the chemical and mass differences are higher. One could take EtI-*d*₅ for peralkylation, but this reagent is very expensive, and perethylation is sterically more demanding. Furthermore, permethylation is performed in any case for the determination of the ethyl groups in the glucosyl units. Thus, it is interesting to study and understand the behavior of ethyl/methyl derivatives and to find out, whether discrimination in MS can be corrected or overcome. As seen in 4.1 there are many factors affecting the Rel. Int. like chemistry, molecular weight, concentration, or instrumental parameters which limit data from ESI-MS for direct quantitative analysis. To investigate all these parameters, defined CM and BM of Me-CD and Et-CD derived mixtures of *O*-Me and *O*-Et maltooligosaccharides were prepared as described in *chapter 3*.

4.2.1 Dependence of relative sensitivities in ESI-MS on the MR of Me and Et glucan analytes

All the CM of Me and Et ethers shown in Table 5 were analyzed by ESI-IT-MS within a concentration range of 10^{-6} to 10^{-5} M in methanol. Relative sensitivities of these mixtures at different MR of [Et/Me] are shown in Figure 50. From the results it can be observed that the change of MR in this concentration range has no influence on relative sensitivity coefficients. Figure 50f summarizes the average values of $k_{\text{Et}}/k_{\text{Me}}$ at different MR ($n=18$, n is the total number of measurements, 6 samples measured 3 times) and total concentration (10^{-6} to 10^{-5} M) with uncertainty limits with 95% confidence (4.4). Like for Me-*d*₃/Me

oligosaccharides, the relative sensitivities are decreasing with DP, however, more pronounced and starting at much higher value above 3 for $(I_{Et}/I_{Me})/MR$ for DP 2, reaching 1.6 for DP 6. The difference in chemistry as well as in molecular weight of the Me and Et analogs is much larger compared to $Me-d_3/Me$. Hence, the decrease of relative sensitivities with DP can probably partly be attributed to the decrease in the electrophilic mobility of the higher molecular weight component (Et). With respect to variation of MR in the range of total concentration of 10^{-6} to 10^{-5} M, there is no clear trend visible, neither within the change in MR, nor within repeated measurements of the same mixture. Scattering of measurement ($n=3$) is often in the range of about 5% and in some cases even up to 15%. Since there is no significant difference for the samples of various total concentration and MR, all data were summarized in Figure 50f for DP 2-6.

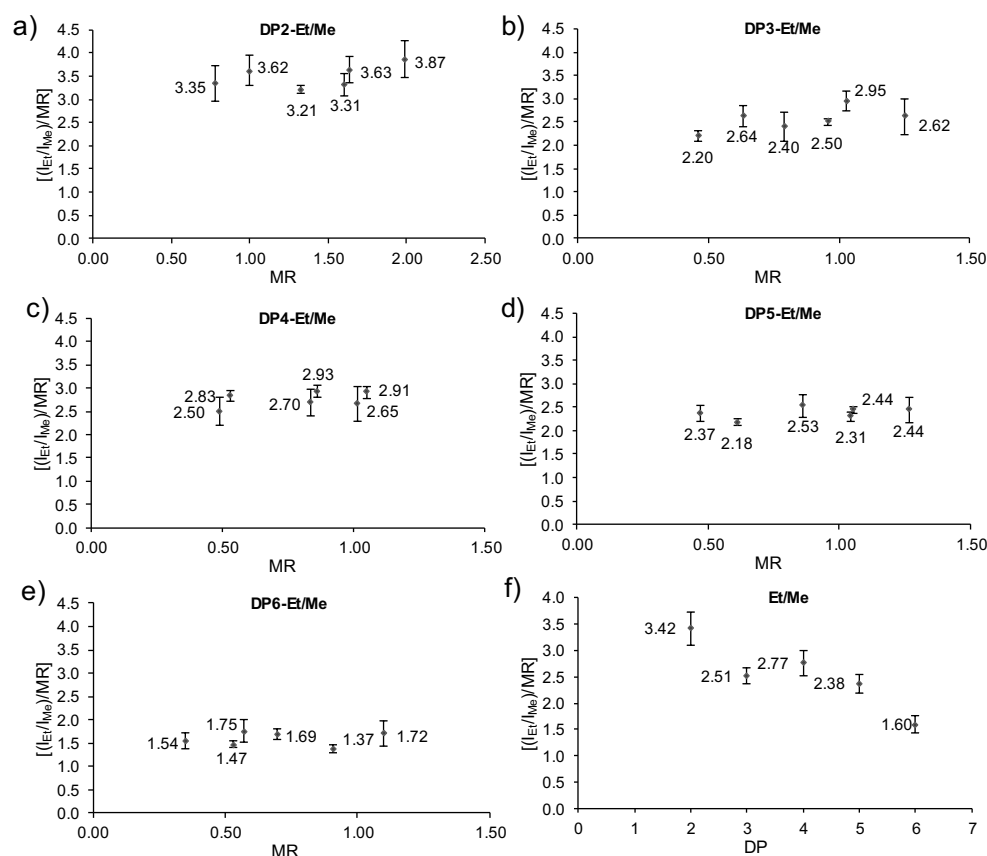


Figure 50. Relative sensitivities for all CM given in Table 5 measured at three different total concentrations (10^{-6} to 10^{-5} M) in methanol while keeping the MR of the components constant. Graphs a - e show the averaged values for DP 2-6, measured by syringe pump infusion under conditions given in *materials and methods* (Sec. 7.3; each data point shows the standard deviation for $n=3$). Graph f shows the summarized values of relative sensitivity coefficients of DP 2-6 from all CM measurements ($n=18$, six samples measured three times); U limits with 95% confidence (Table 19) in all graphs.

4.2.2 Comparison of CM and BM

Binary mixtures of Me and Et oligosaccharides given in Table 15 were measured at a concentration of approximately 10^{-5} M. Average results of each DP, both in BM 1 and BM 2, each measured 3 times, are given in Figure 51, with uncertainty limits calculated with 95% confidence (4.4). Comparison of the results obtained for CM (Figure 50f) and BM (Figure 51) shows that with the decrease in competition from other DPs, $[(I_{Et}/I_{Me})/MR]$ of DP5 and DP6 also decreases, the relative sensitivity for DP 2, however, was even higher for BM than for CM.

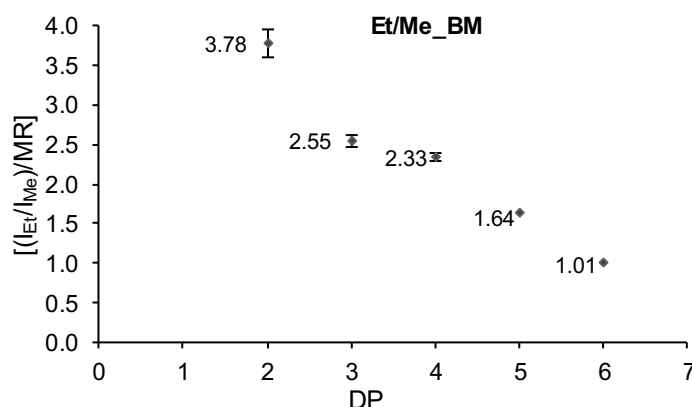


Figure 51. Summarized relative sensitivities (Et/Me) of different BM given in Table 15 at a concentration of approximately 10^{-5} M; $n=6$ for each DP. Error bars show the uncertainty limits with 95% confidence (4.4, Table 19). Samples were measured in ESI-MS, positive ion mode.

4.2.3 Influence of total concentration on relative sensitivity $(I_{Et}/I_{Me})/MR$

As described in 4.1.2, Tang and Kobarle (1993)¹¹⁵ reported on change of relative sensitivity coefficients with total concentration of the samples solution infused. As reported above, the decreasing trend of relative sensitivity found for Me and Me- d_3 -mixtures did not change with total concentration, as the difference for these chemically nearly equal mixtures probably is less due to chemistry, but caused by the diverging molecular weight. But in case of Et/Me mixtures, the relative sensitivity coefficients start at approximately 3.5 for DP 2, going down to 1.0 for DP 6 in case of BM. To study the effect of total concentration of the Et/Me oligosaccharides on relative sensitivity, CM 4 from Table 5 was gradually diluted from a concentration of ca. 10^{-5} to 10^{-8} M (diluted 200 times until S/N is 2/1). As mentioned above,

there are two factors affecting the relative sensitivity, surface activity and electrophilic mobility. As seen in Figure 52, as the sample is diluted the relative sensitivity coefficients decrease, i.e. discrimination of methyl against ethyl is reduced, even not fully. There remains a gap in relative ion intensity, probably due to surface activity differences as has been discussed by Kebarle et al,¹¹⁶ at a higher concentration the compounds with higher surface activity occupy the outer layer of the surface and there is no space left for analytes in the bulk to reach the surface. But as the concentration is diluted surface space is freed and also analytes with less surface activity, in the bulk of the droplet, have a chance to reach the surface and thus form gas phase ions. Hence the relative sensitivity Et/Me of DP2 decreases from 3.85 to 2.33, similarly for the all the other DPs, for DP6 relative sensitivity decreases from 1.69 to even 0.86. From the result of DP6 it is clear that higher electrophoretic mobility favors DP6 Me.

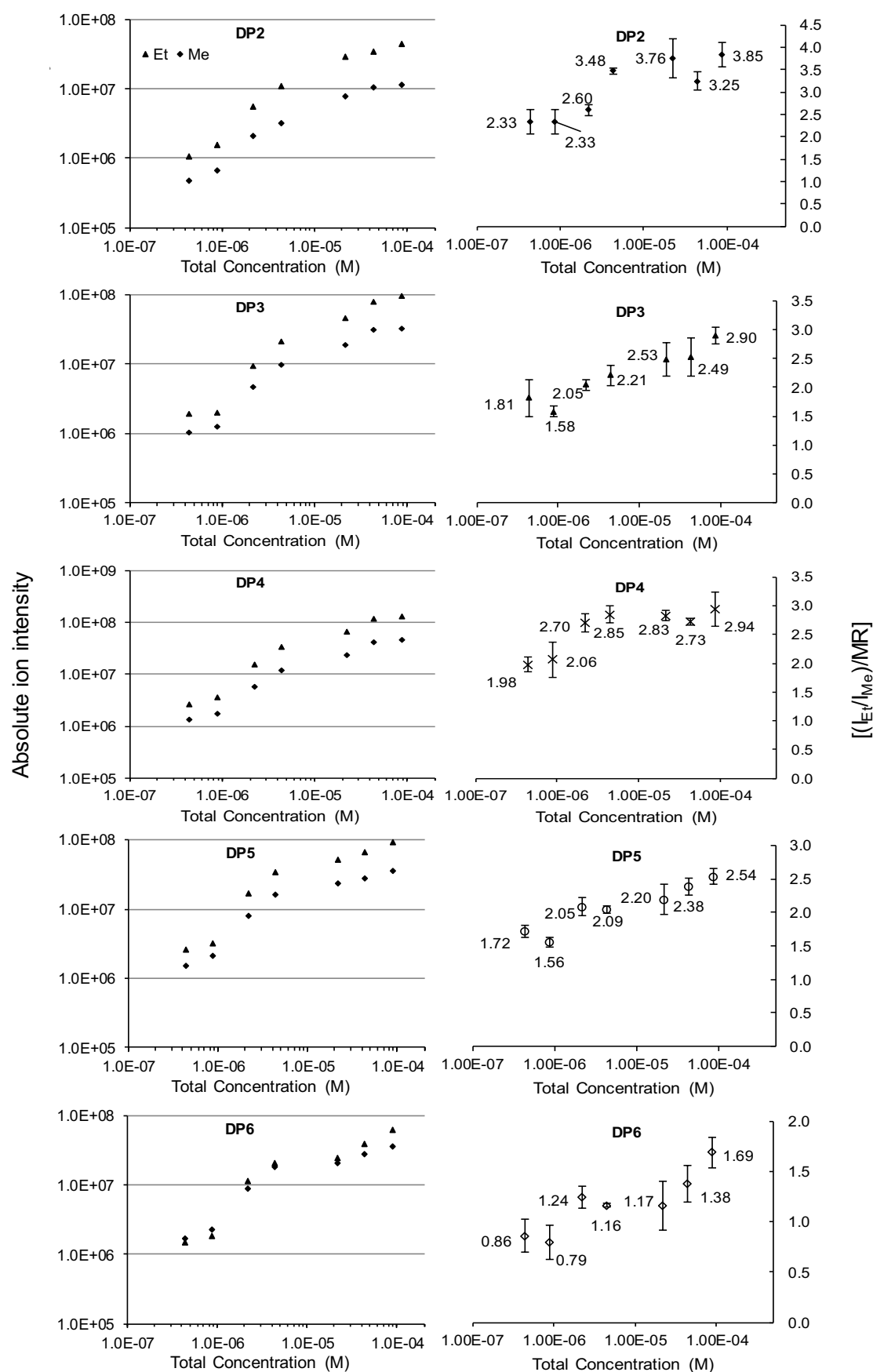


Figure 52. CM 4 of Table 5, measured in ESI-MS at various total concentration of CM while keeping the MR constant; conditions see 7.3. Left: absolute ion intensities (normalized to an equimolar ratio), right: relative sensitivities, at different total concentrations; each data point shown with the standard deviation of n=3.

4.3 Relative sensitivities of Me- d_3 and Et glucan analytes in ESI-MS

Methylated and deuteromethylated oligosaccharides are very similar in chemistry and show almost equal sensitivities in ESI-MS, as described in 4.1.2. Thus, mixtures of analog and homolog Et and Me- d_3 maltooligosaccharides should behave similar to the just described Et/Me mixtures. Et/Me- d_3 mixtures of known molar composition (see Table 6) were prepared. These were analyzed under the ‘defined conditions’ (*sec.* 7.3). Relative sensitivities are almost similar to Et and Me mixtures except a slight difference at DP 5 and DP 6, which could be expected (see Figure 53), as for Me- d_3 /Me the relative sensitivity coefficients for these DPs in CM are 0.87 and 0.71, respectively. Therefore, if we multiply relative sensitivity coefficients of DP 5 and DP 6 Et/Me, i.e., $2.38 \cdot 0.87 = 2.07$ and $1.60 \cdot 0.71 = 1.13$, the expected relative sensitivities for Et/Me- d_3 are around 2.07 and 1.13 respectively.

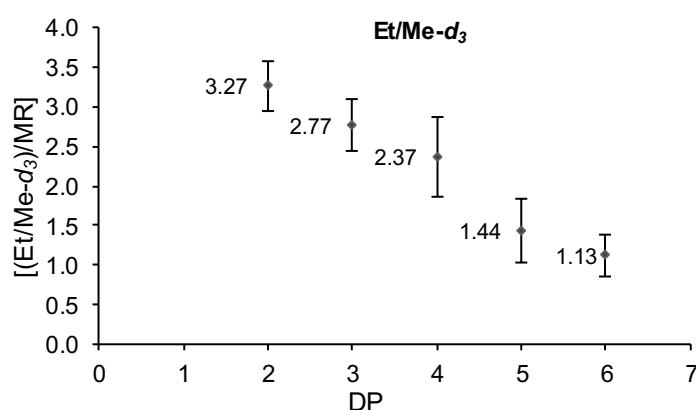


Figure 53. Summarized relative sensitivities of different CM Et/Me- d_3 given in Table 6 in the concentration range (10^{-5} to 10^{-6} M); $n=9$ (three samples with different MR measured three times each) for each DP

4.4 Relative sensitivity coefficients of Me and Me- d_3 and Me and Et with uncertainty

All measurements described have been performed in our laboratory with a Bruker HCT ultra ESI-IT-MS which is intensively used by several research groups for different applications. Since the condition of the instrument is critical with respect to reproducibility of absolute ion intensities a study was performed by syringe pump infusions, five consecutive times each day and on five different days under defined conditions (*sec.* 7.3), with CM 4 of Me- d_3 and Me (Table 4) and Et and Me (Table 5). Figure 54 shows how relative sensitivity of the same

sample varies on same day and different days. The standard deviation of five consecutive measurements on the same day and different days also was around 2 to 14 %. Hence it is essential to assign uncertainty limits to the data of relative sensitivity coefficients. Depending on the parameters causing uncertainty in the measurement ‘Type A’ or ‘Type B’ evaluation can be chosen for uncertainty limits calculation.¹²⁶⁻¹²⁷ Type A is suitable for error caused by repeated measurements and Type B for a probability density function which represents the knowledge about the measurand. Due to the poor reproducibility of repeated measurements here Type A evaluation is chosen for defining uncertainty limits. Uncertainty (u_1) was calculated for each DP for both types of alkylated analytes in BM and CM, respectively. This uncertainty u_1 was combined with uncertainty u_2 from the determination of reference data by HPLC-UV (*chapter 3*), and a combined uncertainty (U) with 95% confidence was calculated by following ‘Type A evaluation’. Averaged k_{Et}/k_{Me} and k_{Me-d_3}/k_{Me} values for DP 2-6, for both, BM and CM at a total concentration of 10^{-5} M with U limits are summarized in Table 19.

Table 19

Relative sensitivities of BM and CM given with U limits (95% confidence) of Me- d_3 /Me and Et/Me

Mixture	DP2	DP3	DP4	DP5	DP6
BM_Me- d_3 /Me	1.01±0.04	0.99±0.03	0.93±0.03	0.84±0.02	0.78±0.02
CM_Me- d_3 /Me	1.06±0.09	0.98±0.06	0.96±0.06	0.87±0.05	0.71±0.05
BM_Et/Me	3.78±0.19	2.55±0.11	2.33±0.08	1.64±0.04	1.01±0.05
CM_Et/Me	3.42±0.32	2.51±0.16	2.77±0.24	2.31±0.18	1.60±0.18

Relative sensitivities for Me- d_3 /Me BM and CM from Figure 39 and Figure 43f, Et/Me CM and BM from Figure 50f and Figure 51 respectively.

4 Results and discussion (Relative sensitivities)

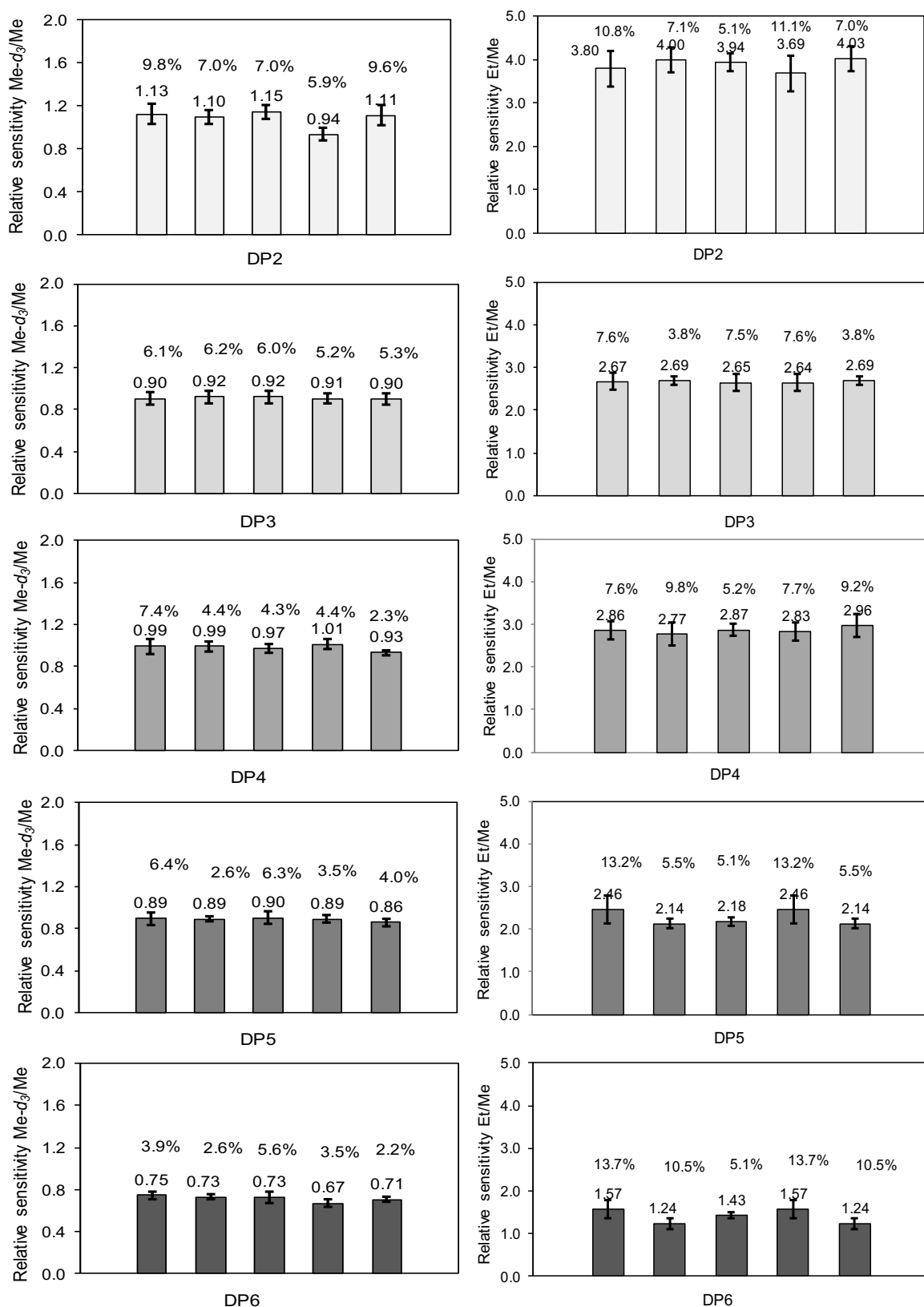


Figure 54. Relative sensitivities of DP 2-6; CM4 of Me and Me- d_3 (Table 4, here left), and Me and Et (Table 5, here: right) were measured on five different days, each day for five consecutive times. Each data bar shows the relative sensitivity of same DP from same mixture measured on different days with percent SD on each day. For conditions see *sec. 7.3*

4.5 Relative sensitivities of higher *O*-alkyl- related to *O*-methyl-maltooligosaccharides

After determination of the relative sensitivity coefficients for Me-*d*₃/Me and Et/Me (Table 19), a study was performed with higher *O*-alkylated analogs, where mixtures were prepared with propylated oligomers as described in *chapter 3*. In case of *O*-alkylated maltooligosaccharides, chemistry of the analyte molecule influences the abundance in ESI-MS, where increase in the non-polar character¹²⁸ increases surface activity and shifts the equilibrium of the analyte in the bulk to outer layer and surface of the droplet. As we analyze oligosaccharides as sodium adducts $[M+Na]^+$ in positive ion mode, sodium complexation ability¹²⁹ also influences the ion abundance in ESI-MS. Formation of sodium adduct of a neutral molecule is of electrostatic nature. As the electron density on the coordinating oxygen atoms of the oligosaccharide increases, the equilibrium is shifted in favor of the sodium adduct formation. With respect to the formation of sodium adducts, however, it is not clear whether it occurs in solution or at the droplet surface.¹³⁰⁻¹³¹ As the alkyl chain length of the *O*-alkyl ethers (without branching) increases electron density and basicity of the linked oxygen increases due to the positive inductive effect,¹⁴¹⁻¹⁴² which probably enhances the sodium complexation ability.

As observed by some researchers, the kinetics of a chemical reaction increases linearly with polarity.¹³²⁻¹³³ We wanted to study whether Rel. Int. in ESI-MS also exhibit such a relationship with the alkyl chain length of the substituents in forming gas phase ions. Hence, as described in Tables 7 and 8, complex mixtures with known composition were prepared. These mixtures were analyzed under ‘defined conditions’ (*sec. 7.3*). Averaged and summarized relative sensitivities from mixtures with different molar ratio are shown in Figure 55 for Pr and Me and Pr and Et. From Table 19 and Figures 50 and 55 it can be interpreted that oligomers which are nearly equal in chemistry (Me-*d*₃/Me) show almost equal relative sensitivity in ESI-MS up to DP 4. At DP 5 the relative intensity drops for Me-*d*₃/Me

probably due to the increasing difference ($\Delta 45$) in molecular weight. This drop is more prominent already at DP 3 for all the other types of mixtures, for example $\Delta 126.2$ for Et/Me DP 3, $\Delta 252.3$ for Pr/Me DP 3. As we have seen above, mixtures of Et/Me and Et/ Me- d_3 show almost equal relative sensitivities. From the comparison of DP 2-4 of higher alkylated compounds mixed with methyl derivatives shown in Figures 50 and 55, it can be seen that relative sensitivity of DP 2 of $(I_{Et}/I_{Me})/MR$ is 3.42 and $(I_{Pr}/I_{Et})/MR$ is 2.44 with certain uncertainty, hence the relative sensitivity of $(I_{Pr}/I_{Me})/MR$ could be expected to be close to $3.42 \cdot 2.44$, i.e., 8.3. Indeed, a value of 9.6, close to the multiplicative estimation, is experimentally found for $(I_{Pr}/I_{Me})/MR$ of DP2. The estimated and experimental values of DP 3 and DP 4 are 4.5/5.3 and 3.0/4.3, respectively, and thus also following the trend, while being lower than the real Rel. Int..

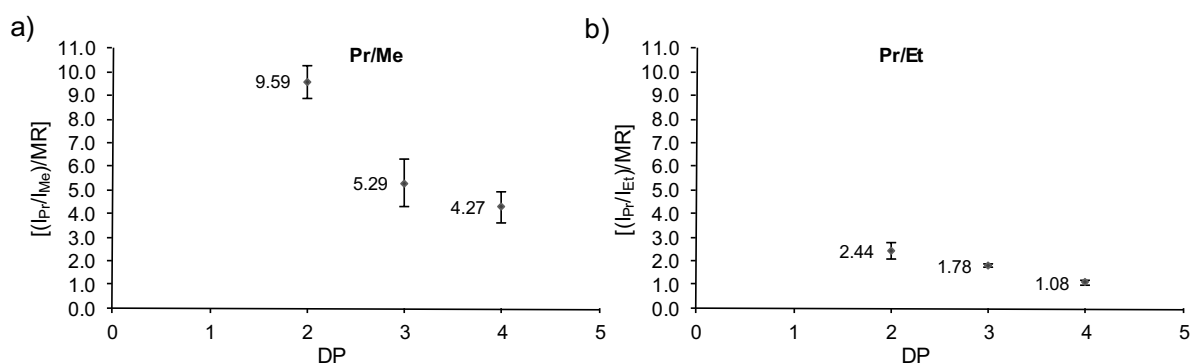


Figure 55. Relative sensitivity coefficients of complex mixtures with higher *O*-alkyl substituents; a) results from DP 2-4 of Pr/Me (Table 7), b) results from DP 2-4 of Pr/Et (Table 8). Each data point is the average of 9 measurements, total concentration of the sample is 10^{-5} M in methanol. Samples were measured under defined conditions in ESI-MS, (Sec. 7.3).

Hence it can be assumed that with the addition of each ‘CH₂’ to chain, as long as it is linear, relative sensitivity factor increases by a certain factor, which might be due to increase of hydrophobicity,⁶⁰ and then surface activity and sodium complexation ability. But due the increasing difference in molecular weight and hence decrease in electrophoretic mobility this multiplicative relation is no longer visible from DP 3. Hence to estimate the increase in relative sensitivity with each additional ‘CH₂,’ each DP has to be considered separately, to calculate the increase in relative sensitivity with increasing ‘ ΔC ’ on the oligomer unit.

Figure 56 shows the graphs for each DP, where, relative sensitivities are plotted against increasing number of C (considering the data from Table 19 and Figure 55). For DP 2-4 polynomial equations are obtained. It shall be tested if these equations could be used to normalize the Rel. Int. within each DP in oligomeric mixtures obtained from partially hydrolyzed per higher alkylated/methylated cellulose ethers to obtain the molar composition from Rel. Int. in ESI-MS. Considering Me_n as '0' and calculating for each oligomer with ΔC ($\text{Me}_{n-1}\text{Alk}_1$) within each DP, until the border case Alk_n . Application of these equations, however, have to be proved experimentally. By applying the correction factors from these equations the average DS of each DP should approximate to the overall sample DS calculated from the GC analysis of the constituents.⁷⁸ Application of these equations for Et/Me oligomeric mixtures is described in *chapter 5*.

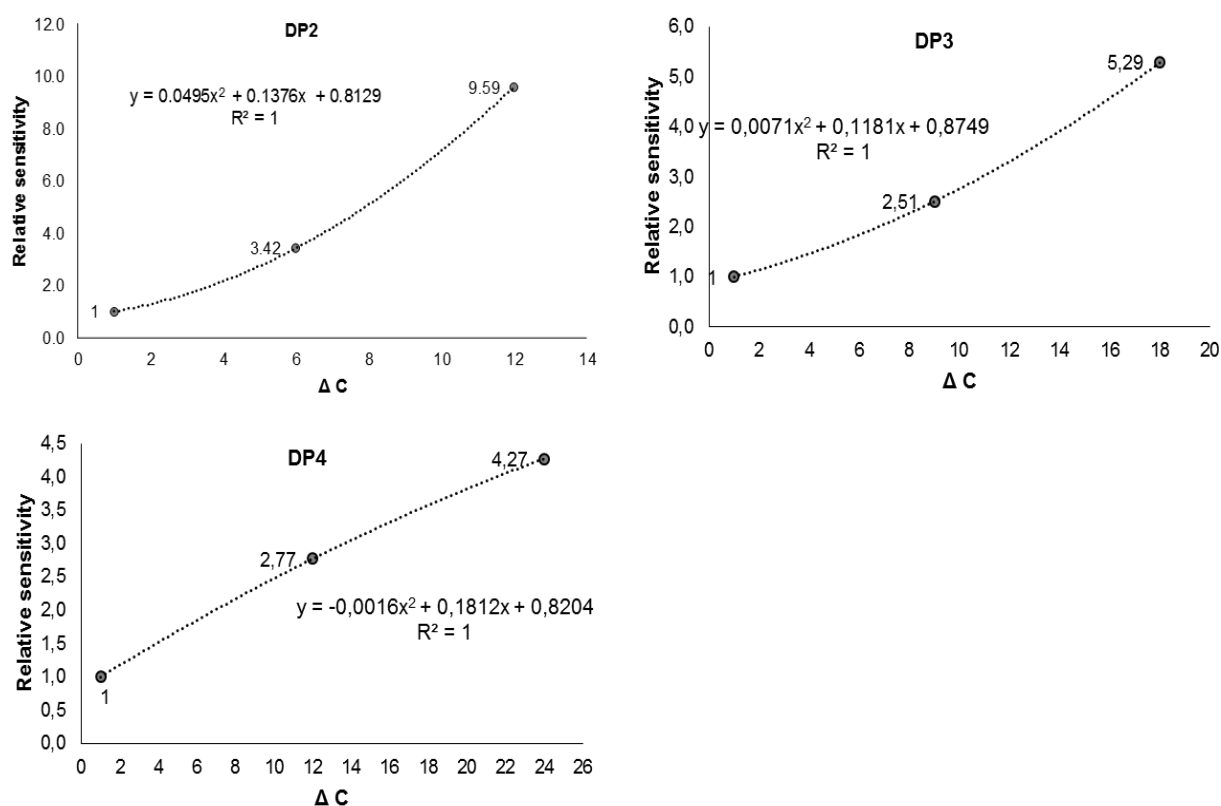


Figure 56. Equations for individual DP to obtain relative sensitivity with each additional 'CH₂' within each DP from methylated to propylated oligomers. Relative sensitivities are taken from CM (Table 19 and Figure 55).

4.6 Relative sensitivities of *O*-methoxyethyl related to *O*-alkyl-maltooligosaccharides

Methoxyethyl ethers are obtained in the analysis of HECs and HEMCs.^{92,93} For hydroxyalkyl derivatives of glucans in general, a strongly enhanced ion yield has been observed in ESI-MS causing severe problems in quantitative analysis. Thus, methoxyethyl ethers were included in this study (Tables 9, 10 and 11). By going from propyl to a methoxyethyl group, an additional oxygen is introduced which increases the number of complexation sites for sodium with the additional effect of conformational freedom. While the positions of the oxygens of the carbohydrate backbone are fixed because of the direct binding to the rigid pyranoside ring, hydroxy- or methoxyalkyl groups are flexible and can adapt the best conformation for interaction with sodium or other alkali ions.^{57,104} From Figure 57c it can be seen that relative sensitivity of DP 2 of $(I_{\text{MeOEt}}/I_{\text{Pr}})/\text{MR}$ is 3.29. From the relative sensitivities of DP 2 of Et/Me and Pr/Et, it can be expected that $(I_{\text{MeOEt}}/I_{\text{Et}})/\text{MR}$ would be around 6 which is indeed observed in Figure 57b. Relative sensitivity of DP 2 $(I_{\text{MeOEt}}/I_{\text{Me}})/\text{MR}$ can be estimated from $(I_{\text{MeOEt}}/I_{\text{Pr}})/\text{MR}$ (3.29) and $(I_{\text{MeOEt}}/I_{\text{Et}})/\text{MR}$ (5.60) to be close to 18.4. In Figure 57a it can be seen that $(I_{\text{MeOEt}}/I_{\text{Me}})/\text{MR}$ is approximately '20' scattering between 18-22. Here, DP3 also fits in such a multiplicative relation, however, DP4 does not. It is not clear what causes the deviation from DP 3, but the relative sensitivities between compounds with different chemistry can be used for estimation of molar composition as long as their relative sensitivity coefficients are known with defined uncertainty limits. There is clearly a certain type of multiplicative relation between relative sensitivity and chemistry, but due the deviation from DP 3, each type of mixture has to be studied and relative sensitivity coefficients must be defined for each DP with certain uncertainty limits. Similar to Figure 56, with increasing 'Δ C' on each oligomer unit within each DP, here a relationship with increasing number of 'CH₂' groups on the oligomer unit to relative sensitivity can be obtained for each DP. Figure 58 shows the relative sensitivity plotted against Δ C for each DP. The equations shown in Figure 58 could be used to normalize Rel. Int. for MeOEt/Me, MeOEt/Et and MeOEt/Pr

oligomeric mixtures to obtain the molar composition from Rel. Int. in ESI-MS, but it has to be experimentally proven.

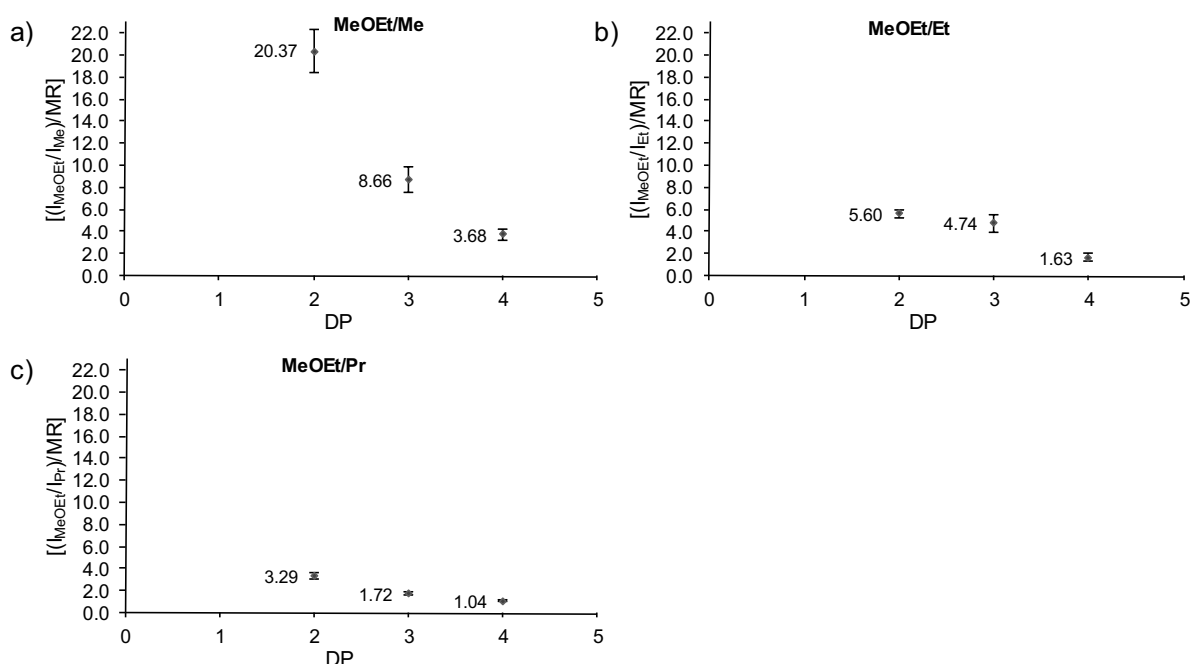


Figure 57. Relative sensitivity coefficients of mixtures of methoxyethylated compounds with methyl, ethyl and propyl oligosaccharides; a) results from DP 2-4 of MeOEt/Me (Table 9), b) results from DP 2-4 of MeOEt/Et (Table 10), c) results from DP 2-4 of MeOEt/Pr (Table 11). Each data point is the average of 9 measurements, total concentration of the sample 10^{-5} M in methanol. Measured under defined conditions see (sec. 7.3).

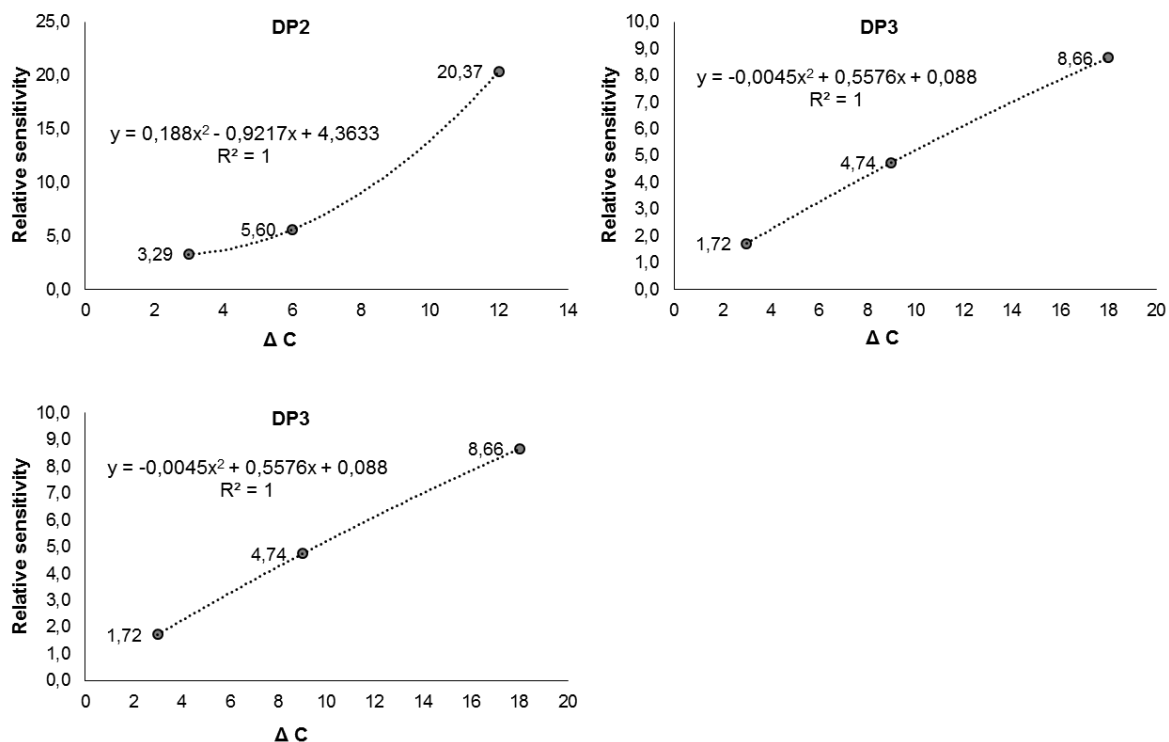


Figure 58. Equations for individual DP to obtain relative sensitivity with each additional O and CH_2 within each DP for MeOEt/Me, MeOEt/Et and MeOEt/Pr oligomers. Relative sensitivities are taken from CM (Figure 57).

4.7 Comparison of relative sensitivities of alkyl oligosaccharides obtained by syringe pump infusion or LC/MS

All the results presented up to now have been obtained by analyzing the sample solutions by syringe pump infusion. This means that all analytes are present at the same time and compete with each other to reach the outer layer/surface from bulk of the droplet. In contrast, by analyzing the sample with LC separation prior to ESI, compounds are fully or partly separated. Not only the components are separated prior to ESI, but also the spray dynamics⁴⁷⁻⁴⁹ like flow rate (increased flow rate) and solvent composition (when a gradient elution is used) are drastically changed. With the change of flow rate and depending on the vapor pressure of the solvent, temperature and flow of nebulizer gas has to be adjusted to obtain a stable spray. To conclude, whether the relative sensitivity coefficients obtained with syringe pump infusion change with the elimination of competition from other DPs, to check the influence of changed solvent composition and other instrumental parameters, the complex mixtures of Et/Me (CM 4), Pr/Me (CM 1), Pr/Et (CM 2), MeOEt/Me (CM 5), MeOEt/Et (CM 5) and MeOEt/Pr (CM 1) were selected from Tables 5 and 7-11, respectively) and were measured with LC-ESI-MS. Hence, by a comparison of relative sensitivity coefficients obtained from infusion from methanol solution by syringe pump, with those applying LC coupling, where acetonitrile/water (gradient) was applied, not only competition, but also other parameters change which might affect the results. In Figure 59 a and d it can be observed that relative sensitivity coefficients of Et/Me and Pr/Me CM are similar, both for syringe and LC-ESI-MS. Corresponding results were observed for Me-*d*₃/Me CM (4.1.4). Thus, it is concluded that, if parameters are set for a stable spray (temperature, flow rate, nebulizer gas flow) both in syringe and LC-ESI-MS or for BM/CM, relative sensitivity coefficients remain constant with certain uncertainty despite of using a different solvent.

However, for methoxypropyl glucans, gradient elution in HPLC has been shown to effect ionization yield.⁹¹ In this study, MeOEt/Alk also behaved different from the alkylated

mixtures. All the mixtures with MeOEt show a decrease in relative sensitivity ($I_{\text{MeOEt}}/I_{\text{Alk}})/\text{MR}$ with $\text{Alk} = \text{Me}, \text{Et}$ and Pr , when measured in LC-MS mode instead of syringe infusion (Figure 59). This is probably at least partly caused by a higher sodium complexation ability¹⁰⁴ of MeOEt compounds compared to the corresponding alkylated oligomers, which will favor the ion formation of these compounds over that of alkylated analogs, when competing for sodium in syringe pump infusions. In LC-ESI-MS all the components are eluted separately which avoids competition and hence gives higher chance for other analytes. Therefore, relative sensitivity coefficients decreased in LC/MS. For mixtures with Pr oligosaccharides, only the results from DP 2 can be evaluated, because propylated oligomers of higher DP only elute with a combination of acetonitrile/isopropanol from an RP C_{18} HPLC column. (For all the other CM a gradient of water/acetonitrile was applied, whereas, for CM in combination with Pr a gradient system with water/acetonitrile/isopropanol was used.) The mass spectra obtained from these non-polar solvents like acetonitrile/isopropanol could not be evaluated, since there was a lot of background noise and no sample peaks. DP 2 of Pr elutes earlier than DP 3-7 in a gradient elution which contains some water in the elution system. Hence a mass spectrum is obtained for DP 2 Pr with good S/N but not for higher DPs. From Figure 59d it can be observed that relative sensitivity coefficients for DP 2 ($(I_{\text{Pr}}/I_{\text{Me}})/\text{MR}$ and $(I_{\text{Et}}/I_{\text{Me}})/\text{MR}$ CM are independent on sample application by syringe pump infusion or LC.

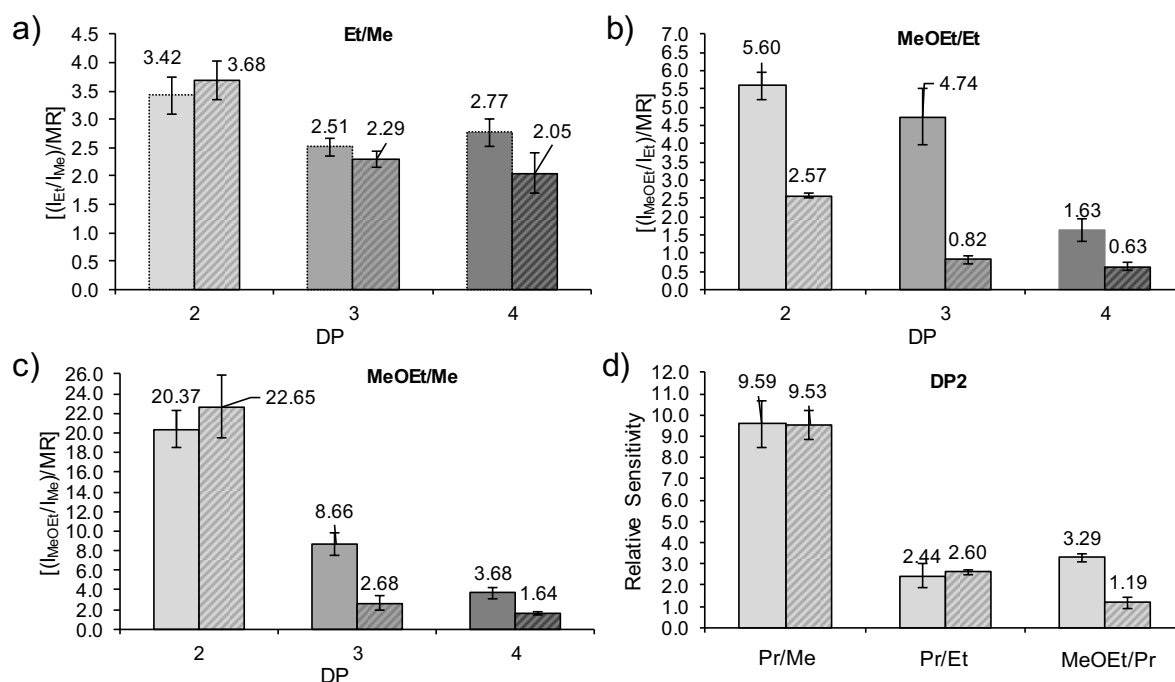


Figure 59. Relative sensitivities in comparison between syringe pump (solid fill) infusion and LC-ESI-MS (pattern fill) a) Et/Me CM 4 (Table 5), b) MeOEt/Me CM 4 (Table 9), c) MeOEt/Me CM 4 (Table 104) and d) sensitivity coefficients of DP 2 mixtures with propylated compounds CM 2,1 and 5 of Table 7, 8 and 11 respectively. Each data point is the average of 3 measurements, total concentration of the sample 10^{-5} M. Measured under defined conditions for LC see sec. 7.3.

4.8 Effect of total concentration

As described in 4.1.3, Tang and Kebarle¹¹⁵ reported the influence of total concentration of the sample on relative sensitivity coefficients. For Me- d_3 /Me mixtures total concentration did not influence relative sensitivity since both the components have similar surface activity and the difference observed at higher DPs was probably due to difference in electrophoretic mobility. To study the influence of total concentration on other types of CM, CM 4 Et/Me (Table 5), CM 2 Pr/Me (Table 7), CM 1 Pr/Et (Table 8), CM 5 MeOEt/Me (Table 9), CM 5 MeOEt/Et (Table 10) and CM 2 MeOEt/Pr (Table 11) were gradually diluted from a concentration of approximately 10^{-4} to 10^{-7} M (diluted 200 times until S/N is 2/1), to study the effect of total concentration of the sample on relative sensitivities. Figure 60 shows the mass spectra of MeOEt/Me with changing total concentration as an example. The results of concentration studies are shown for Pr/Me (Figure 61), Pr/Et (Figure 62), MeOEt/Me (Figure 63), MeOEt/Et (Figure 64) and MeOEt/Pr (Figure 65). Relative sensitivities of all CM

which differ in chemistry and hence surface activity are highly dependent on total concentration. As observed in the Figures, at the lowest measurable total concentration of 10^{-7} M, where, the concentration of individual DP 2-4 in each CM is approximately around 10^{-9} M, relative sensitivities of DP 2-4 are 2.33, 2.20 and 2.03 (Pr/Me), 1.21, 1.51 and 1.02 (Pr/Et), 3.53, 2.14 and 0.77 (MeOEt/Me), 1.77, 1.58 and 0.44 (MeOEt/Et) and 1.59, 1.29 and 0.29 (MeOEt/Pr). When the values are compared to the relative sensitivities from Figures 55 and 57, there is a decrease in relative sensitivity coefficients. The decrease of relative sensitivity coefficients with increasing DP means a reduction in electrophoretic mobility, however, for all mixtures with MeOEt the relative sensitivity coefficients show an additional strong drop with DP. For DP 4 ($I_{\text{MeOEt}}/I_{\text{Alk}}$)/MR was even <1 (Me: ca. 0.8, Et: ca. 0.5, Pr: ca. 0.3). From a concentration of approximately 10^{-7} to 10^{-4} M the absolute ion intensities increase and are saturated at a concentration range of 10^{-6} to 10^{-5} M. Unlike, the relative sensitivities of Me- d_3 /Me mixtures the relative sensitivities of all the other mixtures are highly dependent on concentration of the sample. As discussed by Tang and Kebarle¹¹⁵ the differences due to surface effects were decreased with decrease in total concentration in these chemically different CM. Although, the effects in sensitivity raised by differences of analytes with respect to surface activity and electrophoretic mobility are reduced by dilution, the interpretation of results suffers from high scattering and interference from background noise. For quantitative evaluation relative sensitivity coefficients must be determined at concentration higher than 10^{-5} M, but care must be taken to keep the concentration below cluster formation. Sometimes both sodium and potassium adducts were observed in the mass spectra, normally the intensity from these two peaks can be combined to interpret relative sensitivities. But to avoid any possible errors in the interpretation the ESI-MS system was flushed with a solution of methanol/water (50/50) by syringe pump for one hour before measuring which avoided potassium adducts.

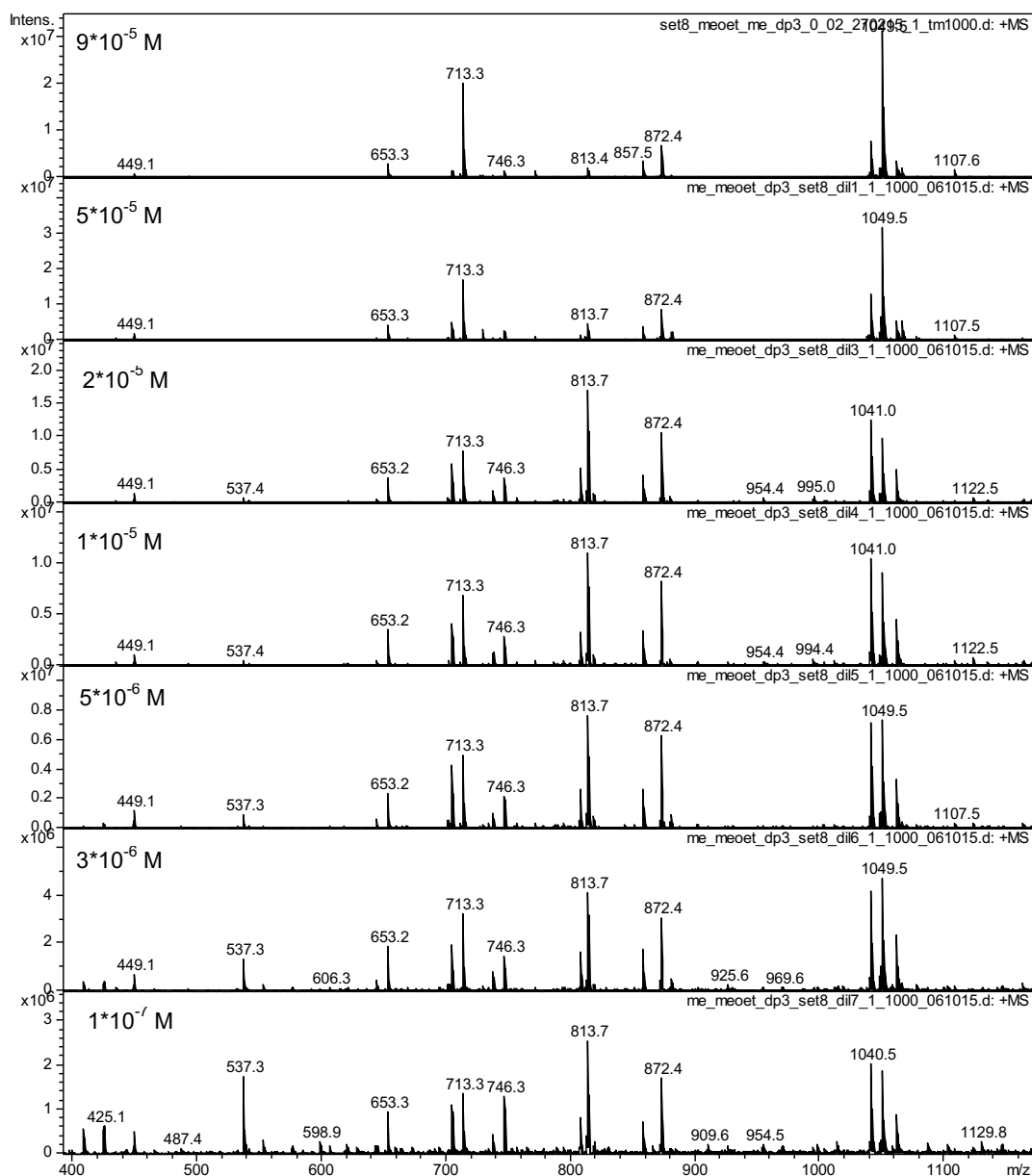


Figure 60. ESI-MS spectra of MeOEt and Me maltooligosaccharides from a concentration of 10^{-4} to 10^{-7} M in methanol, measured in positive ion mode as sodium adducts conditions see *sec. 7.3*. To show the change of peaks with total concentration, only the section up to DP 3 MeOEt is shown. (For full spectra see appendix). 449.2, 653.3 and 857.5 are peaks from Me DP 2, DP 3 and DP 4, respectively, 713.3 and 1049.5 are from DP 2 and DP 3 MeOEt. All the additional peaks seen in the first mass spectrum are from doubly and triply charged peaks of higher DPs. With the decrease of concentration intensity of doubly and triply charged peaks and background noise increases. Evaluation see Figure 63.

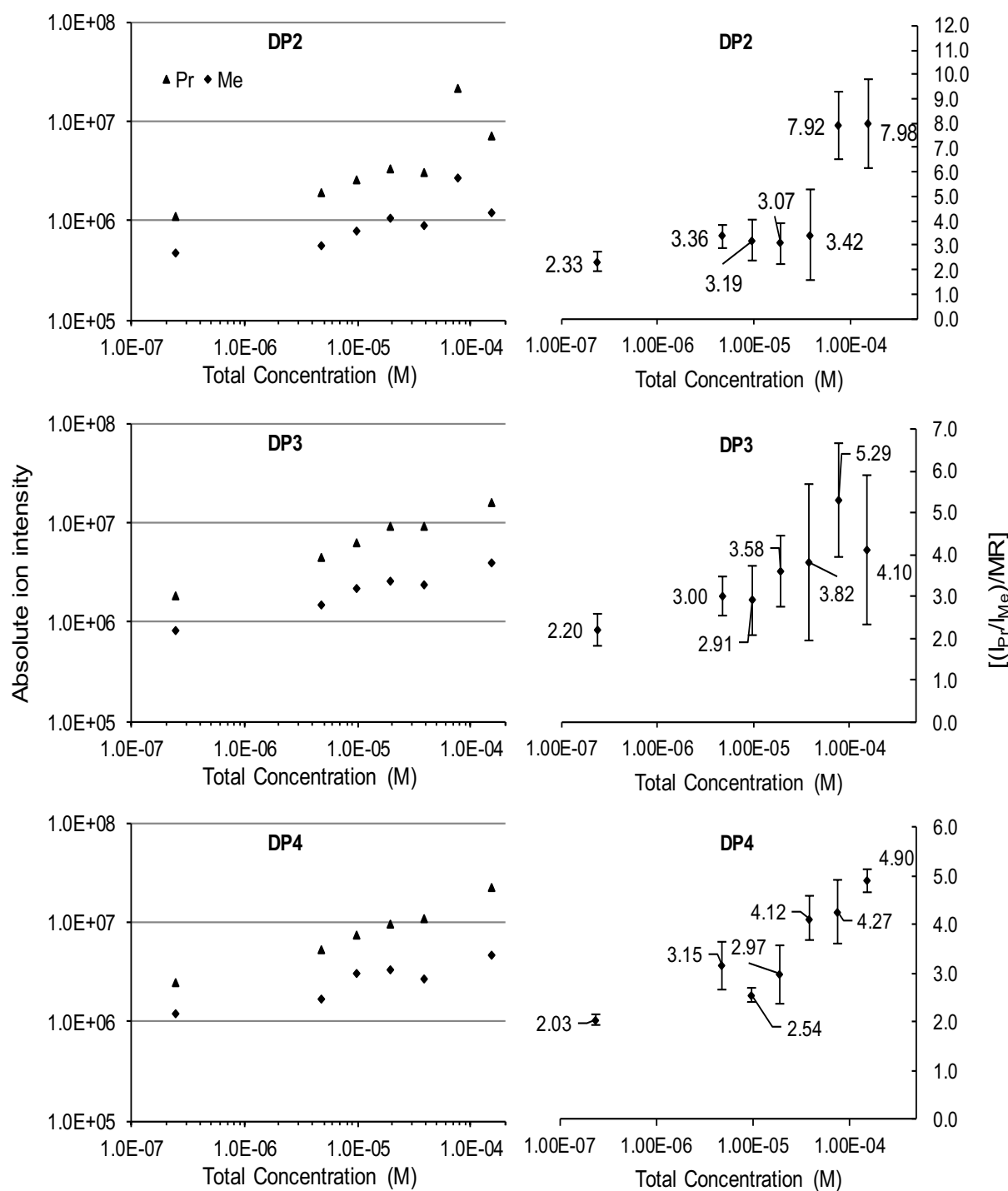


Figure 61. Pr/Me CM 2 of Table 7; measured at varying total concentration of CM while keeping the MR constant; conditions see *sec.* 7.3. Left-absolute ion intensities (normalized to an equimolar ratio), right-relative sensitivities, at different total concentrations; each data point shows the standard deviation of three measurements ($n=3$).

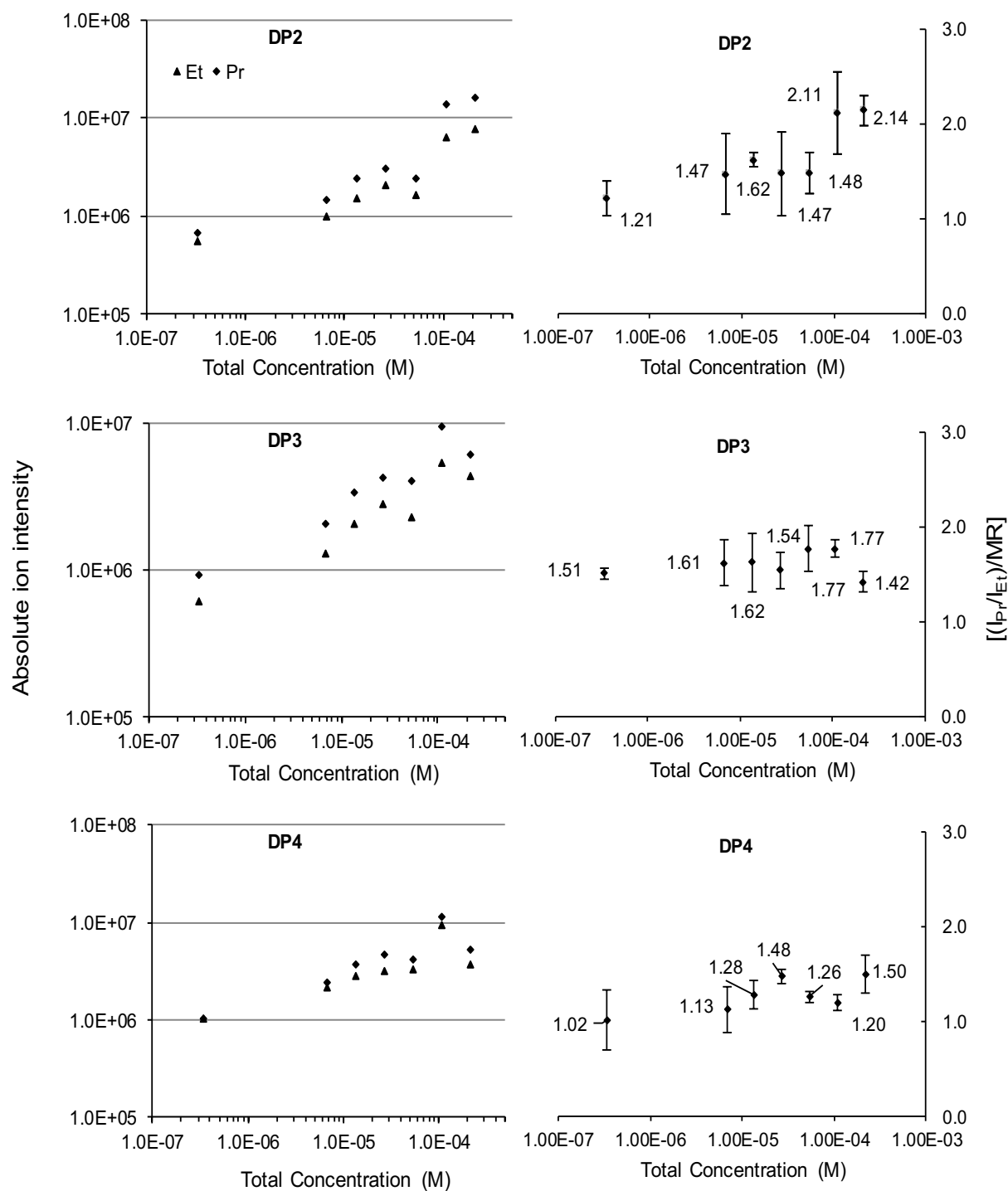


Figure 62. Pr/Et CM 1 of Table 8; measured at varying total concentration of CM while keeping the MR constant; conditions see *sec. 7.3*. Left-absolute ion intensities (normalized to an equimolar ratio), right-relative sensitivities, at different total concentrations; each data point shows the standard deviation of three measurements ($n=3$).

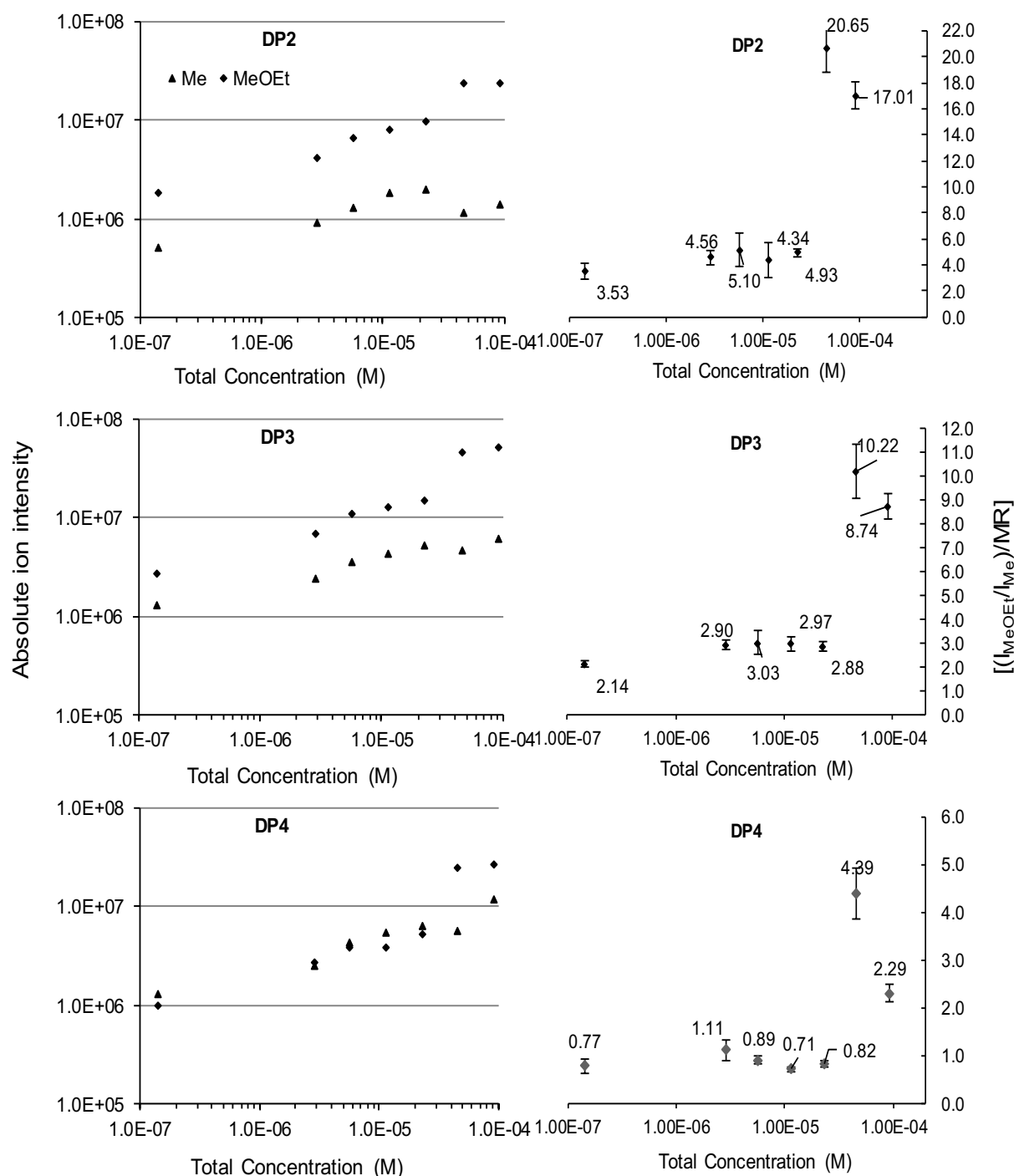


Figure 63. MeOEt/Me CM 5 of Table 9; measured at varying total concentration of CM while keeping the MR constant; conditions see *sec. 7.3*. Left-absolute ion intensities (normalized to an equimolar ratio), right-relative sensitivities, at different total concentrations; each data point shows the standard deviation of three measurements ($n=3$).

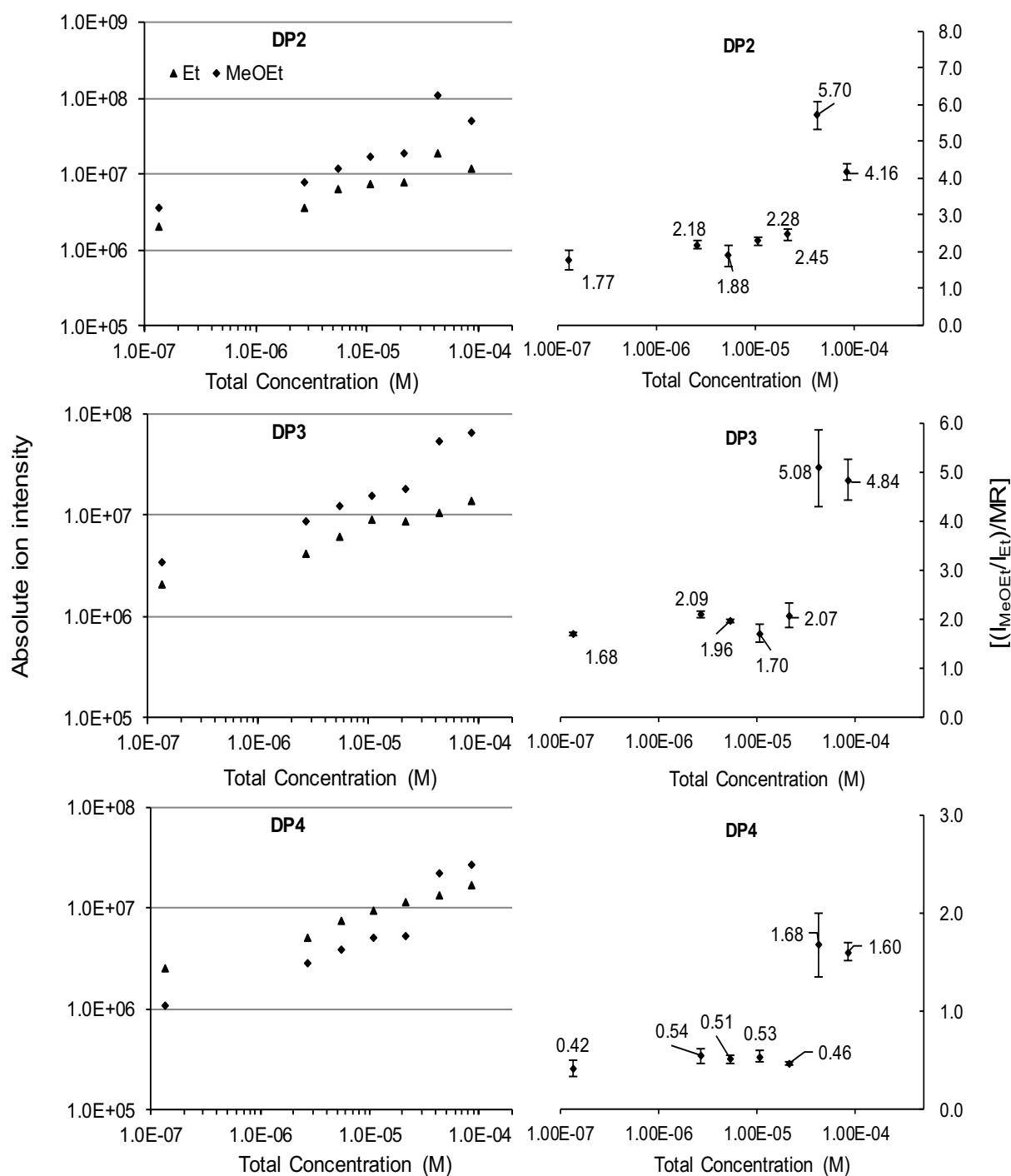


Figure 64. MeOEt/Et CM 5 of Table 10; measured at varying total concentration of CM while keeping the MR constant; conditions see *sec. 7.3*. Left-absolute ion intensities (normalized to an equimolar ratio), right-relative sensitivities, at different total concentrations; each data point shows the standard deviation of three measurements ($n=3$).

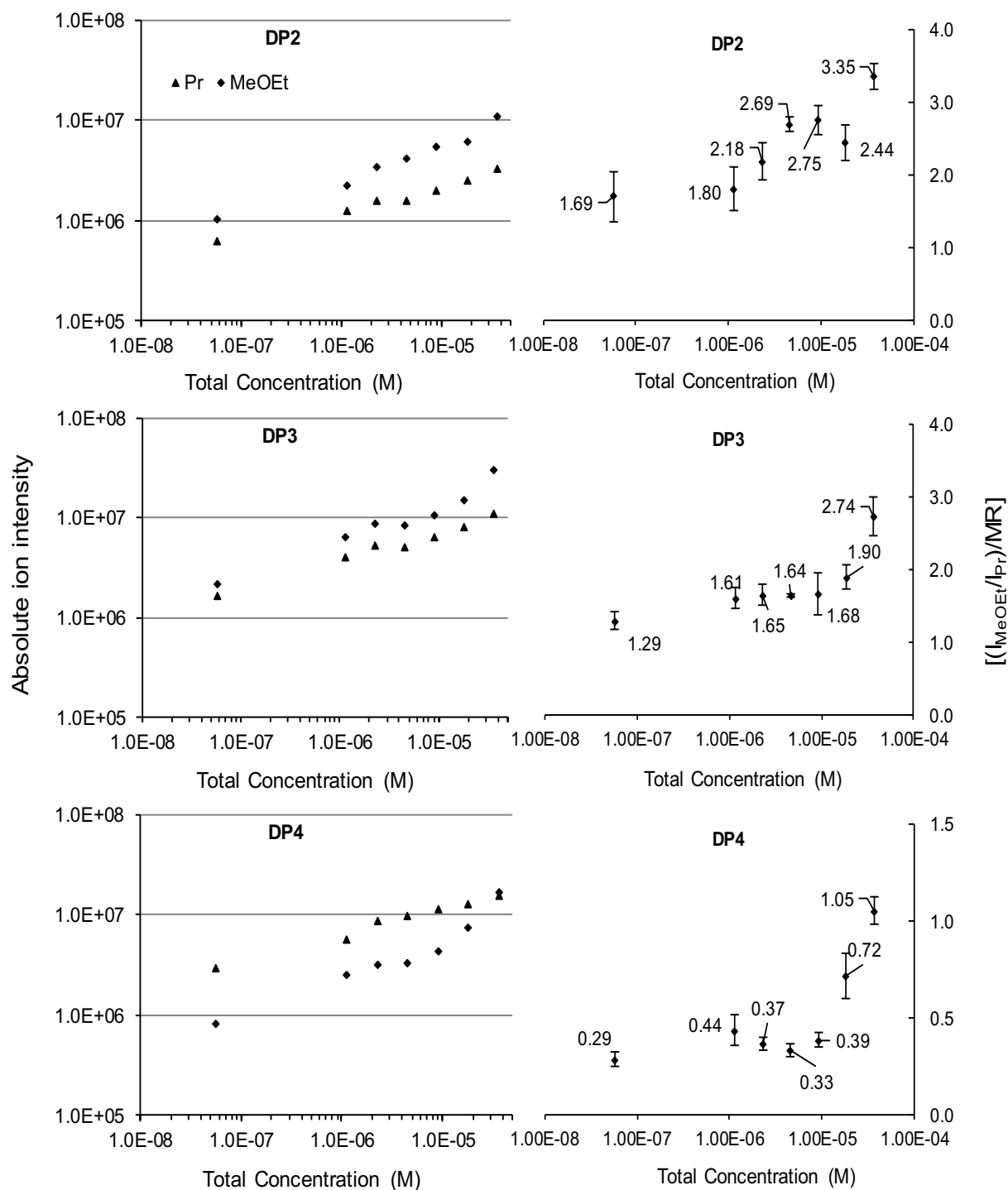


Figure 65. MeOEt/Pr CM 1 of Table 11; measured at varying total concentration of CM while keeping the MR constant; conditions see *sec. 7.3*. Left-absolute ion intensities (normalized to an equimolar ratio), right-relative sensitivities, at different total concentrations; each data point shows the standard deviation of three measurements ($n=3$).

4.9 Comparison between ESI and nano-ESI-MS

As described in 4.1.5 discrimination of Me- d_3 /Me oligosaccharides of DP 5 and DP 6 can be overcome by applying nano-ESI-MS. Since much smaller droplets are produced in nano-ESI-MS surface and electrophoretic effects on ion yield are eliminated⁹⁴⁻⁹⁷. Similarly, all the other CM were measured in nano-ESI-MS, equipped with ion trap or with orbitrap. Results from Et/Me, Pr/Me, Pr/Et, MeOEt/Me, MeOEt/Et and MeOEt/Pr are shown in Figures 66-71, respectively. As expected, relative sensitivity coefficients decreased by reducing the droplet size, but did not reach 1.0 as in case of Me- d_3 /Me. Surprisingly, the values obtained from nano-ESI-MS were comparable to the values obtained in ESI-MS at a concentration of 10^{-7} M. Hence, both parameters, reducing the droplet size and reduction of population in droplet bulk show similar effects on relative sensitivity coefficients.

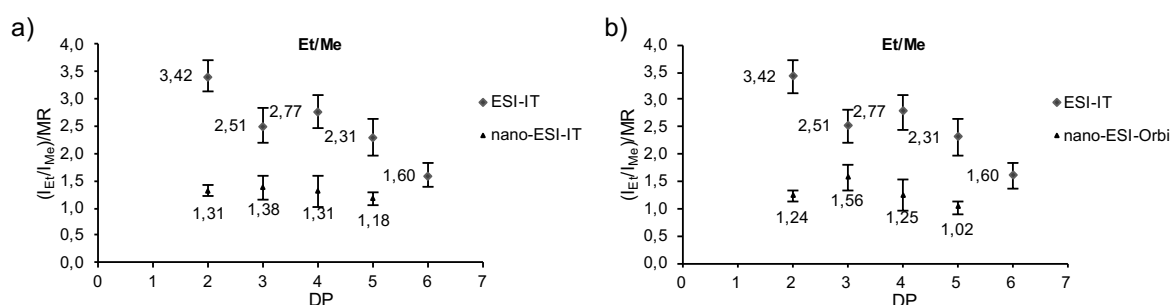


Figure 66. a) Comparison of average relative sensitivities of CM 4, 5, and 6 from Table 5, measured in ESI-IT-MS and nano-ESI-IT-MS. b) Comparison of average relative sensitivities of CM 4, 5, and 6 from Table 5, measured in ESI-IT-MS and nano-ESI-Orbitrap-MS. Samples were dissolved in methanol at a total concentration of ca. 10^{-6} M, measured under the conditions see *sec. 7.3* for ESI-MS and nano-ESI-MS, respectively.

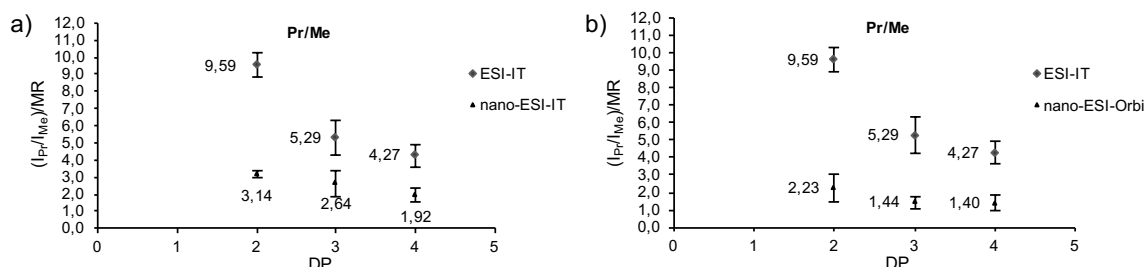


Figure 67. a) Comparison of average relative sensitivities of all CM in Table 7 measured in ESI-IT-MS and nano-ESI-IT-MS. b) Comparison of average relative sensitivities of all CM in Table 7 measured in ESI-IT-MS and nano-ESI-Orbitrap-MS. Samples were dissolved in methanol at a total concentration of ca. 10^{-6} M, measured under the conditions see *sec. 7.3* for ESI-MS and nano-ESI-MS, respectively.

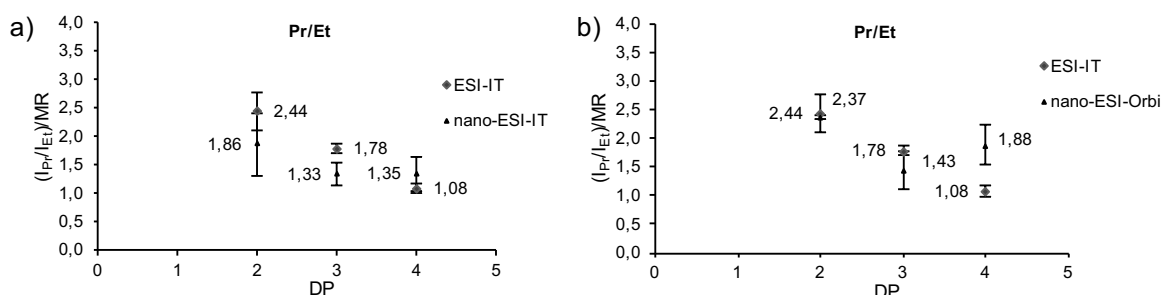


Figure 68. a) Comparison of average relative sensitivities of all CM in Table 8 measured in ESI-IT-MS and nano-ESI-IT-MS. b) Comparison of average relative sensitivities of all CM in Table 8 measured in ESI-IT-MS and nano-ESI-Orbitrap-MS. Samples were dissolved in methanol at a total concentration of ca. 10^{-6} M, measured under the conditions see *sec. 7.3* for ESI-MS and nano-ESI-MS, respectively.

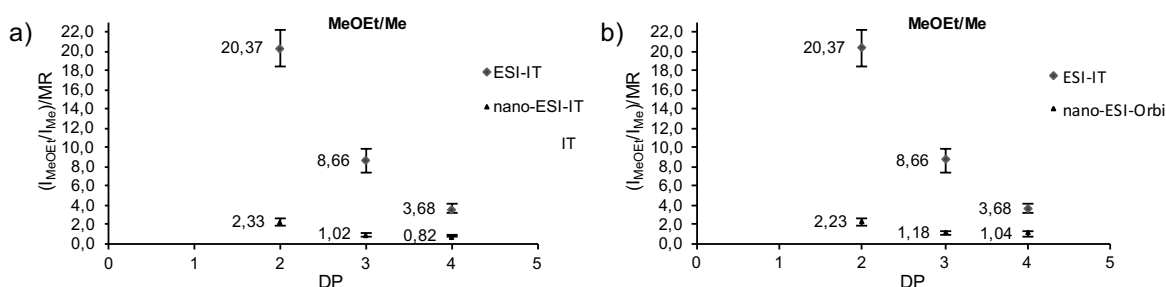


Figure 69. a) Comparison of average relative sensitivities of all CM in Table 9 measured in ESI-IT-MS and nano-ESI-IT-MS. b) Comparison of average relative sensitivities of all CM in Table 9 measured in ESI-IT-MS and nano-ESI-Orbitrap-MS. Samples were dissolved in methanol at a total concentration of ca. 10^{-6} M, measured under the conditions see *sec. 7.3* for ESI-MS and nano-ESI-MS, respectively.

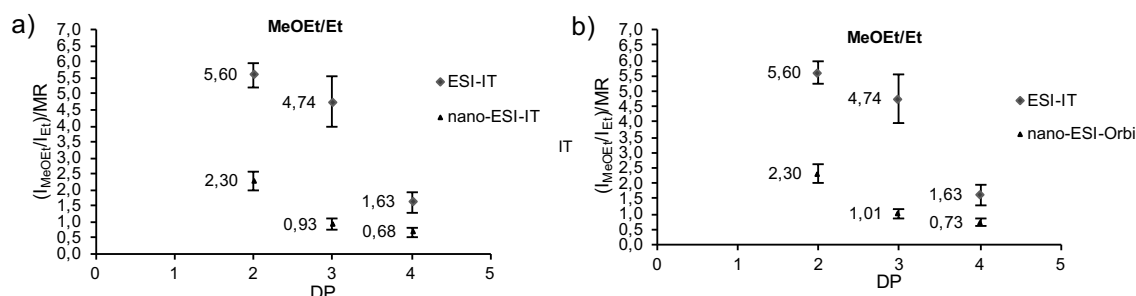


Figure 70. a) Comparison of average relative sensitivities of aCM 3-5 in Table 10 measured in ESI-IT-MS and nano-ESI-IT-MS. b) Comparison of average relative sensitivities of CM 3-5 in Table 10 measured in ESI-IT-MS and nano-ESI-Orbitrap-MS. Samples were dissolved in methanol at a total concentration of ca. 10^{-6} M, measured under the conditions see *sec. 7.3* for ESI-MS and nano-ESI-MS, respectively.

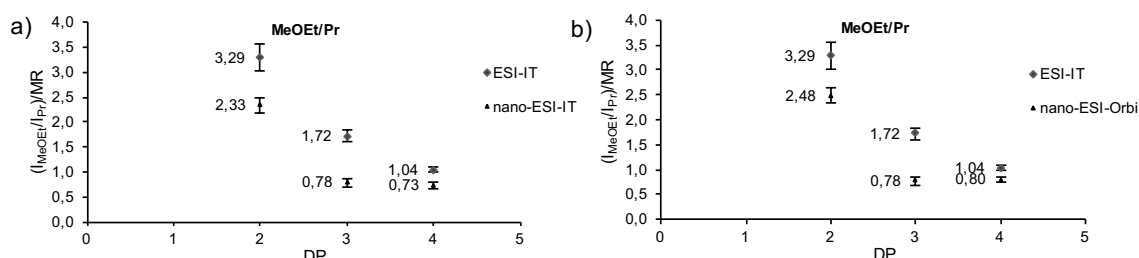


Figure 71. a) Comparison of average relative sensitivities of all CM in Table 11 measured in ESI-IT-MS and nano-ESI-IT-MS. b) Comparison of average relative sensitivities of all CM in Table 11 measured in ESI-IT-MS and nano-ESI-Orbitrap-MS. Samples were dissolved in methanol at a total concentration of ca. 10^{-6} M, measured under the conditions see *sec. 7.3* for ESI-MS and nano-ESI-MS, respectively.

4.10 Comparison between non-labeled and labeled compounds

As described in 4.1.6 introducing a charge on the oligomer unit can enhance the detection sensitivity. Since the charge is provided by the tag, there is no discrimination from sodium complexation ability.¹⁰⁴ All the CM were reductively aminated¹¹² with *m*ABA and measured with LC/MS in negative ion mode. Introduction of *m*ABA increases the mass of the analytes by '97' units. Since we used ion trap as mass analyzer, selection of target mass is critical (*see* 4.1.3) at and above DP 4 of labeled oligomers of Et, Pr, and MeOEt. Use of a target mass of '1500' gave good peak intensities of the higher oligomers. But corresponding Me oligomers should be measured at a target mass of '1000' for comparison with other results. Hence to allow comparison and eliminate the effect from different target masses only results of DP2 and DP 3 are presented. Results for DP 2 and DP 3 of Et/Me, MeOEt/Me and MeOEt/Et are given in Figure 72. As expected, the relative sensitivity coefficients decreased with the introduction of a charge, for samples with similar concentration as unlabeled samples (10^{-5} M), but anyhow do not give a 1:1 response for an equimolar mixture. Interestingly, the "switch" from sodium adducts to negatively charged analytes leveled the discrimination of Me against MeOEt from factor '22.65' in unlabeled to '1.89' in labeled mixtures.

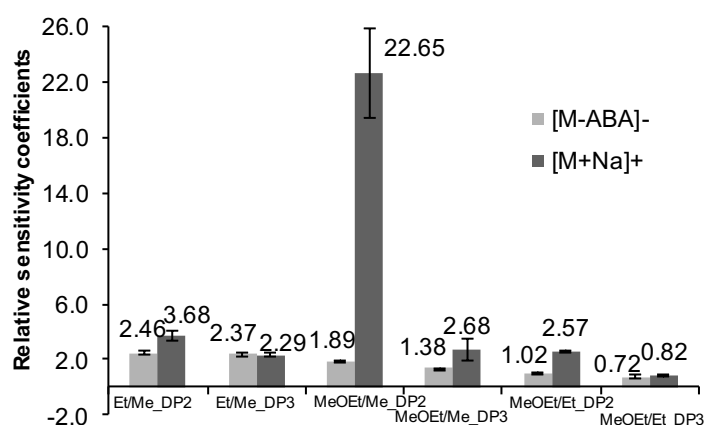


Figure 72. Comparison of relative sensitivities of unlabeled and labeled oligomers (DP 2-3; Et/Me, MeOEt/Me and MeOEt/Et) in positive and negative ion mode, respectively, measured by LC-ESI-MS. Total concentration of the sample 10^{-5} M; each data point is an average of 3 measurements; conditions *see sec. 7.3*.

5. Application of Me- d_3 /Me and Et/Me sensitivity coefficients

As given in Table 19, relative sensitivity coefficients of Me- d_3 /Me and Et/Me from DP 2-6 have been studied in detail. Within the concentration range tested for Me- d_3 /Me, molar composition can be calculated from relative ion intensities in ESI-MS, the difference observed from DP 5 can be overcome by labeling and hence the analysis can be extended at least up to DP 6. Therefore, Rel. Int. obtained from a complex oligomeric mixture of Me- d_3 /Me cellulose ethers after partial hydrolysis and labeling, can be used without any correction factors to calculate the average DS of each DP and the experimentally determined substituent distribution within each DP will match the calculated distribution for randomly substituted compounds. This has been previously proved by many researchers.⁸⁹ Similarly, for Et/Me the application of relative sensitivity coefficients for the calculation of molar ratio from relative ion intensities should be tested. Due to higher difference in chemistry the difference was not levelled off by labeling in this case. But as described in *chapter 3*, these model compounds are only the extreme cases in the analysis of per-alkylated partially hydrolyzed 1,4-glucan ethers. To obtain the relative sensitivities of ‘in between cases’ for each DP as shown in Figure 20, the relative sensitivities from border cases in each DP might be used, as described in *sec. 4.5*. Relative sensitivities of ‘in between cases’ i.e., with each additional ‘CH₂’ (ΔC), for each DP were calculated from the polynomial equations given in Figure 56 which were obtained from border cases of individual DP. By applying the thus obtained relative sensitivity coefficients of Et/Me oligomers and correcting Rel. Int., the average DS of each DP (obtained by partial hydrolysis of MEC) should match the overall DS of the sample (usually determined by GC) and the calculated and experimental distribution profiles should be similar.

To test the applicability of Et/Me sensitivity coefficients, a MC sample (MC 5 from Unterrieser’s thesis¹³⁶) was chosen. The DS is 2.01 and molar portions c_0 , c_1 , c_2 and c_3 are 3.19, 21.16, 47.33 and 28.32 Mol%, respectively. Distribution of the substituents can be

calculated from this data. A comparison of experimental (ESI) and calculated (based on monomer data) substituent distribution in DP 2-3 after perdeuteromethylation of MC 5 is given in Figure 73. The distribution profile of perethylated MC 5 should be similar to perdeuteromethylated MC 5. To test the application of Et/Me sensitivity coefficients to calculate DS and substituent distribution, perethylated MC 5 was partially hydrolyzed and measured by ESI-MS, mass spectrum of which is shown in Figure 20. DS and DP distribution profiles have been calculated for DP 2-6. The comparison of DS values from DP 2-6 before and after application of correction factors according to the relative ion intensities is shown in Figure 74. Similarly, comparison of distribution profiles in DP 2-6 before and after application of corrections factors is shown in Figure 75.

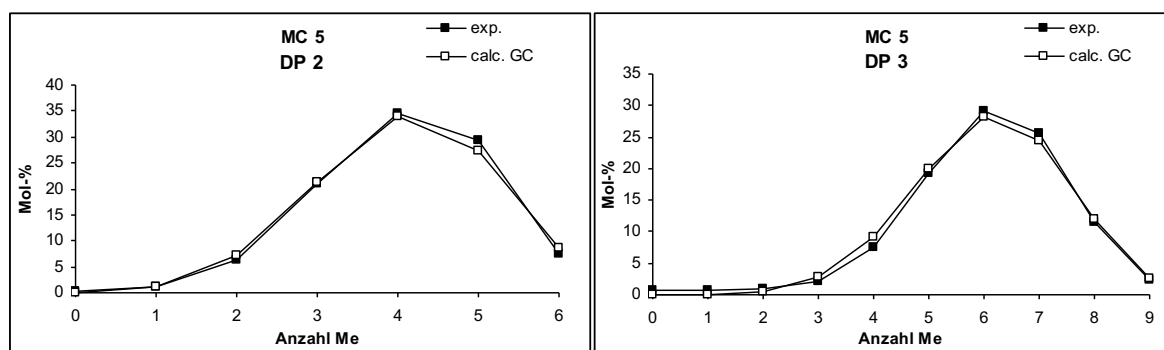


Figure 73. Comparison of calculated (GC) and experimental (ESI-MS) distribution profiles of substituents (Me) distribution in DP 2-3 of perdeuteromethylated MC 5. Source: Unterrieser's thesis.¹³⁶

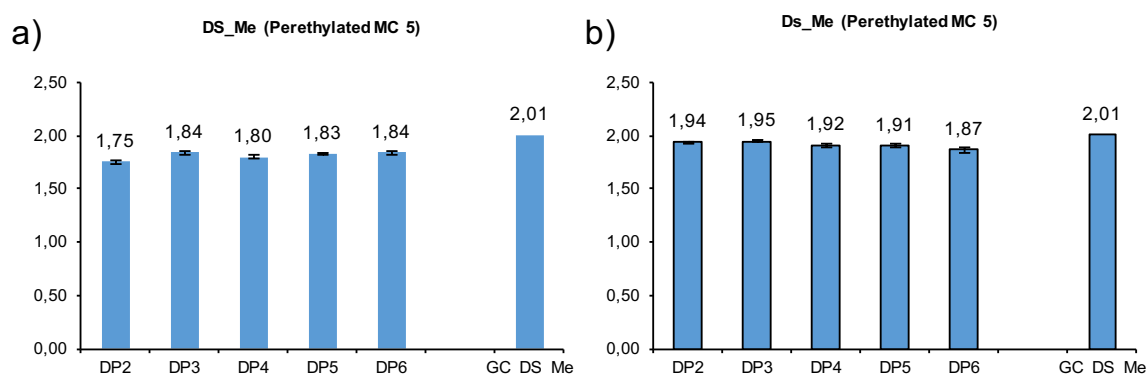


Figure 74. DS: DP 2-6 determined from the ESI-MS mass spectrum of partially hydrolyzed perethylated MC 5 in comparison to DS of the sample MC 5 determined by GC analysis. a) DS of DP 2-6 before applying Et/Me correction factors b) DS of DP 2-6 after applying Et/Me correction factors obtained from relative sensitivity coefficients.

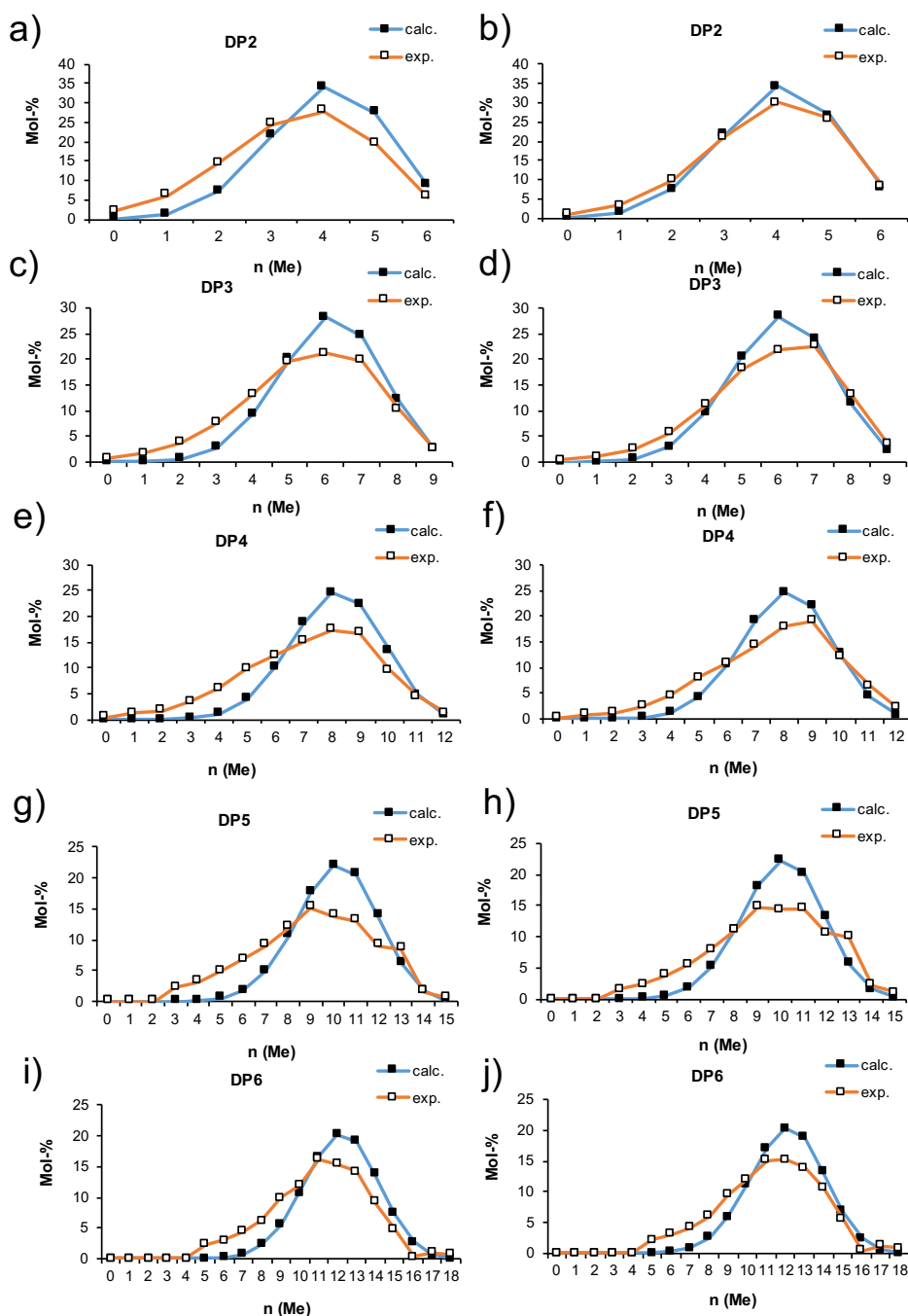


Figure 75. Comparison of calculated to experimentally (ESI-MS) obtained substituent distribution (Me) in DP 2-6, of partially hydrolyzed perethylated MC 5. Measured by syringe pump infusion in methanol, conditions (see 7.3); a, c, e, g and i show the distribution in DP 2-6, respectively, before correcting the Rel. Int.; b, d, f, h and j shows the distribution in DP 2-6, respectively, after applying Et/Me correction factors obtained from relative sensitivity coefficients.

From Figure 74 it can be observed that by application of correction factors the DS of DP 2-6 becomes closer to the independently determined average DS, however, it still deviates by 0.05- 0.14. By applying corrections factors to Rel. Int., experimentally (ESI-MS) obtained substituent distribution of DP 2 approximates calculated distribution. With the increase of DP, however, there is an increase in the distortion from the calculated profile, also DS is decreasing with increasing DP. One reason could be that depending on the position of the substituents, sodium complexation ability⁵⁷ might differ. This might be influenced by the configuration of the glucosidic linkage. Cellooligomers are β -linked, while maltooligomers are α -linked. Furthermore, the mutual suppression of analytes is much more complex, so that a simple correction by type of response factors cannot probably not be applied. As unlike ‘border cases’, where C-2,3,6 are completely alkylated, there is a significant variety in substitution positions for ‘in between’ cases. Therefore, better results might be observed after labeling the partially hydrolyzed MEC and then measuring in ESI-MS, but for labeled compounds new sensitivity coefficients have to be defined. As seen in Figure 72, sensitivity coefficients change after labeling. However, these results can be considered as preliminary and further experiments to test the applicability of sensitivity coefficients have to be performed to confirm the output of the data.

6. Summary and outlook

ESI MS is a breakthrough technique in the field of protein and polysaccharide analysis. When the method was first proposed by Fenn, he illustrated biomolecules as ‘flying elephants’. As it produces single molecular ions of large biomolecules, without destroying the structure, it is a quick technique for qualitative analysis. Quantitative analysis, however, is hampered by various chemical, physical and parametrical influences of analyte, solvent and instrument. In the field of polysaccharide analysis, the determination of substitution pattern over the chains of modified polymers is important to understand their properties such as film formation or thermoreversible gelation. To determine the substitution pattern the polysaccharide is depolymerized by partial hydrolysis to yield a complex oligomeric mixture. The molar composition, i.e. the DS profile for each particular DP, is important for pattern evaluation. Within a DP, however, depending on the type of derivative there are components of different chemistry, for example *O*-methyl-*O*-ethyl ethers with different number of each type of substituent. These substituents cause different ionization yields of analytes. Hence, the data from relative intensities cannot be converted into molar ratio. To increase the applicability of ESI-MS for quantitative evaluation of chemically different analytes, we determined the concentration-dependent relative ionization efficiencies of chemically different oligosaccharides, measured as sodium adducts in ESI, and to estimate coefficients for correction of intensities, if possible.

In the first part of the project uniform derivatives of β -cyclodextrin (methylated, deuteromethylated, ethylated, propylated and methoxyethylated β -cyclodextrin) were prepared. By partial hydrolysis β -CD, maltooligomers from DP 1-7 were available. Composition with respect to individual DP was determined and standard mixtures with desired composition were prepared. To have accurate reference data with respect to the real composition of each sample used for quantitative MS studies, the final sample solutions were

labeled with *m*ABA and analyzed by HPLC/UV up to 3 times. Standard deviation of this determination was in the range of 0.02 to 0.4 %. Beside these ‘complex mixtures’ (CM), ‘binary mixtures’ (BM) of only two components of same DP, but different chemistry were prepared from the isolated oligosaccharides. First, Me-*d*₃/Me mixtures were evaluated to understand the ‘rules’ oligomeric mixtures follow in ESI-MS. It was found that relative ionization efficiencies of these chemically equal isotopomers are not significantly influenced by total concentration of sample solution (10^{-9} to 10^{-5} M), molar ratio, whether applied as BM or CM, or whether infused by syringe pump (samples measured in methanol) or LC (samples measured in ACN/H₂O) using different solvents. But a suppression for Me-*d*₃ by Me was observed at DP ≥ 5 . One reason might be the difference in electrophoretic mobility, arising from increasing differences in molecular weight. To overcome this discrimination nano-ESI has been applied, which reduces the initial droplet size and thus also the number of Coulomb explosions (consecutive droplet fissions) also prone to discrimination due to surface activity. In fact, the difference in relative sensitivity for DP 5 and 6 were leveled. Also introducing a charged tag by labeling the maltooligosaccharides at their reducing end was appropriate to overcome the discrimination found for the non-labeled sodium adducts. Labeling influences both: ionization and chemistry and thus surface activity.

In the next step, studies were extended to chemically more different compounds. To study the effect of increasing chain length (Me, Et, Pr) on oligomer unit, mixtures with increasing chemical difference (Et/Me, Pr/Me and Pr/Et) were prepared. These mixtures were analyzed under defined conditions to investigate the inter-dependence of relative ionization efficiencies on the type of substituent. At a total concentration range (10^{-5} to 10^{-4} M) where the absolute ion intensities are saturated, the relative ion intensities, normalized to an equimolar mixture remained constant regardless of molar ratio of measurement, BM or CM. Provided the target mass was properly adjusted, it also made no difference whether sample

solutions were infused by syringe pump, where, methanol was used as solvent or by LC/MS coupling, where ACN/H₂O, with a gradient elution was used as solvent, provided the temperature, pressure and flow of the nebulizer gas was properly adjusted depending on the solvent and flow rate. But unlike for Me-*d*₃/Me, relative ion yields are highly dependent on total concentration due to saturation effect and difference in polarity and thus surface activity for the higher alkylated analogs. Considering only DP 2, relative ion intensities from Et/Me to Pr/Me increased approximately 3 times (3.4→9.6), which showed a multiplicative relation (3.4·2.4) from the relative ion intensities observed for Pr/Et DP2 (2.4). These relative ion intensities are decreasing with DP, and from DP 3 this multiplicative relationship can no longer be seen probably due to an additional effect of increasing molecular weight. Therefore, within each DP, certain type of relation depending on the increasing ΔC with each additional 'CH₂' can be assumed. From the relative ion intensities obtained from these mixtures, graphs were plotted for each DP with Me_nPr₀, Me_{n-1}Pr₁.....Me₀Pr_n, from these graphs polynomial second order equation are obtained. From these equations 'relative sensitivity coefficients' for Alk/Me (Alk= Me, Et and Pr) were calculated for each DP and were applied to ethyl methyl celooligomers to find out whether the real molar composition can be obtained from Rel. Int. in ESI-MS. The DS improved with the correction factors close to the real DS of the sample for DP 2, but did not match the sample DS and profile with increasing DP. This might due the differences in the sodium complexation of α and β glucans or or more complex suppression effects depending on concentrations of these multi-component mixture.

Later, due to the strong influence of additional oxygen atoms, mixtures with methoxyethyl (MeOEt) were also prepared, resembling permethylated hydroxyethyl starches or, more general, glucans. MeOEt/Me, MeOEt/Et and MeOEt/Pr were also analyzed similar to Alk/Me mixtures. Again, at a total concentration range (10⁻⁵ to 10⁻⁴ M) where the absolute ion intensities are saturated, the relative ion intensities became constant. Relative ion intensities,

however, were highly dependent on total concentration and decreased when analyzed by LC/MS. The reason might be due to the higher sodium complexation ability of MeOEt compounds and stronger suppression effects in syringe pump infusion, compared to LC/MS analysis where all the analytes are eluted separately. Relative sensitivities of DP2 MeOEt/Pr, MeOEt/Et and MeOEt/Me are 3.3, 5.6 and 20.4 respectively. Here also certain type of multiplicative relationship is seen for DP2, which is no longer visible from DP3. Hence, similar to Alk/Me here also for each DP graphs have been plotted with increasing ΔC from MeOEt/Pr to MeOEt/Et to MeOEt/Me, second order polynomial equations have been obtained. By introduction of a charged tag the relative sensitivity coefficient of MeOEt/Me for DP2 reduced from approximately 22.7 to 1.9 independent on concentration.

When Alk/Me and MeOEt/Alk CM mixtures were measured by nano-ESI-MS relative ion intensities approximated the value of molar ratio (MR), scattering around 1.3 for Et/Me (for MR 1), while the decrease with DP was no longer relevant. Mixtures with MeOEt more or less showed similar ion intensities and were decreasing with DP (DP 2-4: 2.3, 0.8-1, 0.7-0.8). At a lower concentration range in ESI-MS (10^{-8} to 10^{-7} M), relative intensities of Pr/Me, Pr/Et, MeOEt/Me, MeOEt/Et and MeOEt/pr were similar to those in nano-ESI-MS at 10^{-6} M. This indicates that in nano-ESI the differences due to surface effects can be minimized. Similarly, at a lower concentration, due to availability of surface space analytes from the bulk of the droplet can reach the surface and are ionized with equal efficiency as in nano-ESI.

From all these studies it is observed that, within the droplet, analyte molecules can be assumed competing for droplet surface. By increasing the chance of the analyte to become charged and be located in the droplet surface layer (introduction of permanent charge by labelling, dilution, nano-ESI) suppression is reduced and in some cases completely leveled. At lower concentration the difference observed due to chemistry is reduced but the relative ion intensities might not be reliable due to higher scattering and interference from background

noise. At a concentration where the absolute ion intensities are saturated ($>10^{-5}$ M), the relative ion intensities of compounds very similar in chemistry showed a response with respect to molar ratio. For compounds which have larger difference in chemistry the relative ion intensities changed with the total concentration, but at a concentration where the absolute ion intensities were saturated the relative sensitivity became constant with certain scattering. Hence relative ionization efficiencies can be defined at a concentration of $>10^{-5}$ M for all types of mixtures with defined uncertainty limits. But for compounds which differ in chemistry the dependence of relative ion intensities on molar ratio at a concentration in the saturation range is not yet fully understood. As unlike compounds with similar chemistry, along with competition for surface space other parameters like sodium complexation ability, electron density, electrophilic mobility, polarity, etc., also play a major role in ionization.

From the studies described, an overview of the effects influencing intensities in ESI-MS has been obtained, some of which were only known theoretically for alkylated oligosaccharides, and only some of which had been practically proven previously.

7. Materials and methods

7.1 Reagents

All chemicals purchased were of highest purity and used without further purification. Reagents and materials were purchased from Sigma Aldrich. Solvents used for ESI-MS were LC-MS grade and were purchased from Fluka.

7.2 Materials

Alkylating agents: Iodomethane (MeI), iodomethane- d_3 (Me- d_3 -I), iodoethane (EtI), methoxyethyl bromide (MeOEtBr) and propyl bromide (PrBr). β -Cyclodextrin was purchased from Sigma Aldrich. *m*-Aminobenzoic acid (*m*ABA), 2-picoline borane, matrices used for MALDI-ToF-MS, (2-(4-hydroxyphenylazo) benzoic acid (HABA), 2,5-dihydroxybenzoic/2-hydroxy-5-methoxybenzoic acid (sDHB) and α -cyano-4-hydroxycinnamic acid (CHCA)), and Lewis acid BF_3OEt_2 were also purchased from Sigma Aldrich.

7.3 Instruments and methods

ESI-IT-MS

(referred as defined parameters in text for syringe pump infusions)

Instrument	HCT Ultra ETDII (Bruker Daltonics, Bremen, Germany)
Software	Bruker Data Analysis
Flow	200 $\mu\text{L/h}$
Dry gas	N_2 , 4L/min (direct infusion) and temperature 300 $^\circ\text{C}$
Nebulizer gas	N_2 , 10 psi (direct infusion)
Mode	positive or negative ion mode, respectively
ICC target	100,000 (positive mode) and 70,000 (negative mode)
Average scans	100
Capillary voltage	4.5 kV
End plate offset	500 V
Capillary exit	280 V
Skimmer	40 V

Compound stability	1000%
Trap drive level	100%
Target Mass	Normally 1000, sometimes varied to 300, 500, 1500 and 2000 depending on the requirement. Also in some cases target mass of the m/z of interest was used as specified in the text.
Solvent	Methanol

LC-IT-MS (*referred as defined parameters in text*)

Instrument	HCT Ultra ETDII (Bruker Daltonics, Bremen, Germany)
Software	Bruker Data Analysis
Flow	0.2 mL/min (short column), 0.4 mL/min (long column)
Column	RP-C ₁₈ (Phenomenex, Gemini, 250 x 4.60 mm, 5 micron)
Mobile phase	A: H ₂ O/HOAc (99/1, v/v) B: Acetonitrile/HOAc (99/1, v/v) B: Acetonitrile/Isopropanol/HOAc (48.5/48.5/1, v/v); for propylated mixtures
Pump	Binary pump, series 1100, G1312A, Agilent technologies
Autosampler	Series 1200, G1392B, Agilent technologies
DAD-Detector	200-600 nm, series 1100, G1315B, Agilent technologies
Gradient system	40% B (0 min) → 100% B (50 min) 30% B (0 min) → 100% B (50 min) 20% B (0 min) → 100% B (50 min) 10% B (0 min) → 100% B (50 min)
Dry gas	N ₂ , 9 L/min (direct infusion) and temperature 365 °C
Nebulizer gas	N ₂ , 40 psi (direct infusion)
Voltages	similar syringe pump infusions

Nano-ESI-MS (HZI Braunschweig)

Instrument	Thermo Scientific LTQ Orbitrap Velos Pro mass spectrometer equipped with both, orbitrap and linear ion trap
Software	X calibur
Capillary temperature	300 °C
Spray voltage	1 kV
Spray current	0.06 µA
Resolution	60,000
Scan mode	full (200-2000 m/z)

Source fragmentation 'ON' 100%

MALDI-ToF-MS (At KTH Stockholm, Fiber and Polymer technology)

Instrument	Bruker UltraFlex mass spectrometer was used equipped with a gridless SCOUT-MTP ion source from Bruker Daltonics Software
Software	Bruker Data Analysis
Laser	N ₂ , 337 nm
Mode	positive ion
Molecular weight range low (20-2500 Da)	
Ion source 1	25 kV
Ion source 2	22 kV
Lens voltage	9 kV
Reflector voltage	26.36 kV
Reflector voltage 2	13.75 kV
Frequency	50.0 Hz
Laser power	35-60%
No. of shots	1000
Matrices	HABA, sDHB, HCHA

Analyte solution (1 mg/mL) and matrix solution (10 g/L) in methanol were mixed in 1:10 weight ratio. Approximately 0.3 µL of sample solution was spotted on the target plate and was dried at ambient temperature before insertion into instrument.

Preparative HPLC

Instrument	HPLC (Knauer, well chrome) equipped with pump K-1001
Column	RP-C ₁₈ -column (Phenomenex, Luna, 5 micron, 250x15.00 mm)
Flow rate	5 mL/min
Mobile phase	A: H ₂ O/HOAc (99/1, v/v) B: Acetonitrile/HOAc (99/1, v/v)
Gradient system	20% B (0 min) → 100% B (50 min)
Sample concentration	20 mg/mL
Injection volume	200 µL

As non-labeled compounds are not UV-active, the eluent from the column was collected every one minute in separate tubes. Fractions were monitored by TLC, and oligosaccharides of the same DP were combined, evaporated, and the residue dissolved in MeOH. Results were further confirmed by syringe pump infusions of the unified fractions in the ESI-IT-MS instrument. In addition, the individual concentration of each DP in combined solutions was determined by HPLC-UV.

Gas chromatography

Instrument	GC-2010, Shimadzu
Column	ZB-5MS, phenomenex, l = ca. 30 m, ID = 0.25 mm, film thickness = 0.25 μ m
Injector mode	splitless
Carrier gas	hydrogen, linear gradient 45 cm/s
Detector	FID, hydrogen (40 mL/min), synthetic air (400 mL/min) and nitrogen (make-up-Gas 30 mL/min)
T-programme	60 $^{\circ}$ C (1 min isotherm), 20 $^{\circ}$ C/min \rightarrow 200 $^{\circ}$ C, 4 $^{\circ}$ C/min \rightarrow 250 $^{\circ}$ C. 20 $^{\circ}$ C/min \rightarrow 310 $^{\circ}$ C (10 min isotherm)
Data analysis	GC. Solution, Shimadzu

GC-MS

Instrument	GC-5890A, Hewlett Packard
Mode	EI, positive, 70 eV
Column	same as GC
Injector	Split 1:20
T-programme	same as GC

IR-spectrometer

Instrument	Tensor 27, Bruker
Type	Diamond-ATR
Scan range	600 – 4000 cm^{-1} (32 scans)

¹H NMR

Instrument	DRX 400 MHz, Bruker
Solvent	CD ₃ OD

7.4 Synthesis (per-*O*-alkylated β -cyclodextrins)**7.4.1 Reaction procedure (Ciucanu and Kerek¹⁰⁵)**

Me-CD, Me₃-CD, Et-CD and MeOEt-CD were synthesized following the same process. The β -cyclodextrin (β -CD) was dissolved in DMSO by stirring (data for amounts of substrate and reagents are summarized in Table 20) for 20 min at room temperature. To this, freshly pulverized NaOH (3 equiv./OH) was added and, stirred for further 20 min. Then, alkylating agent (3 equiv./OH) was added. The reaction was carried out at room temperature under nitrogen, to avoid additional access of humidity. After stirring for 24 h, half of the first amount of base and alkylating agent was added to the reaction. After 48 h the reaction was quenched by diluting with 120 mL of ice-cold water. The product was extracted with CH₂Cl₂ from DMSO/water mixture 4-5 times. The combined CH₂Cl₂ phases was washed 5 times with water to remove residual DMSO. The organic phase was dried over Na₂SO₄ and evaporated to dryness.

7.4.2 Reaction procedure (Hakomori)

A second compound of Me-CD (2) was also synthesized using Li-dimsyl as base (modified method of Hakomori¹³⁴)

Preparation of base Li dimsyl (Li methylsulfinylmethanide)

To 35 mL of DMSO 35 mL of methyl lithium in ether (1.6 M) was added under nitrogen and excluding humidity. The mixture was stirred under nitrogen at room temperature until all diethylether and methane formed had been evaporated, and the volume was reduced to the original volume of DMSO.

Addition of base to substrate in DMSO

β -Cyclodextrin (0.97 g, 0.85 mmol) was dissolved in 50 mL of DMSO under nitrogen. The mixture was allowed to stir for 20 min. to completely dissolve β -cyclodextrin. To this Li-dimsyl (34.8 mL, 55.5 mmol, 3 equiv./OH) was added and stirred for 40 min.. After 40 min. alkylating agent (3 equiv./OH) was added. After stirring for 24 h at room temperature under nitrogen, half of the first amount of base and alkylating agent were added. After 48 hrs the reaction was quenched by diluting with 120 mL of ice-cold water. The product was extracted 4-5 times with CH_2Cl_2 from DMSO/water mixture. The CH_2Cl_2 phase was washed 5 times with water to remove residual DMSO. The organic phase was dried over Na_2SO_4 and evaporated to dryness.

7.4.3 Synthesis of Heptakis[2,3,6-tri-*O*-propyl]- β -cyclodextrin (Pr-CD)

O-Propyl- β -cyclodextrin was synthesized in three steps. In step 1 the substrate was alkylated according to the procedure according to Ciucanu and Kerek,¹⁰⁵ described under 7.4.1. The product obtained in step 1 was not completely alkylated (checked by IR spectroscopy, OH peak was visible in the range 3000-3500 cm^{-1}). Due to decreased polarity and thus change in solubility, step 2 was performed according to Tamura and Imanari¹³⁵ in THF using sodium hydride as base. This step was repeated to achieve completeness of propylation.

Propylation in THF with NaH/propylbromide)

Partly *O*-propylated β -CD from step 1 was dissolved in dry THF and stirred for 20 min until it was completely dissolved. To this solution, 3 equiv./OH NaH, washed free of mineral oil with petroleum ether) was added. The reaction was stirred for 1 h at a temperature of 30 - 35 $^{\circ}\text{C}$. Then propyl bromide (3 equiv./OH) was added. The reaction was carried out at room temperature under nitrogen. After stirring for 24 h, half of the first amounts of base and alkylating agent were added to the reaction. After 48 hours the reaction was stopped first by

adding cold methanol to neutralize the unreacted NaH, later the reaction was quenched with cold water. The product was extracted 4-5 times with diethyl ether from THF/water mixture. The diethyl ether phase was washed 5 times with water to remove residual THF. The organic phase was dried over Na₂SO₄ and evaporated to dryness. Amounts of materials taken in alkylation of β -cyclodextrins are given Table 20.

Table 20

Summary of the amount of substrate, solvent, base and alkylating agent used in the synthesis

Abbreviation	β -Cyclodextrin [g] / mmol CD	Solvent DMSO, THF [mL]	Base (3 equiv./OH) NaOH, NaH [g] Dimsyl [mL]	Alkylating agent (3 equiv./OH) [mL]
Me-CD	1.00/0.88	28	2.25 NaOH	3.5 MeI
Me-CD (2)	0.97 / 0.85	50	34.8 Dimsyl	4.0 MeI
Me- <i>d</i> ₃ -CD	1.00 /0.88	28	2.25 NaOH	3.5 MeI- <i>d</i> ₃
Et-CD	1.01 / 0.89	35	2.25 NaOH	4.5 EtI
Et-CD-2	1.20*	35	2.25 NaOH	4.5 EtI
MeOEt-CD	1.01 /0.89	40	2.25 NaOH	5.3 MeOEtBr
Pr-CD	1.00 /0.88	28	2.25 NaOH	6.8 Pr-Br
Pr-CD-2	2.07*	35 (THF)	4 NaH in petroleum ether	6.8 Pr-Br
Pr-CD-3	2.04*	35 (THF)	4 NaH in petroleum ether	6.8 Pr-Br

Half of the prior amount of base and alkylating agent was added to the reaction after 24 h

**Et-CD-2 was prepared using Et-CD as substrate. Similarly, Pr-CD was used for Pr-CD-2 and Pr-CD-2 for Pr-CD-3*

7.5 Monomer analysis

Methanolysis and trimethylsilylation¹⁰⁷ (MeTMS)

To 1-2 mg of sample in a 1 mL V-vial 1 mL of methanolic HCl (1.5 M) was added. The mixture was heated at 90 °C for 90 min. During heating the vial was shaken several times. After 90 min. the samples were cooled to room temperature and HCl was co-distilled with methanol under the stream of nitrogen. To the residue 10 μ L of pyridine, 50 μ L of CH₂Cl₂ and 50 μ L of BSTFA were added. The mixture was heated for 1 h at 100 °C. After cooling to

room temperature, 890 μL of CH_2Cl_2 was added. The diluted sample was analyzed by GLC-FID (data given in Table 21).

Preparation of alditol acetates¹⁰⁸ (AA)

Hydrolysis:

To 1-2 mg of sample in a 1 mL V-vial 1 mL of 2 M TFA was added and heated at 120 $^{\circ}\text{C}$ for 120 min. During heating the vial was shaken several times. After cooling to room temperature the aqueous acid was removed in a stream of nitrogen, until the solid residue was nearly but not completely dry. The residue was neutralized with drops of ammonia prior to reduction and the ammonia was evaporated after addition of a droplet toluene under nitrogen.

Reduction:

To the residue from hydrolysis a solution of 0.5 mL of 0.25 M NaBD_4 in 2 M NH_3 is added and heated for 120 min. at 60 $^{\circ}\text{C}$. During heating the vial was shaken several times. After cooling to room temperature aqueous ammonia was removed under a stream of nitrogen.

Acidic Acetylation:

To the above residue from reduction 250 μL acetic anhydride and 100 μL of concentrated TFA are added and mixed thoroughly by shaking the vial. Acetylation of the free OH groups was carried out for 30 minutes at 60 $^{\circ}\text{C}$. During heating the vial was shaken several times. After cooling the samples to room temperature, the solution is transferred into 5 mL vial. The 1 mL vial is washed three times with CH_2Cl_2 . The combined dichloromethane phases are once washed with saturated NaHCO_3 . After phase separation the aqueous phase is carefully removed with a Pasteur pipette. The organic phase is then washed four times with distilled water, the aqueous phase is removed by Pasteur pipette. After fourth washing the organic phase is carefully removed with syringe, transferred into appropriate glass vessel and dried over small pieces of CaCl_2 . After transfusing, the organic phase is used for GLC-FID analysis (data given in Table 21).

Table 21Monomer data from GLC analysis of per-*O*-alkylated β -cyclodextrins

Mol %	Me-CD (MeTMS)	Me-CD (AA)	Me-CD (2) (MeTMS)	Et-CD (MeTMS)	MeOEt-CD (MeTMS)
un	0.02	0.04	0.01	0.02	0.00
2	0.01	0.01	0.10	0.01	0.06
3	0.00	0.00	0.00	0.00	0.00
6	0.01	0.43	0.13	0.02	0.00
23	1.22	0.42	0.62	5.78	0.61
26	0.65	0.22	0.16	0.36	0.79
36	0.39	0.14	0.34	0.17	0.56
236	97.71	98.75	97.63	93.04	97.98
DS	2.98	2.98	2.97	2.94	2.98

Unsubstituted glu-un, 2-substituted:2, 3-substituted:3, 6-substituted:6, 23-substituted:23, 26-substituted:26, 36-substituted:36, 236-substituted:236.

7.6 Partial hydrolysis

Peralkylated- β -cyclodextrins were submitted to partial hydrolysis in a 1 mL V-Vial. Ca. 2 mg in 1 mL of 1 M TFA was heated at 120 °C for various times. After cooling to room temperature, aqueous acid was removed in a stream of nitrogen and finally co-distilled with toluene and the remainder evaporated to dryness. The obtained *O*-maltooligosaccharides of DP 1–7 were dissolved in 1 mL of methanol. Composition with respect to DP was determined after reductive amination by HPLC-UV-MS for each sample.

7.7 Reductive amination

To ca. 2 mg of the substrate in 0.5 mL MeOH, 0.3 mL *m*ABA in methanol (containing 2.6 mg/19 μ mol *m*ABA) and 0.15 mL glacial acetic acid was added, and the mixture was heated to 40 °C for 30 min. Subsequently, 50 μ L of 2-picoline borane in MeOH (containing 1.7 mg; \sim 19 μ mol) were added, and the mixture was heated to 40 °C for 45 min. Subsequently the solvent was removed in a stream of nitrogen and the residue was dissolved in 1 mL of MeOH. The completeness of labeling was determined by TLC and by ESI-IT-MS in positive ion mode for the presence of unlabeled sample.

7.8 Preparation of mixtures

From the stock solutions given in Table 2 and Table 3 complex mixtures were prepared by mixing certain proportions of the two compounds of interest. The volumes of the stock solutions taken are given in Table 22.

Table 22

Amounts of stock solutions taken to prepare complex mixtures

(v/v) μL	Me- <i>d</i> ₃ / Me	Et/Me	Et/Me- <i>d</i> ₃	Pr/Me	Pr/Et	MeOEt/ Me	MeOEt/ Et	MeOEt/ Pr
CM1	148/100	138/100	110/100	697/100	817/100	153/100	180/100	194/100
CM2	134/100	231/100	70/100	483/100	355/100	144/100	106/100	133/100
CM3	187/100	298/100	59/100	379/100	235/100	141/100	87/100	109/100
CM4	148/100	117/100				153/100	106/100	
CM5	134/100	136/100				288/100	212/100	
CM6	187/100	161/100						
CM7	357/100							
CM8	280/100							
CM9	258/100							

For the exact molar ratio in DP 2-6 in different complex mixtures see Tables 4-11

7.9 Calculation of uncertainty limits

Depending on the relation between various factors that cause scattering uncertainty limits can be calculated either by Type A or Type B evaluation.¹²⁶⁻¹²⁷ As here the relationship between reference data and relative ion intensities is linear uncertainty limits are calculated by following Type A evaluation. The uncertainty of a measurement can be defined by the formula:

$$U = \sqrt{u_1^2 + u_2^2 + \dots + u_n^2}$$

Where U is the combined uncertainty, u is the uncertainty from each factor which can be obtained from $\frac{\sqrt{s}}{n}$. Where, s is the standard deviation and n is the number of measurements.

After obtaining the combined uncertainty, uncertainty limits can be obtained by multiplying the k factor from t-distribution table depending on the probability interval.

In our case there are three factors that cause uncertainty: determination of the concentration of individual stock solution (u_1 is obtained by calculating SD from three measurements), determination of the concentration of the mixtures (u_2 is obtained by calculating SD from three measurements), and standard deviation of the measurement itself (ESI-MS, u_3) which has been obtained by measuring the samples 5 consecutive times on 5 different days. Combining all these uncertainties combined uncertainty has been obtained as described above. Uncertainty limits were calculated by multiplying 'U' with a K factor of '2' for 95% probability from t-distribution table.

8. References

- [1] M. Barber, R. S. Bordoli, R. D. Sedgwick, A.N. Tyler, *Nature.*, **293**, 270-275 (1981).
- [2] J. Zeleny, *Phys. Rev.*, **3**, 69 (1914).
- [3] J. Zeleny, *Phys. Rev.*, **10**, 1 (1917).
- [4] J. Zeleny, *Phys. Rev.*, **16**, 102 (1920).
- [5] M. Dole, L.L. Mack, R.L. Hines, R.C. Mobley, L.D. Ferguson, *Chem. Phys.*, **49**, 2240–2249 (1968).
- [6] L.L. Mach, P. Kralik, A. Rheude, M. Dole, *J. Chem. Phys.*, **52**, 4977 (1970).
- [7] M. Yamashita, J. B. Fenn, *J. Phys. Chem.*, **88**, 4451–4459 (1984).
- [8] M. Yamashita, J. B. Fenn, *J. Phys. Chem.*, **88**, 4671 (1984).
- [9] A.P. Bruins, T. Covey, J. D. Henion, *Anal. Chem.*, **59**, 2642–2646 (1987).
- [10] M.E. Ikononou, A.T. Blades, P. Kebarle, *Anal. Chem.*, **63**, 1989–1998 (1991).
- [11] T. R. Covey, R. F. Bonner, B. I. Shushan, J. Henion, *Rapid Commun. Mass Spectrom.*, **2**, 249–256 (1988).
- [12] E. C. Huang, J. D. Henion, *Anal. Chem.*, **63**, 732–739 (1991).
- [13] K. L. Duffin, T. Wachs, J. D. Henion, *Anal. Chem.*, **64**, 61–68 (1992).
- [14] G. J. Van Berkel, G. L. Glisch, J. A. McLuckey, *Anal. Chem.*, **62**, 1284–1295 (1990).
- [15] S. F. Wong, C. K. Meng, J. B. Fenn, *ASMS Conf. Mass Spectrom. Allied Top.*, **May 24-29**, (1987).
- [16] G. I. Taylor, *Proc Roy Soc L.*, **A**, 280–283 (1964).
- [17] A. P. Bruins, *ESI source design and dynamic range considerations. In: R.B. Cole ed. Electrospray Ionization Mass Spectrometry. Newyork: Wiley, 1997, Chap.3.*
- [18] A. P. Bruins, *J Chromatogr. A.*, **794**, 345–357 (1998).
- [19] J. S. Gaskell, *J Mass Spectrom.*, **32**, 677–688 (1997).
- [20] A. Gomez, K. Tang, *Phys. Fluids.*, **6**, 404-414 (1994).

-
- [21] L. Rayleigh, *Phil Mag.*, **14**, 401-404 (1882).
- [22] <http://america.pink/images/1/4/0/4/9/7/5/en/3-electrospray-ionization.jpg>, 20-04-2016.
- [23] D. P. H. Smith, *IEEE Trans Ind Appl.*, **IA-22**, 527 (1986).
- [24] G. S. Redecker, L. Battering, F. W. Röllgen, *Int. J. Mass Spectrom. Ion Proc.*, **90**, 139 (1989).
- [25] J. B. Fenn, *J. Am. Soc. Mass Spectrom.*, **4**, 524–535 (1993).
- [26] J. V. Iribarne, B. A. Thomson, *Chem. Phys.*, **64**, 2287–2294 (1976).
- [27] B. A. Thomson, J. V. Iribarne, *J Chem. Phys.*, **71**, 4451-4463 (1979).
- [28] G. J. V. Berkel, F. Zhou, *Anal. Chem.*, **67**, 3958–3964 (1995).
- [29] J. B. Fenn, J. Roswell, C. K. Meng, *J. Am. Soc. Mass Spectrom.*, **8**, 1147–1157 (1997).
- [30] M. G. Castano, J. F. Mora, *Anal. Chem.*, **72**, 1426–1429 (2000).
- [31] M. Sakairi, A. L. Yergey, K. W. M. Siu, J. C. Y. Le Blanc, R. Guevremont, S. S. Berman, *Anal. Chem.*, **63**, 1488–1490 (1991).
- [32] P. Kebarle, Y. Ho, *On the mechanism of electrospray mass spectrometry. In: R.B. Cole, ed. Electrospray Ionization Mass Spectrometry. Newyork: Wiley, 1997, Chap. 7.*
- [33] X. Fang, G. R. Anger, *J. Am. Soc. Mass Spectrom.*, **11**, 393–399 (2000).
- [34] S. A. Shaffer, D. C. Prior, G. A. Anderson, H. R. Udseth, R. D. Smith, *Anal. Chem.*, **70**, 4111–4119 (1998).
- [35] C. N. McEwen, B. S. Larsen, *Electrospray ionization on quadrapole and magnetic sectors mass spectrometers. In: R.B. Cole, ed. Electrospray Ionization Mass Spectrometry. Newyork: Wiley, 1997, Chap. 7*
- [36] R. F. Ferguson, K. E. McKulloh, H. M. Rosenstock, *J. Chem. Phys.*, **42**, 100 (1965).
- [37] W. Paul, H. S. Steinwedel, *Z. Naturforsch.*, **89**, 448 (1953).
- [38] R. E. March, R. J. Hughes, J. F. J. Todd, *Mass Spectrom.*, **102**, (1989).
- [39] R. E. March, *J. Mass Spectrom.*, **32**, 351–369 (1997).
- [40] M. Splendore, F. A. Londry, R. E. March, R. J. S. Morrison, P. Andre, J. Perrier, *Int. J.*

-
- Mass Spectrom. Ion Process.*, **156**, 11-29 (1996).
- [41] R. T. Hilger, R. E. Santini, C. A. Luongo, B. M. Prentice, *Int. J. Mass Spectrom.*, **377**, 329–337 (2015).
- [42] A. Krueve, K. Herodes, I. Leito, *Rapid Commun. Mass Spectrom.*, **24**, 919–926 (2010).
- [43] S. Zhou, K. D. Cook, *J Am Soc. Mass Spectrom.*, **11**, 961–966 (2000).
- [44] J. B. Fenn, M. Mann, C. K. Meng, S. F. Wong, C. M. Whitehouse, *Science.*, **246**, 64–71 (1989).
- [45] R. B. Cole, J. H. Zhu, *Rapid Commun. Mass Spectrom.*, **13**, 607–611 (1999).
- [46] R. R. Ogorzalek, R. D. Smith, *J Am Soc. Mass Spectrom.*, **5**, 221–229 (1994).
- [47] T. D. Covey, E. D. Lee, J. D. Henion, *Anal. Chem.*, **58**, 2453-2460 (1986).
- [48] A. L. Rockwood, M. Busman, H. R. Udseth, R. D. Smith, *Rapid Commun. Mass Spectrom.*, **5**, 582–585 (1991).
- [49] L. Tang, P. kebarle, *Anal. Chem.*, **63**, 2709–2715 (1991).
- [50] M. Mann, J. B. Fenn, S. F. Wong, *Benninghoven A.*, 139–144 (1990).
- [51] R. Guevremont, D. A. Barnett, R. W. Purves, *Anal. Chem.*, **72**, 4577–4584 (2000).
- [52] R. W. Purves, W. Gabryelske, *Rapid Commun. Mass Spectrom.*, **12**, 695–700 (1998).
- [53] K. Tang, R. D. Smith, *J. Am. Chem. Soc.*, **12**, 343-347 (2001).
- [54] S. M. Blair, E. C. Kempen, J. S. Bordbelt, *J. Am. Soc. Mass Spectrom.*, **9**, 1049–1059 (1998).
- [55] S. Lee, T. Wyttenbach, G. V. Helden, *J. Am. Chem. Soc.*, **117**, 10159–10160 (1995).
- [56] N. B. Cech, C. G. Enke, *Anal. Chem.*, **73**, 4632–4639 (2001).
- [57] T. Wyttenbach, G. Von Helden, M. T. Bowers, *Int. J. Mass Spectrom. Ion Proc.*, **166**, 377–390 (1997).
- [58] R. Kostiainen, A. P. Bruins, *Rapid Commun. Mass Spectrom.*, **10**, 1393–1399 (1996).
- [59] C. J. Hogan Jr, P. Biswas, *J. Am. Soc. Mass Spectrom.*, **19**, 1098–1107 (2008).
- [60] N. B. Cech, C. G. Enke, *Mass Spectrom. Rev.*, **20**, 362–387 (2001).

-
- [61] K. Tang, R. D. Smith, *Int. J. Mass Spectrom.*, **187**, 97–105 (1999).
- [62] W. N. Haworth, *Helv. Chem. Acta.*, **11**, 534–548 (1928).
- [63] G. Wang, R. B. Cole, *Org. Mass Spectrom.*, **29**, 419–427 (1994).
- [64] G. S. Jackson, C. G. Enke, *Anal. Chem.*, **71**, 3777–3784 (1999).
- [65] G. Hopfgartner, T. Wachs, K. Bean, J. Henion, *Anal. Chem.*, **65**, 439–446 (1993).
- [66] D. B. Hager, N. J. Dovichi, J. Klassen, P. Kebarle, *Anal. Chem.*, **66**, 3944–3949 (1994).
- [67] D. E. Goeringer, K. G. Asano, S. A. McLuckey, D. Hoekman, S. W. Stiler, *Anal. Chem.*, **66**, 313–318 (1994).
- [68] J. F. Robyt, *Essentials of Carbohydrate Chemistry*, Springer-Verlag New York, 1998.
- [69] [http://chemwiki.ucdavis.edu/Textbook_Maps/General_Chemistry_Textbook_Maps/Map%3A_Chem1_\(Lower\)/07%3A_Solids_and_Liquids/7.03%3A_Hydrogen-Bonding_and_Water](http://chemwiki.ucdavis.edu/Textbook_Maps/General_Chemistry_Textbook_Maps/Map%3A_Chem1_(Lower)/07%3A_Solids_and_Liquids/7.03%3A_Hydrogen-Bonding_and_Water), 20-04-2016.
- [70] A. Reveley, 'A Review of Cellulose Derivatives and their Industrial Applications: Cellulose and its Derivatives'
- [71] D. Klemm, B. Heublein, H. P. Fink, A. Bohn, *Angew. Chemie Int. Ed.*, **44**, 3358–3393 (2005).
- [72] H. Thielking, M. Schmidt, *Cellul. Ethers. Ullmann's Encycl. Ind. Chem.*, (2006).
- [73] P. Mischnick, *Cellulose 00*, 1–13 (2002).
- [74] K. Kobayashi, C. Huang, T. P. Lodge, *Macromolecules.*, **32**, 7070–7077 (1999).
- [75] L. Zhang, Y. Wang, L. Yu, H. Liu, G. Simon, N. Zhang, L. Chen, *Colloid Polym. Sci.*, **293**, 229–237 (2015).
- [76] M. Baiardo, G. Frisoni, M. Scandola, A. Lcciardello, *J. Appl. Polym. Sci.*, **83**, 38–45 (2001).
- [77] M. Gohdes, P. Mischnick, *Carbohydr. Res.*, **309**, 109–115 (1998).
- [78] P. Mischnick, D. Momcilovic, *Adv. Carbohydr. Chem. Biochem.*, **64**, 117–210 (2010).
- [79] H. M. Spurlin, *Carbohydr. Res.*, **41**, 2222–2227 (1939).

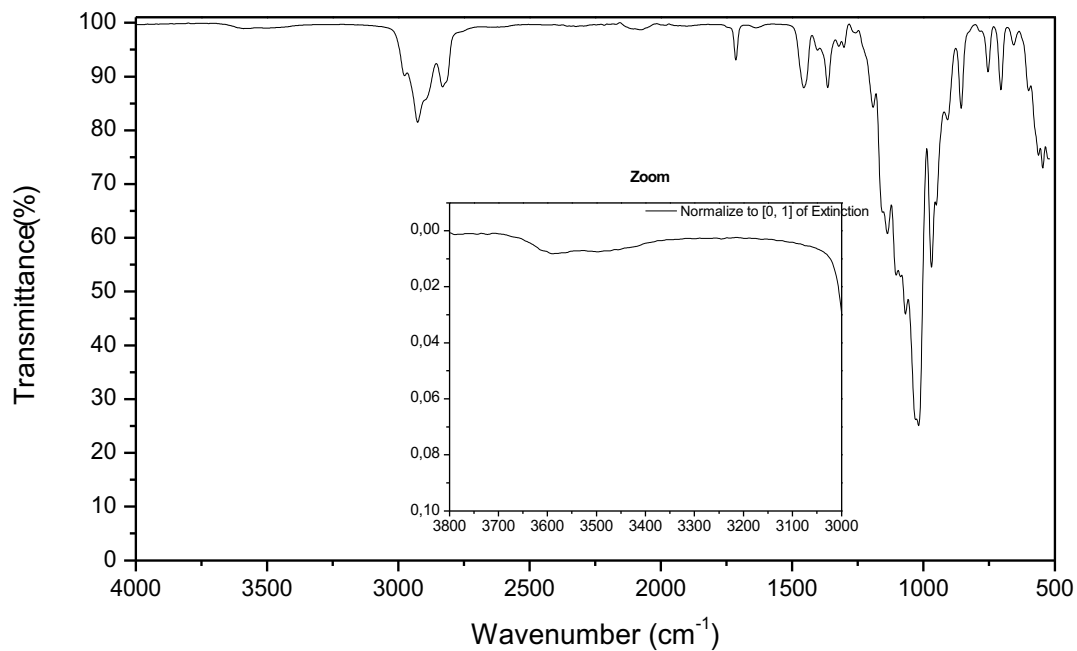
-
- [80] R. Adden, R. Müller, P. Mischnick, *Macromol. Chem. Phys.*, **207**, 954-965 (2006).
- [81] O. Smidsrod, K. I. Draget, *Carbohydr. Eur.*, **14**, 6–13 (1996).
- [82] R. Adden, C. Melander, G. Brinkmalm, L. Gorton, P. Mischnick, *Biomacromol.*, **7**, 1399-1409 (2006).
- [83] C. Melander, R. Adden, G. Brinkmalm, L. Gorton, P. Mischnick, *Biomacromol.*, **7**, 1410-1421 (2006).
- [84] K. Voiges, *Methodenentwicklung zur Analytik von Celluloseethern auf verschiedenen strukturellen Ebenen. Thesis, Technische Universität Braunschweig 2015.*
- [85] P. W. Arisz, H. J. J. Kauw, J. J. Boon, *Carbohydr. Res.*, **271**, 1-14 (1995).
- [86] P. Mischnick, G. Kühn, *Carbohydr. Res.*, **29**, 199–207 (1996).
- [87] P. Mischnick, C. Hennig, *Biomacromolecules*, **2**, 180–184 (2001).
- [88] D. J. Harvey, *Mass Spectrom. Rev.*, **18**, 349–450 (1999).
- [89] J. Cuers, I. Unterrieser, W. Burchard, R. Adden, M. Rinken, P. Mischnick, *Carbohydr. Res.*, **348**, 55-63 (2012).
- [90] P. Mischnick, J. Heinrich, M. Gohdes, O. Wilke, N. Rogmann, *Macromol. Chem. Phys.*, **201**, 1985-1995 (2000).
- [91] J. Cuers, M. Rinken, R. Adden, P. Mischnick, *Anal. Bioanal Chem.*, **405**, 9021-9032 (2013).
- [92] R. Adden, W. Niedner, R. Müller, P. Mischnick, *Anal. Chem.*, **78**, 1146-1157 (2006).
- [93] P. Mischnick, I. Unterrieser, K. Voiges, J. Cuers, M. Rinken, R. Adden, *Macromol. Chem. Phys.*, **214**, 1363-1374 (2013).
- [94] R. Juraschek, T. Dülcks, M. Karas, *J. Am Soc. Mass Spectrom.*, **10**, 300–308 (1999).
- [95] M. S. Wilm, M. Mann, *Int. J. Mass Spectrom. Ion Process.*, **136**, 167–180 (1994).
- [96] M. Karas, U. Bahr, T. Dülcks, *J. Anal. Chem.*, **366**, 669–676 (2000).
- [97] U. Bahr, A. Pfenninger, M. Karas, *Anal. Chem.*, **69**, 4530–4535 (1997).
- [98] P. Mischnick, *Cellulose*, **8**, 245–257 (2001).

-
- [99] D. Momcilovic, H. Schagerlöf, B. Wittergren, K. G. Wahlund, G. Brinkmalm, *Anal. Chem.*, **77**, 2948–2959 (2005).
- [100] R. Adden, P. Mischnick, *Int J. Mass Spectrom.*, **242**, 63–73 (2005)
- [101] A. Bösch, P. Mischnick, *Biomacromolecules*, **8**, 2311–2320 (2007).
- [102] R. Adden, A. Bösch, P. Mischnick, *Macromol. Chem. Phys.*, **205**, 2072–2079 (2004).
- [103] A. Bösch, M. Nimtz, P. Mischnick, *Cellulose*, **13**, 493–507 (2006).
- [104] A. Chapeaurouge, L. Bigler, A. Schafer, S. Bienz, *J. Am. Soc. Mass Spectrom* **6**, 207–211 (1995).
- [105] I. Ciucanu, F. Kerek, *Carbohydr. Res.* **131**, 309 (1984).
- [106] J. R. Johnson, N. Shankland, *Tetrahedron* **41**, 3147–3152 (1985).
- [107] A. Gonera, V. Goclik, M. Baum, P. Mischnick, *Carbohydr. Res.* **337**, 2263–2272 (2002).
- [108] K. Voiges, R. Adden, M. Rinken, P. Mischnick, *Cellulose*, 1–12 (2012).
- [109] D. French, D. W. Knapp, H. Pazur, *J. Am. Chem. Soc.* **72**, 5120 (1950).
- [110] K. Freudenberg, *J. Polym. Sci.*, **23**, 791 (1957).
- [111] A. Pfenninger, M. Karas, B. Finke, B. Stahl, *J. Am. Soc. Mass Spectrom*, **13**, 1331–1340 (2002).
- [112] I. Unterrieser, P. Mischnick, *Carbohydr. Res.*, **346**, 68–75 (2011).
- [113] P. Mischnick, *Adv. Polym. Sci.*, **248**, 105–174 (2012).
- [114] S. Gangula, M. Nimtz, P. Mischnick, *Int. J. Mass Spectrom.*, 15576–15585 (2016).
- [115] L. Tang, P. Kebarle, *Anal. Chem.*, **65**, 3654–3668 (1993).
- [116] P. Kebarle, U. H. Verkerk, *Mass Spectrom. Rev.* **28**, 898–917 (2009).
- [117] J. H. Gross, *Mass Spectrometry*, Springer, Berlin-Heidelberg, 2011.
- [118] R. E. March, J. F. J. Todd, *Pract. Asp. Ion Trap. Mass Spectrom.*, **3**, 39–42 (1995).
- [119] I. Unterrieser, J. Cuers, K. Voiges, J. Enebro, P. Mischnick, *Rapid Commun. Mass Spectrom.*, **25**, 2201–2208 (2011).

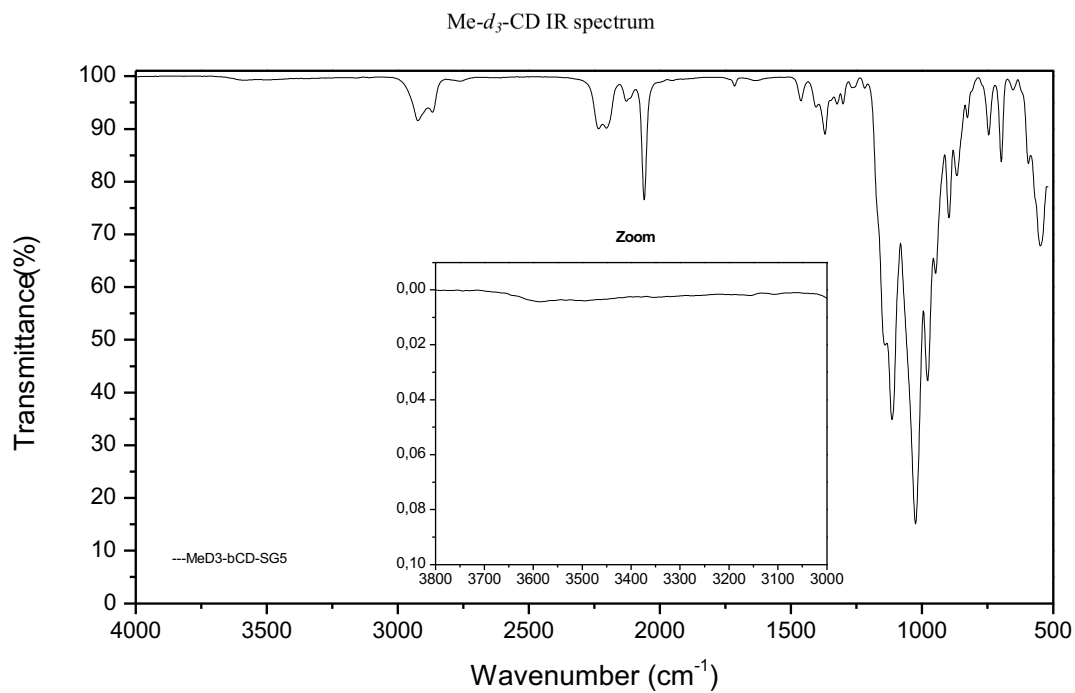
- [120] R. H. Perry, R. G. Cooks, R. J. Noll, *Mass Spectrom. Rev.*, **27**, 661–699 (2008).
- [121] M. Wilm, *Mol. Cell. Proteomics.*, **10**, M111.009407 (2011).
- [122] D. J. Harvey, *Int. J. Mass Spectrom.*, **226**, 1–35 (2003).
- [123] D. J. Harvey, *Mass Spectrom. Rev.* **30**, 1–100 (2011).
- [124] M. Guilhaus, *J. Mass Spectrom.*, **30**, 1519–1532 (1995). E? please check and correct
- [125] W. Gunder, B. H. Lippold, B. C. Lippold, *Eur. J. Pharm. Sci.*, **3**, 203–214 (1995).
- [126] S. L. R. Ellison, A. Williams, *Quantifying Uncertainty in Analytical Measurement*, QUAM:2012.P1.
- [127] *Evaluation of the measurement-Guide to the expression of uncertainty in measurement*, JCGM 100:2008.
- [128] J. V. Iribarne, P. J. Dziedzic, B. A. Thomson, *Int. J. Mass Spectrom. Ion Phys.*, **50**, 331–347 (1983).
- [129] A. Krueve, K. Kaupmees, J. Ligand, M. Oss, *J. Mass Spectrom.*, **48**, 695–702 (2013).
- [130] N. Jonkers, H. Goovers, P. D. Voogt, *Anal. Chim. Acta*, **531**, 217–228 (2005).
- [131] K. Schug, H. M. McNair, *J. Sep. Sci.*, **25**, 760–766 (2002).
- [132] L. S. Levitt, *Z. Naturforsch.*, **34b**, 81–85 (1979).
- [133] H. F. Widing, L. S. Levitt, *Z. Naturforsch.*, **34b**, 321–326, (1979).
- [134] S. Hakomori, *J. Biochem.*, **55**, 205–208 (1964).
- [135] Z. Tamura, T. Imanari, *Chem. Pharm. Bull.*, **12**, 1386–1388 (1964).
- [136] I. Unterrieser, *Quantitative Massenspektrometrie und Fraktionierung nicht-ionischer Celluloseether. Thesis, Technische Universität Braunschweig 2012.*

9. Appendix

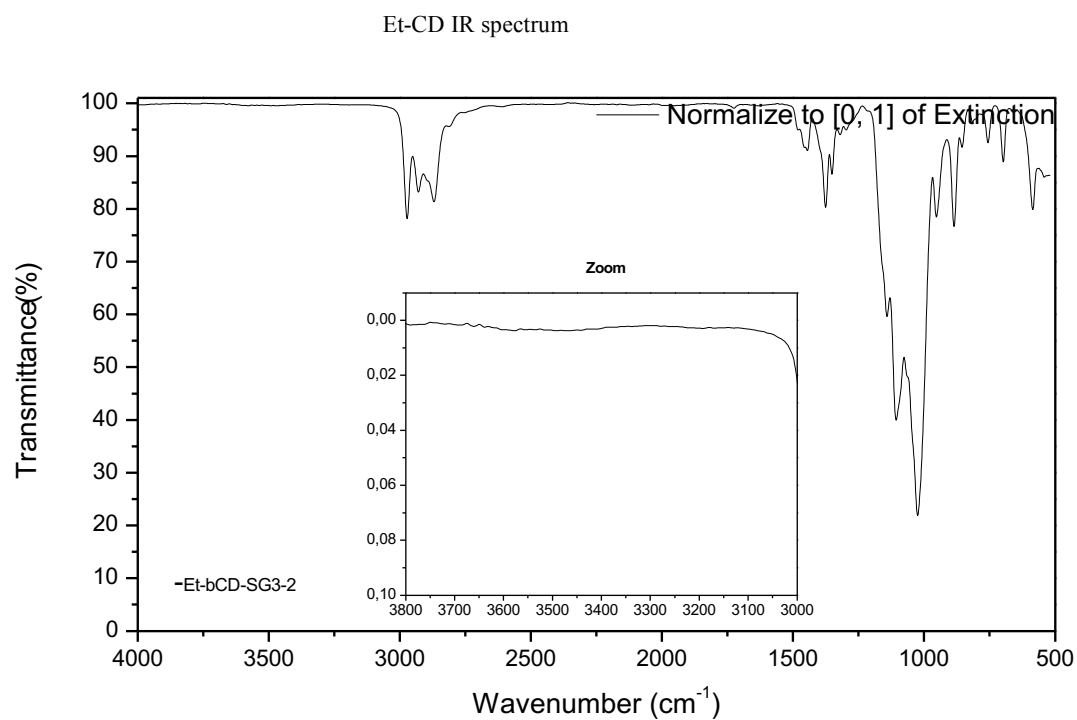
9.1 ATR-IR spectra of peralkylated cyclodextrins



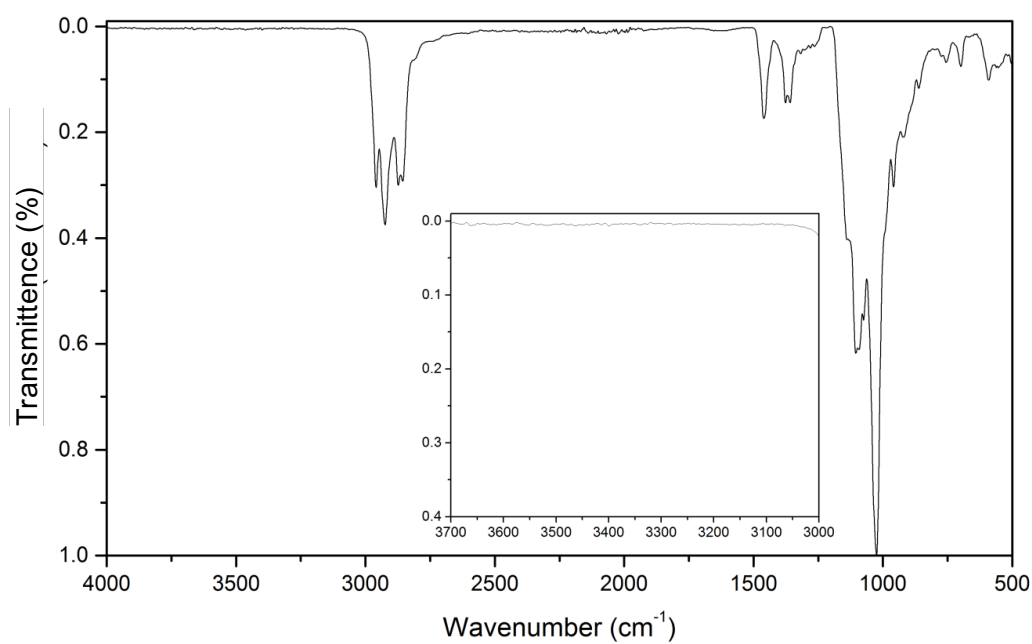
Heptakis [2,3,6-tri-O-methyl] β-cyclodextrin



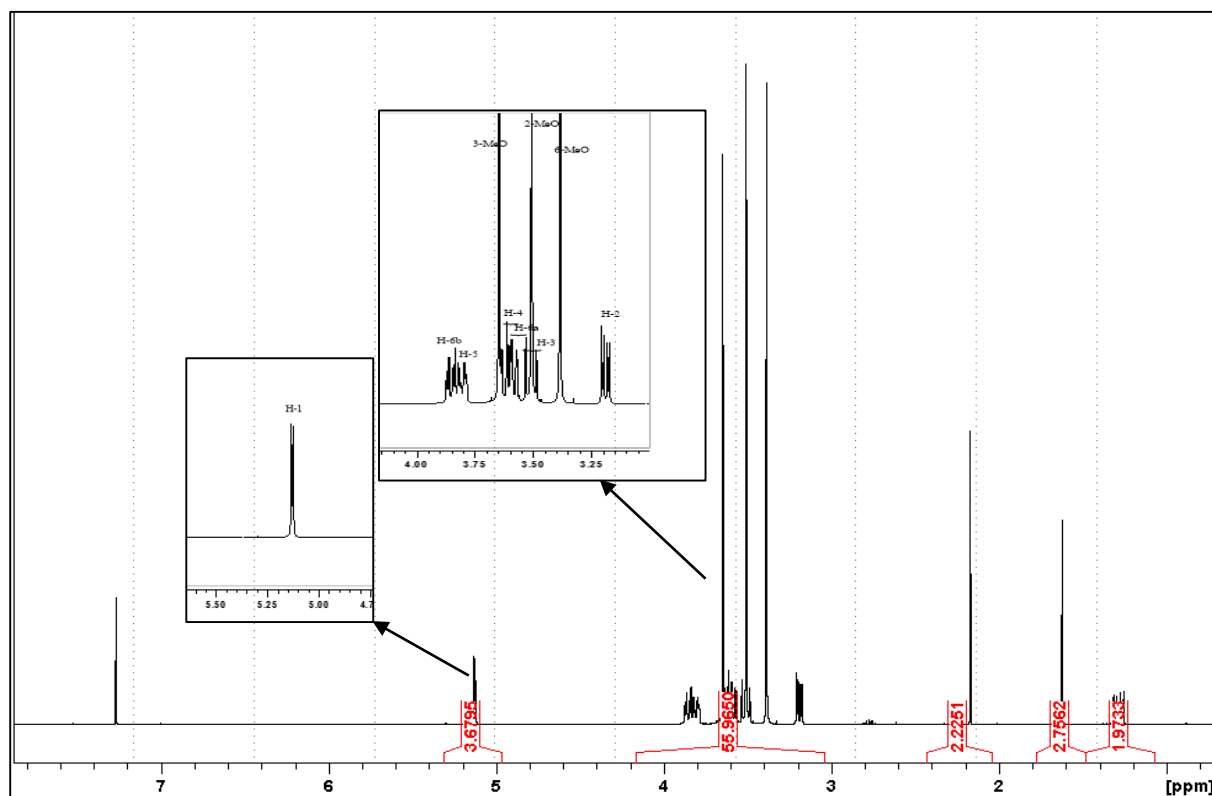
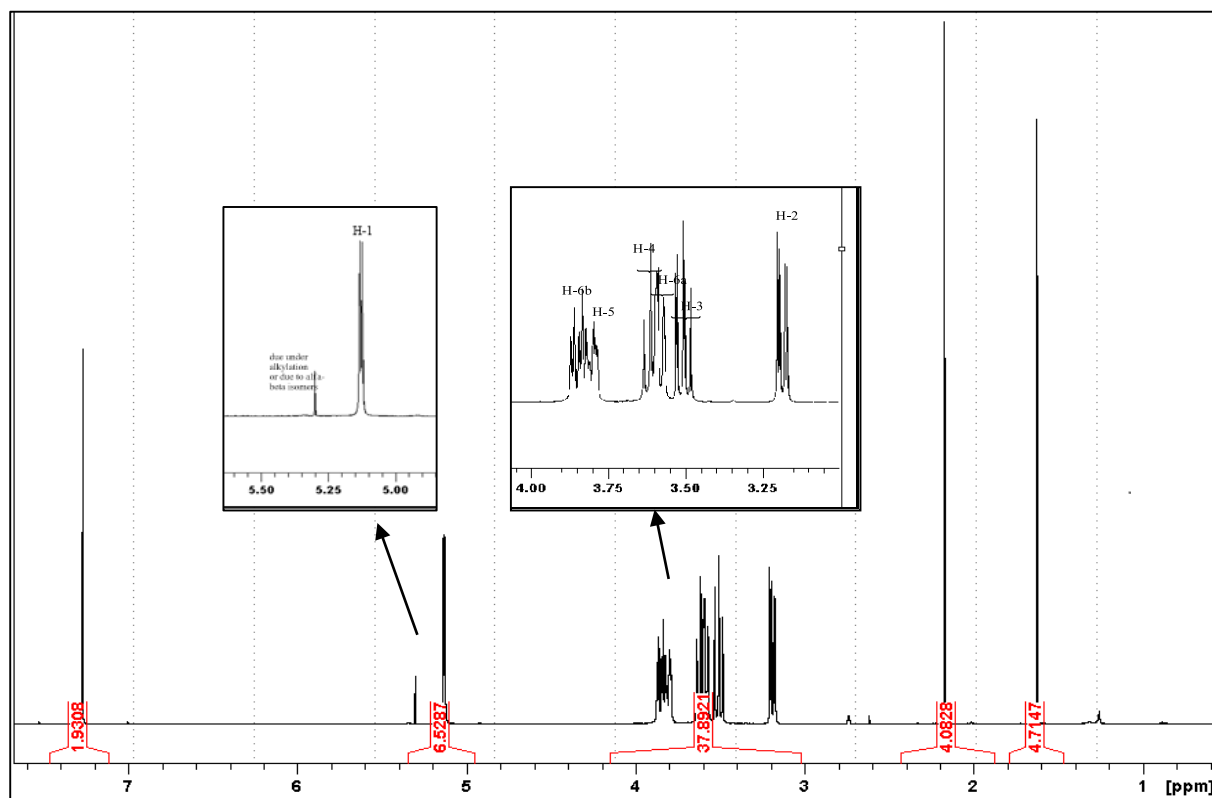
Heptakis [2,3,6-tri-O-deuteromethyl] β-cyclodextrin

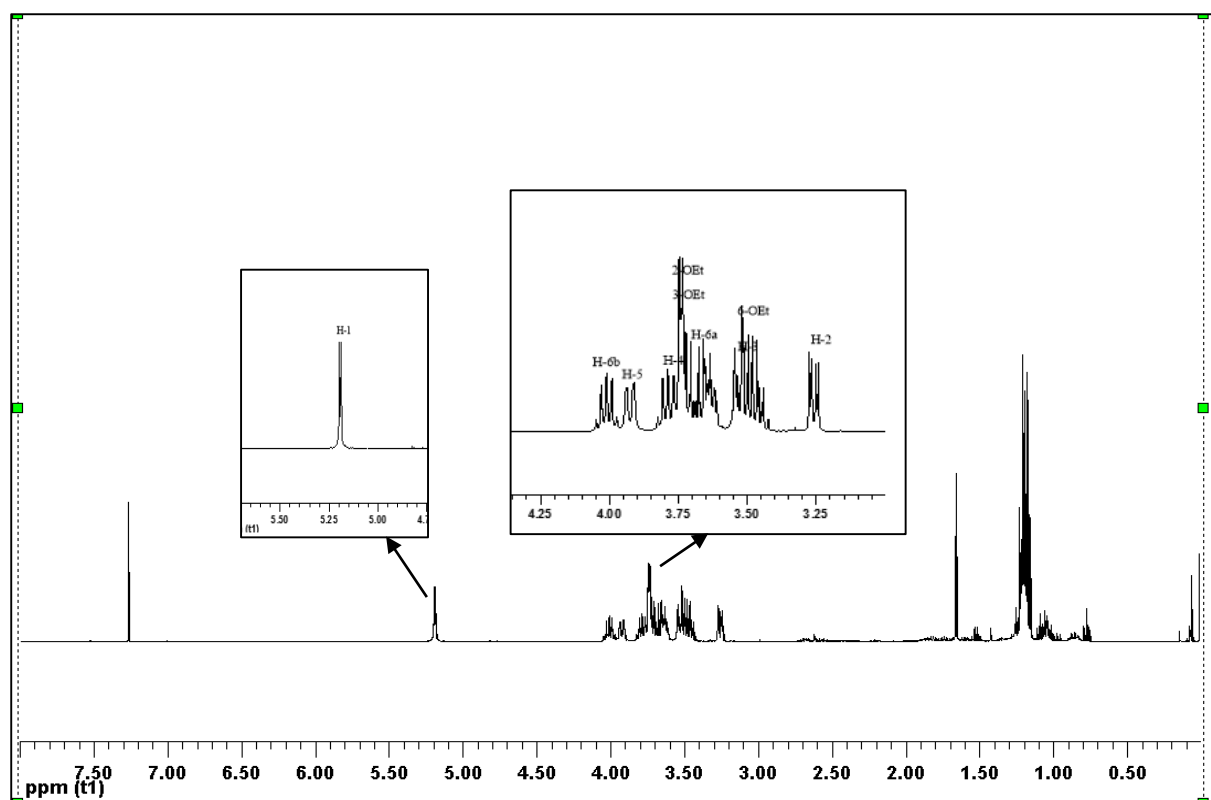


Heptakis [2,3,6-tri-O-ethyl] β-cyclodextrin



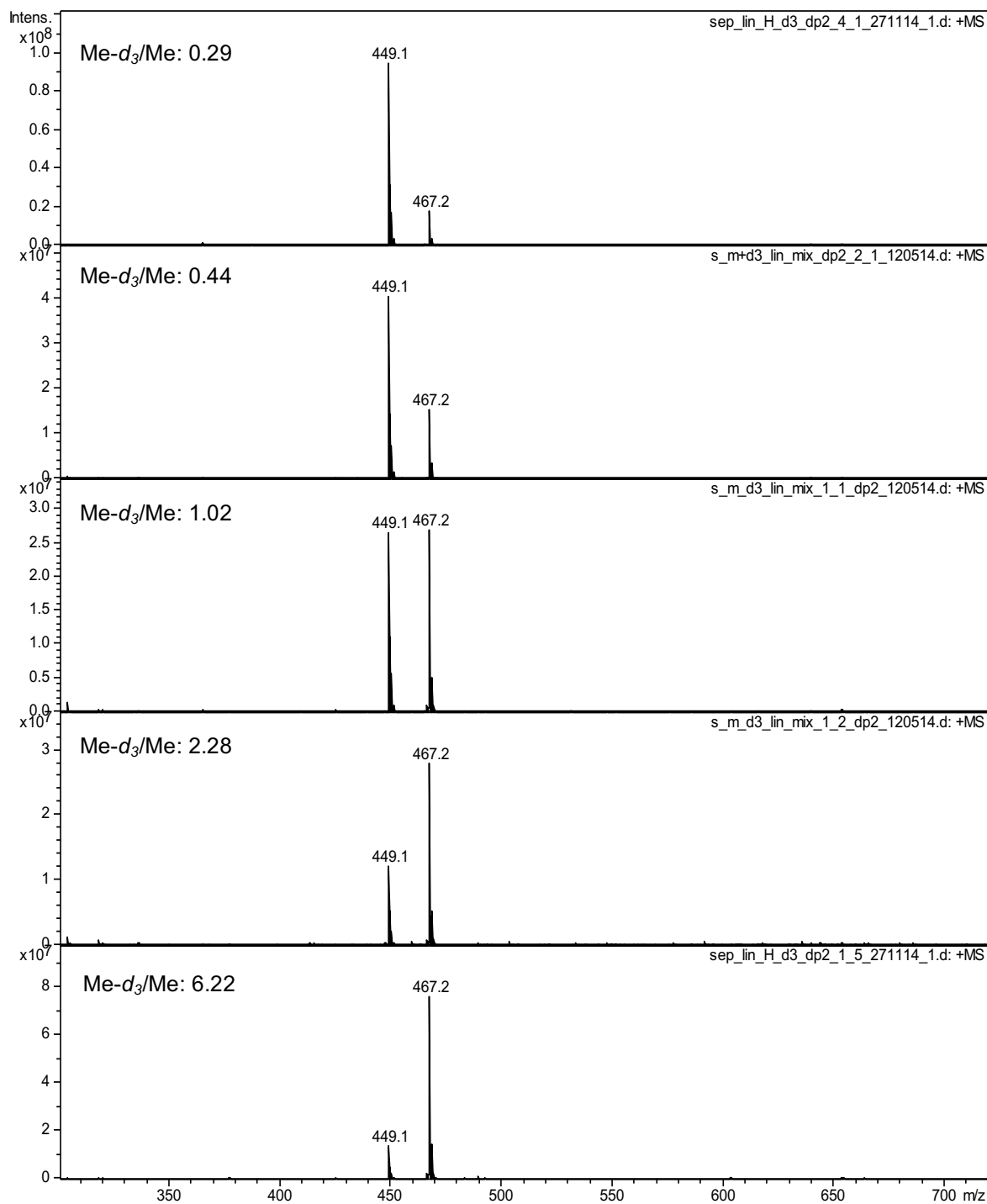
Heptakis [2,3,6-tri-O-propyl] β-cyclodextrin

9.2 ^1H -NMR spectra of peralkylated cyclodextrins measured in CDCl_3 at 400 MHz*Heptakis [2,3,6-tri-O-methyl] β -cyclodextrin**Heptakis [2,3,6-tri-O-deuteriomethyl] β -cyclodextrin*

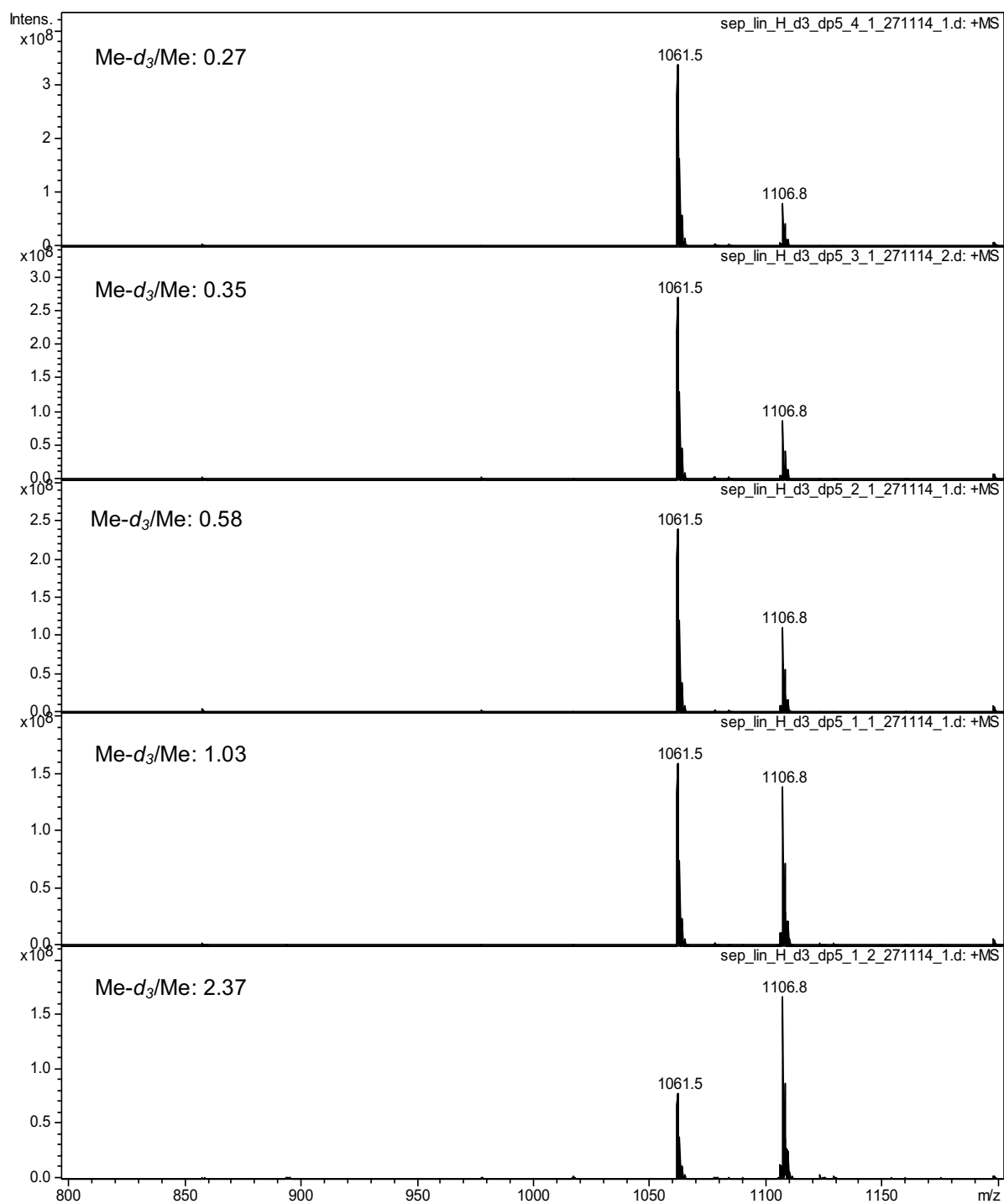


Heptakis [2,3,6-tri-O-ethyl] β -cyclodextrin

9.3 ESI-MS spectra of binary mixtures DP2 and DP5 given in Table 13, prepared with increasing molar ratio

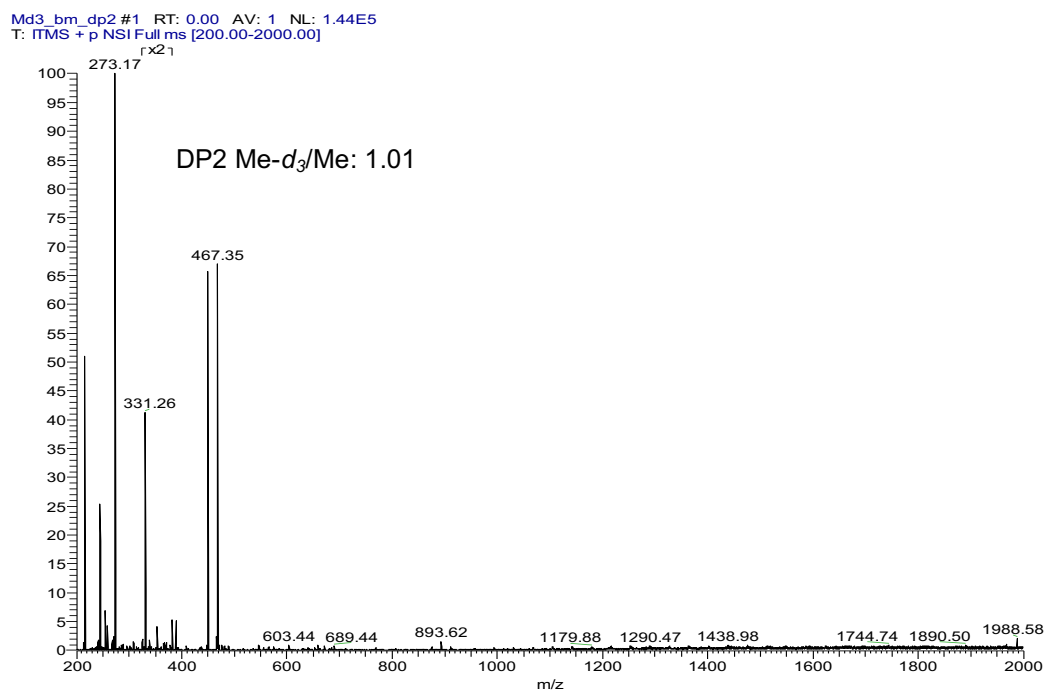


ESI-IT mass spectra of BM DP 2 with varying $\text{Me-d}_3/\text{Me}$ molar ratio (given in each spectrum), measured in methanol in positive ion mode at a concentration of 10^{-5} M, oligomers seen as sodium adducts

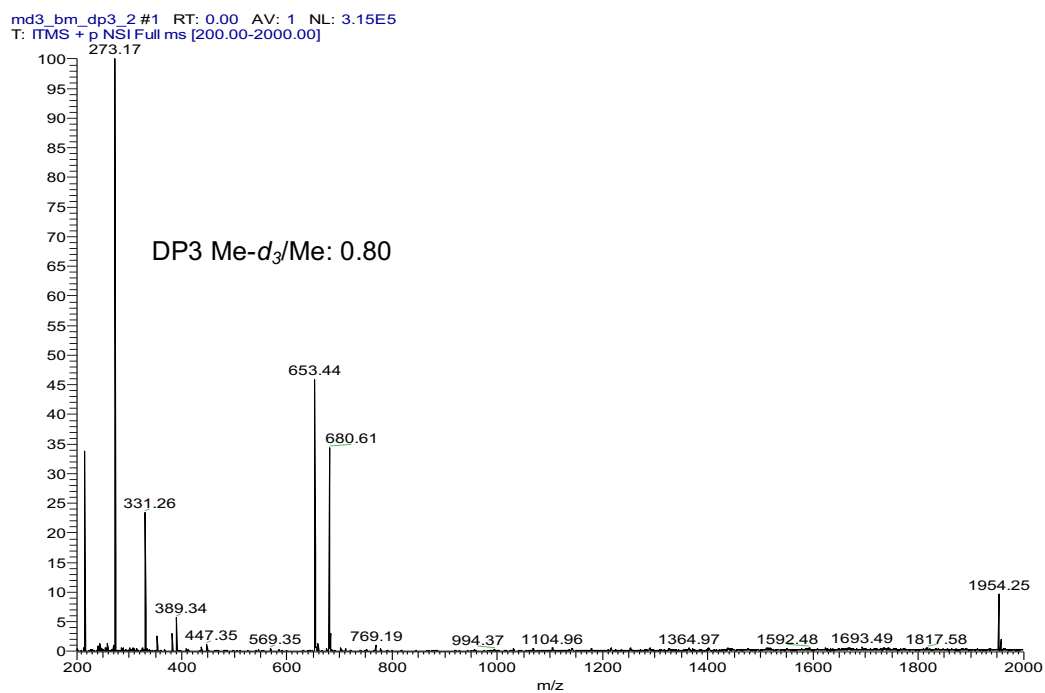


ESI-IT mass spectra of BM DP 5 with varying $\text{Me-d}_3/\text{Me}$ molar ratio (given in each spectrum), measured in methanol in positive ion mode at a concentration of 10^{-5} M, oligomers seen as sodium adducts

9.4 Nano-ESI-IT mass spectrum of Me- d_3 /Me BM 2 given in Table 14, measured in methanol in positive ion mode at a concentration of 10^{-6} M, oligomers seen as sodium adducts. In each spectrum actual molar ratio of the components is given

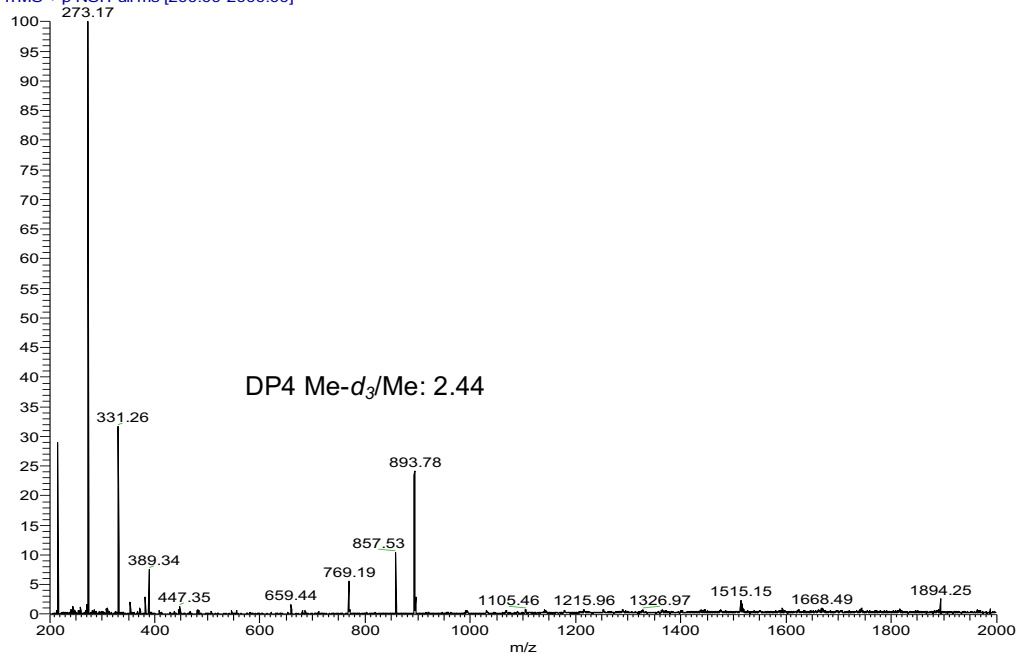


DP2, m/z 449.2 and 467.3 of Me and Me



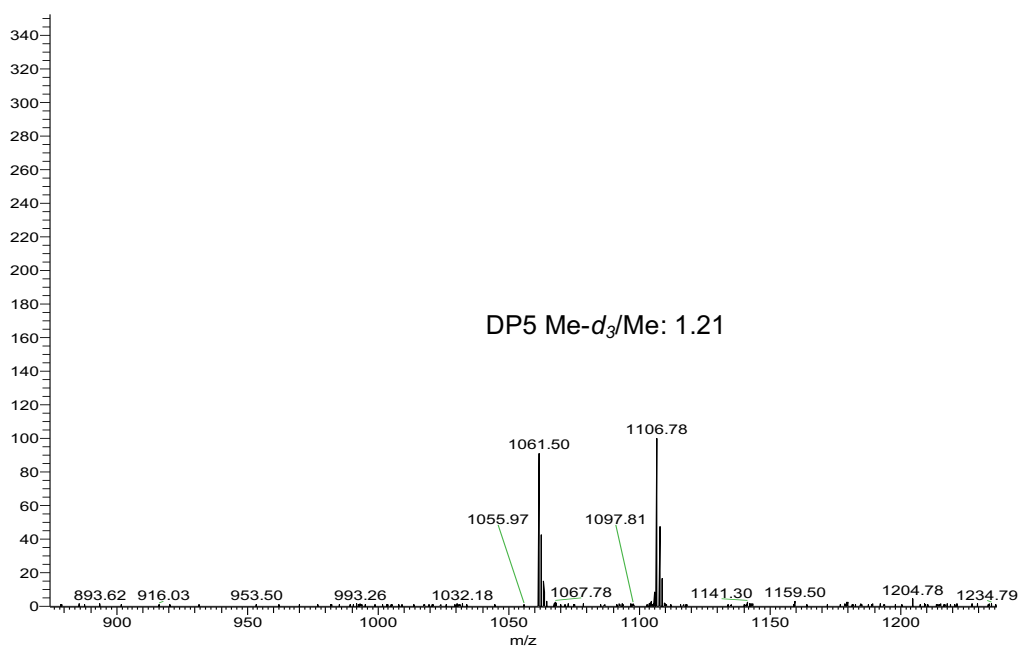
DP3, m/z 653.4 and 680.6 of Me and Me- d_3

md3_bm_dp4 #1 RT: 0.00 AV: 1 NL: 2.17E5
T: FTMS + p NSI Full ms [200.00-2000.00]



DP 4, m/z 857.5 and 893.7 of Me and Me-d₃

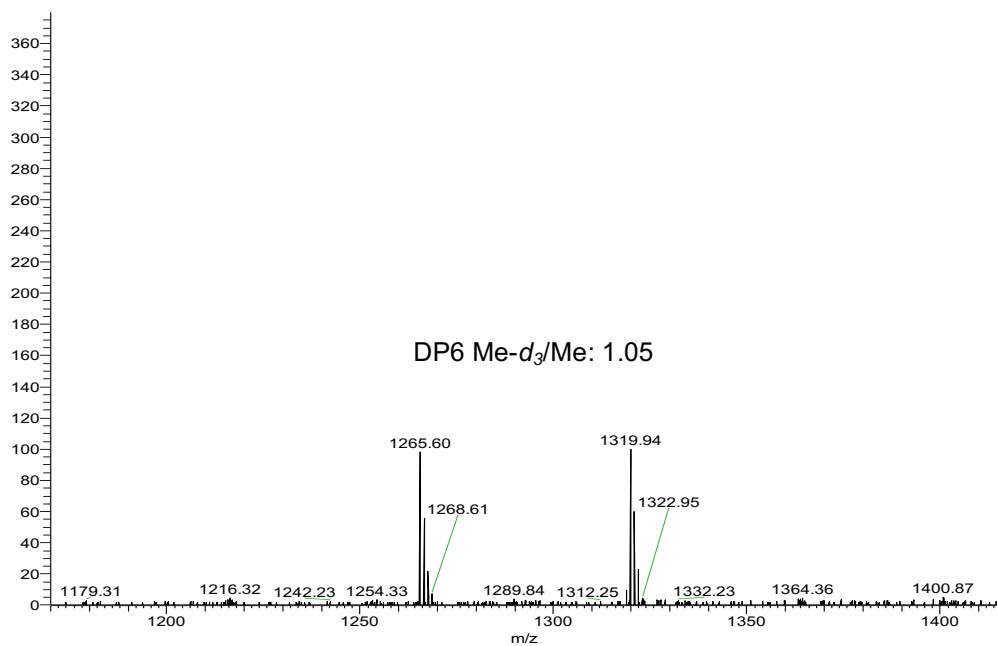
md3_bm_dp5 #1 RT: 0.01 AV: 1 NL: 6.61E4
T: FTMS + p NSI Full ms [200.00-2000.00]



DP 5, m/z 1061.5 and 1106.7 of Me and Me-d₃

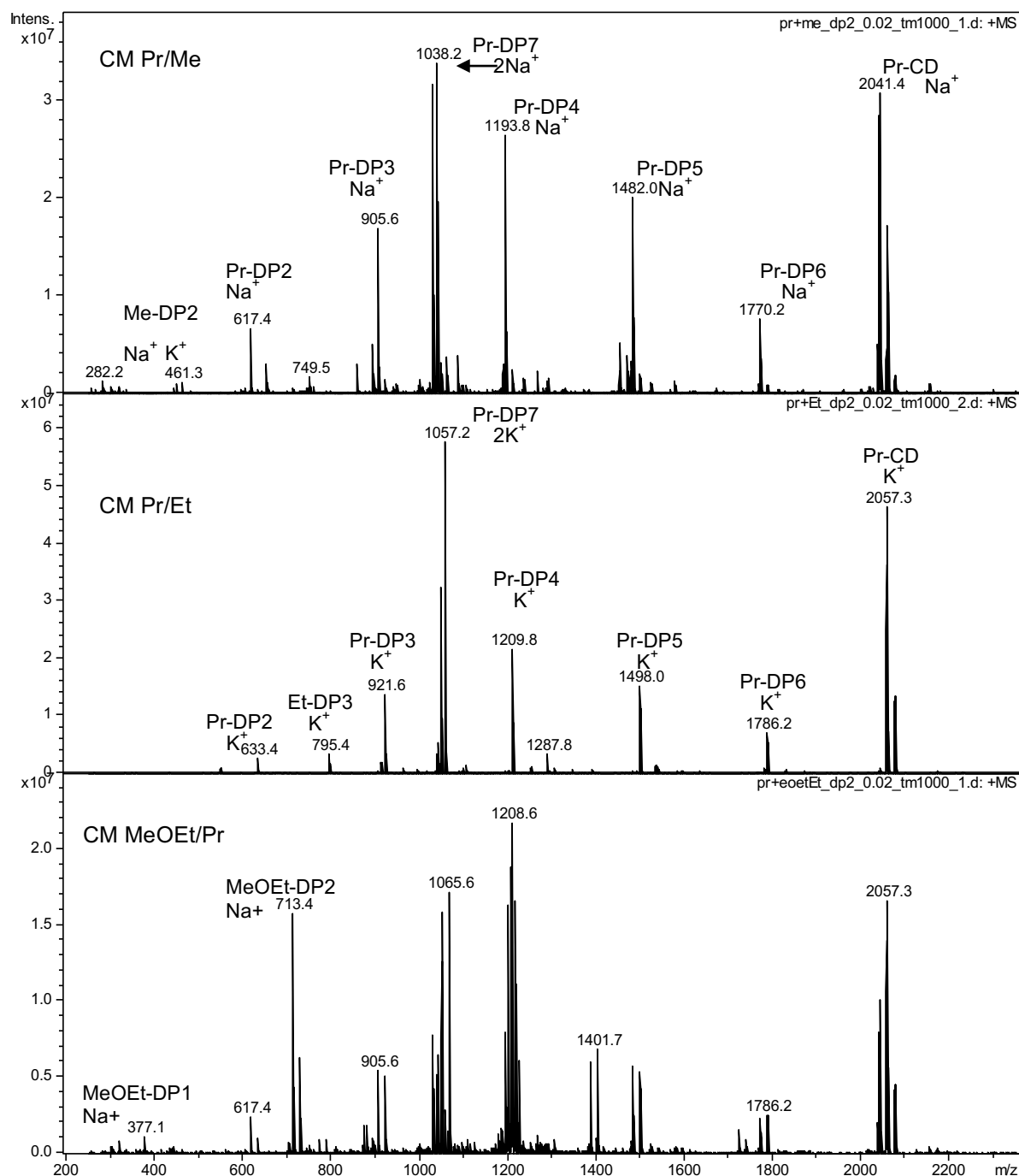
9 Appendix

md3_bm_dp6 #1 RT: 0.01 AV: 1 NL: 4.79E4
T: FTMS + p NSI Full ms [200.00-2000.00]

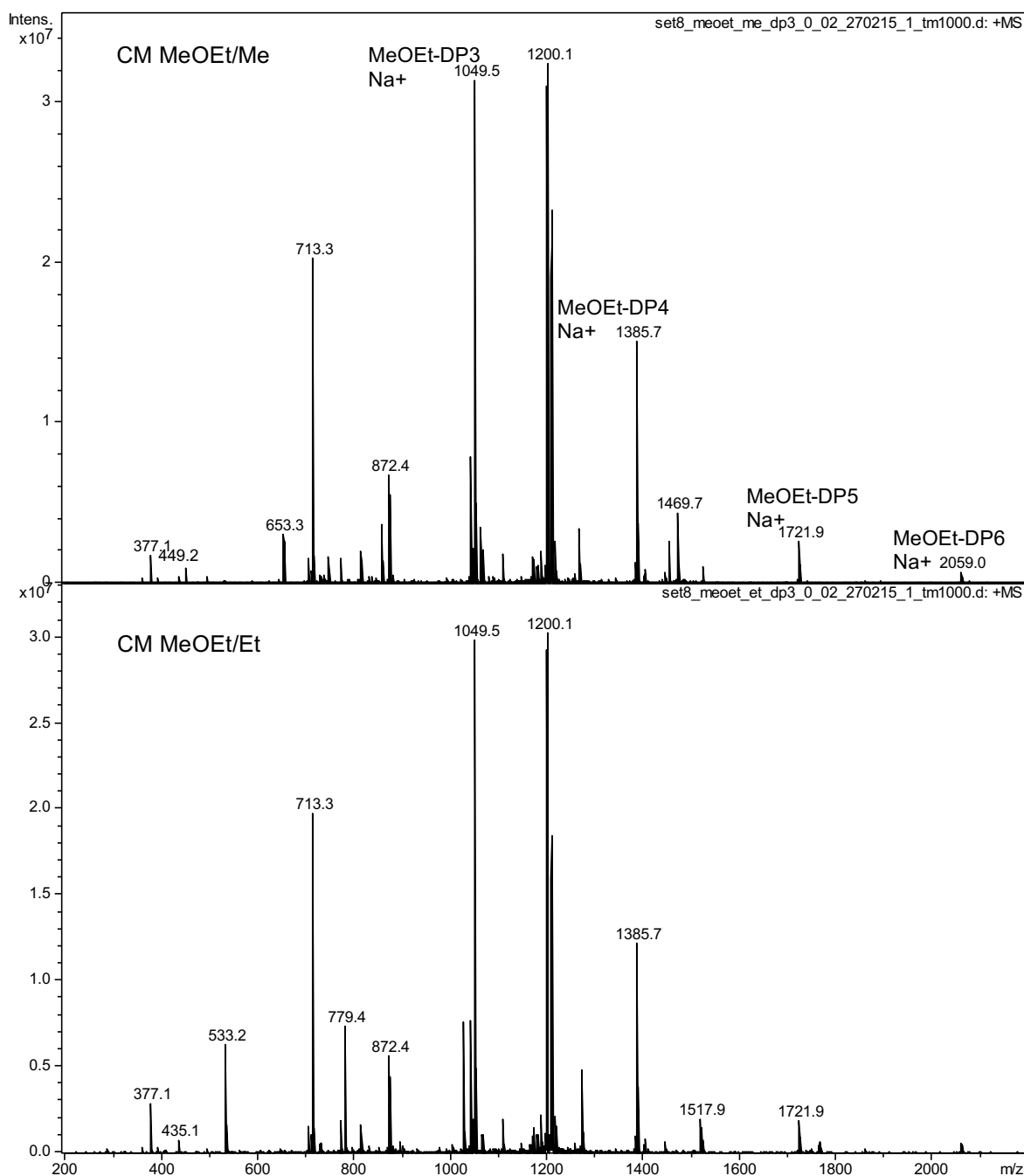


DP6, m/z 1265.6 and 1319.9 of Me and Me- d_3

9.5 ESI-IT mass spectrum of Alk/Me and MeOEt/Alk CM, measured in methanol in positive ion mode at a concentration of 10^{-5} M. Oligomers are seen as sodium adducts, in mixtures with Pr they are seen as both sodium and potassium adducts

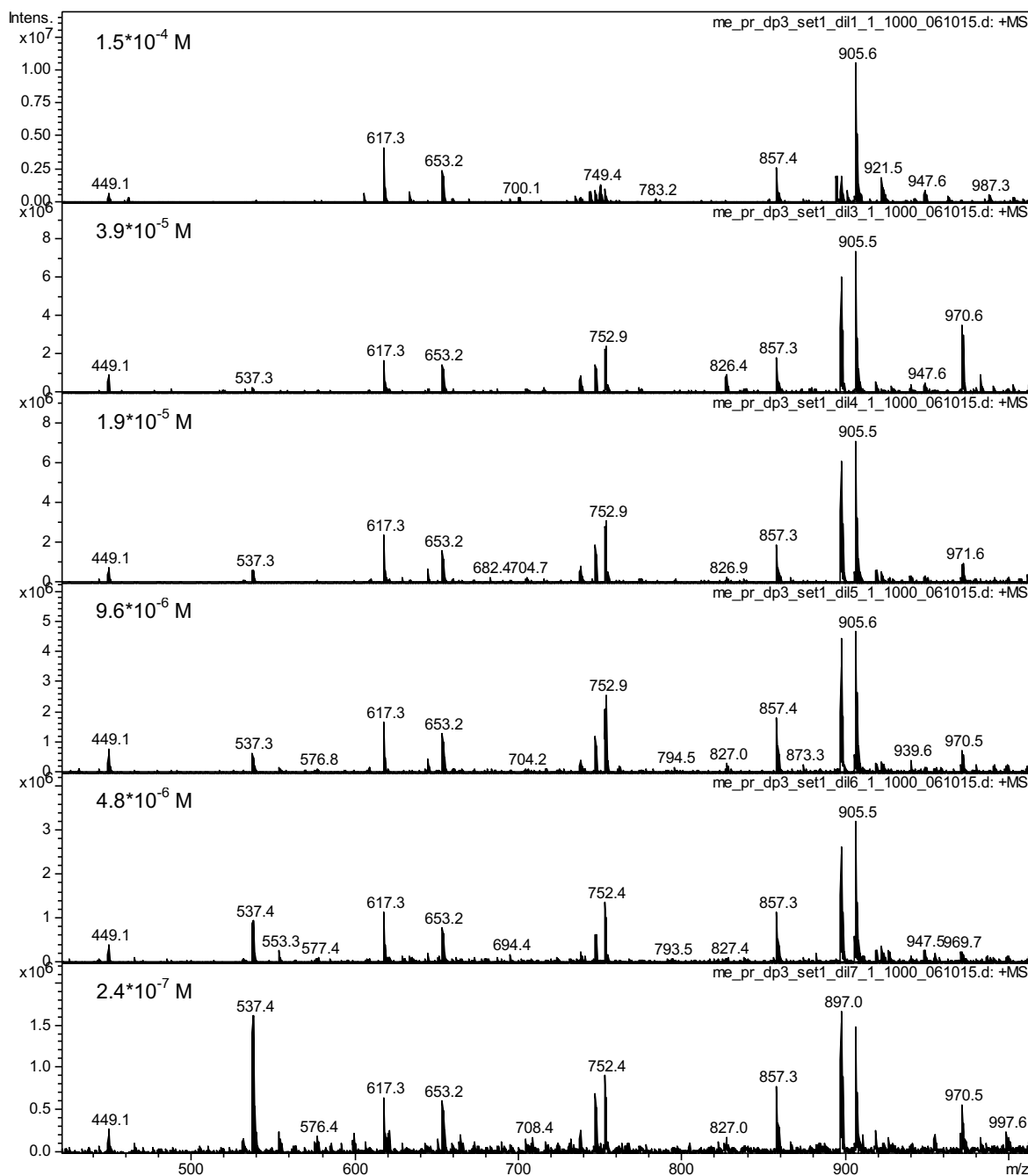


ESI-IT mass spectra of various CM with Pr maltooligomers (CM1 of Pr/Me, Pr/Et and MeOEt/Pr from tables 7, 8 and 11 respectively). 449.2, 653.3, 857.5, 1061.6, 1265.7 and 1469.7 is the m/z of **Me**, 533.3, 779.8, 1025.6, 1271.8, 1517.9 and 1764 of **Et**, 617.2, 905.6, 1193.8, 1482.0, 1770.2 and 2041.4 (Pr-CD) of **Pr**, 713.4, 1049.6, 1385.7, 1721.9, 2059.0 and 2395 of **MeOEt** of DP 2-7 as $[M+Na]^+$. All the additional peaks are from doubly charged sodium adducts and $[M+K]^+$. In all the mass spectra DP2 oligomers are equimolar.

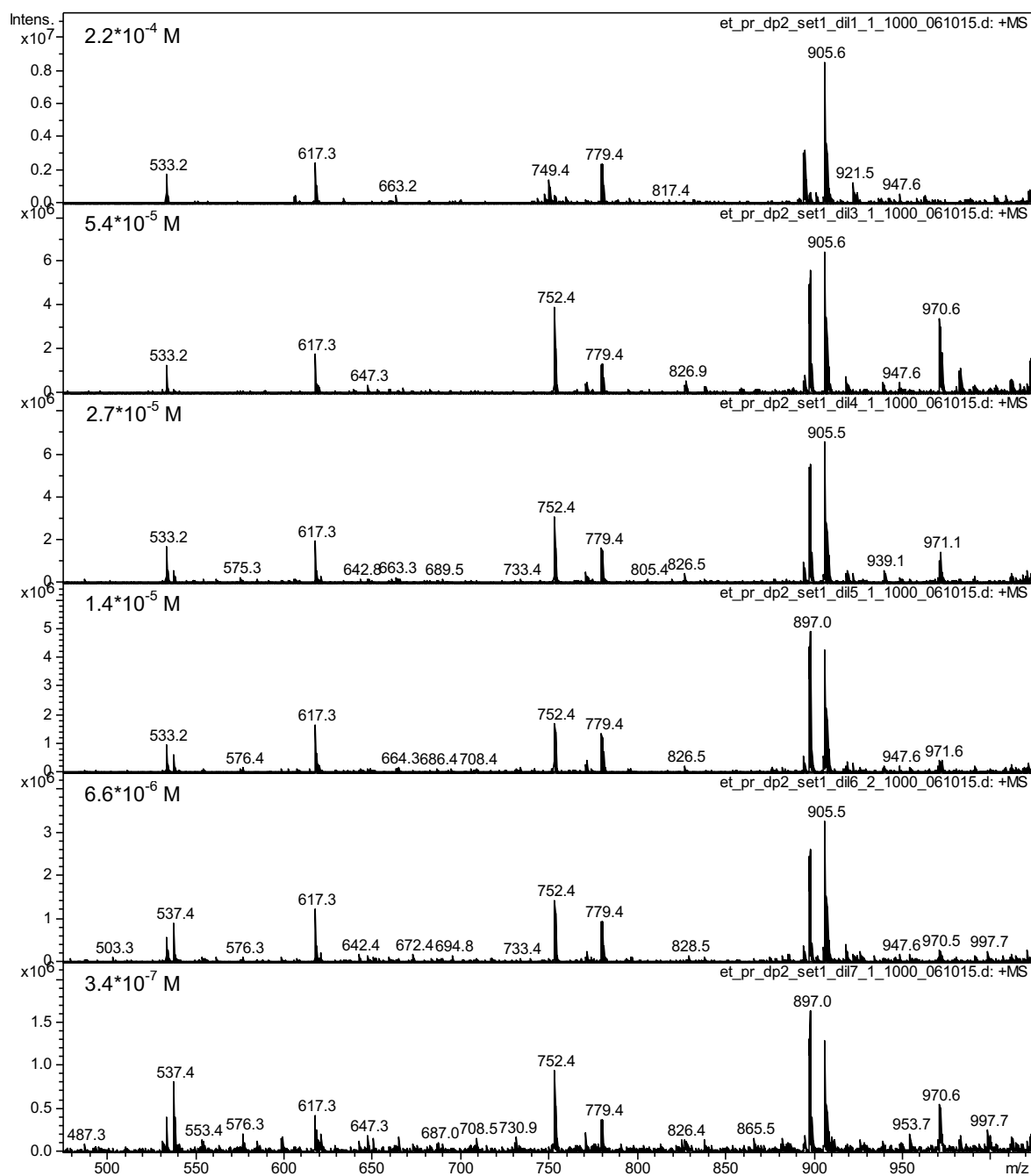


ESI-IT mass spectra of CM5 MeOEt/Me (Table 9) and CM5 MeOEt/Et (Table 10). 449.2, 653.3, 857.5, 1061.6, 1265.7 and 1469.7 is the m/z of **Me**, 533.3, 779.8, 1025.6, 1271.8, 1517.9 and 1764 of **Et** of DP 2-6 as $[M+Na]^+$. 377.1, 713.4, 1049.6, 1385.7, 1721.9, 2059.0 and 2395 of **MeOEt** of DP 1-7 as $[M+Na]^+$. All the additional peaks are from doubly charged sodium adducts, in both mass spectra DP3 oligomers are equimolar.

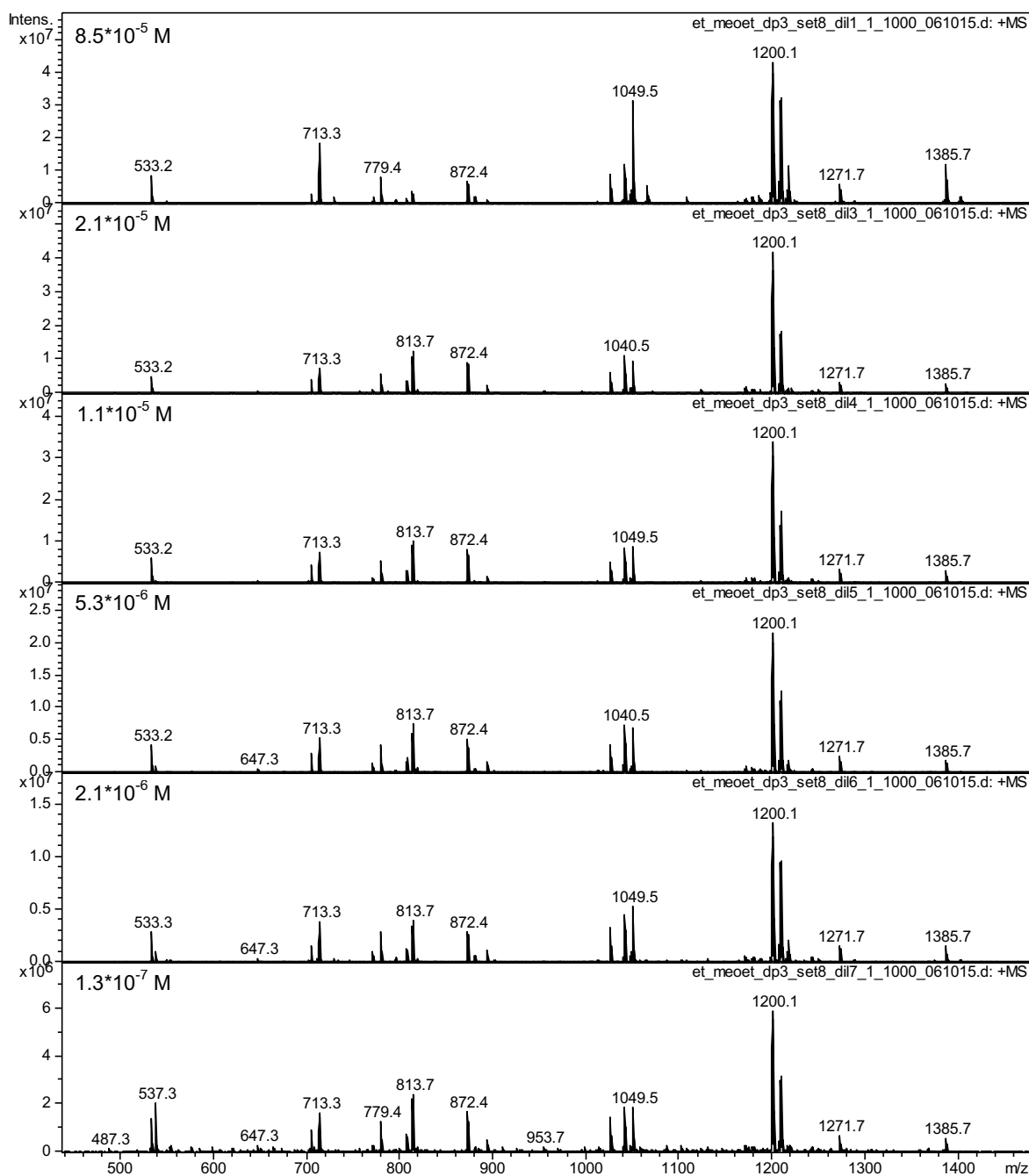
9.6 ESI-IT mass spectrum of Alk/Me and MeOEt/Alk CM, measured in methanol in positive ion mode at a concentration of approximately 10^{-7} to 10^{-4} M.



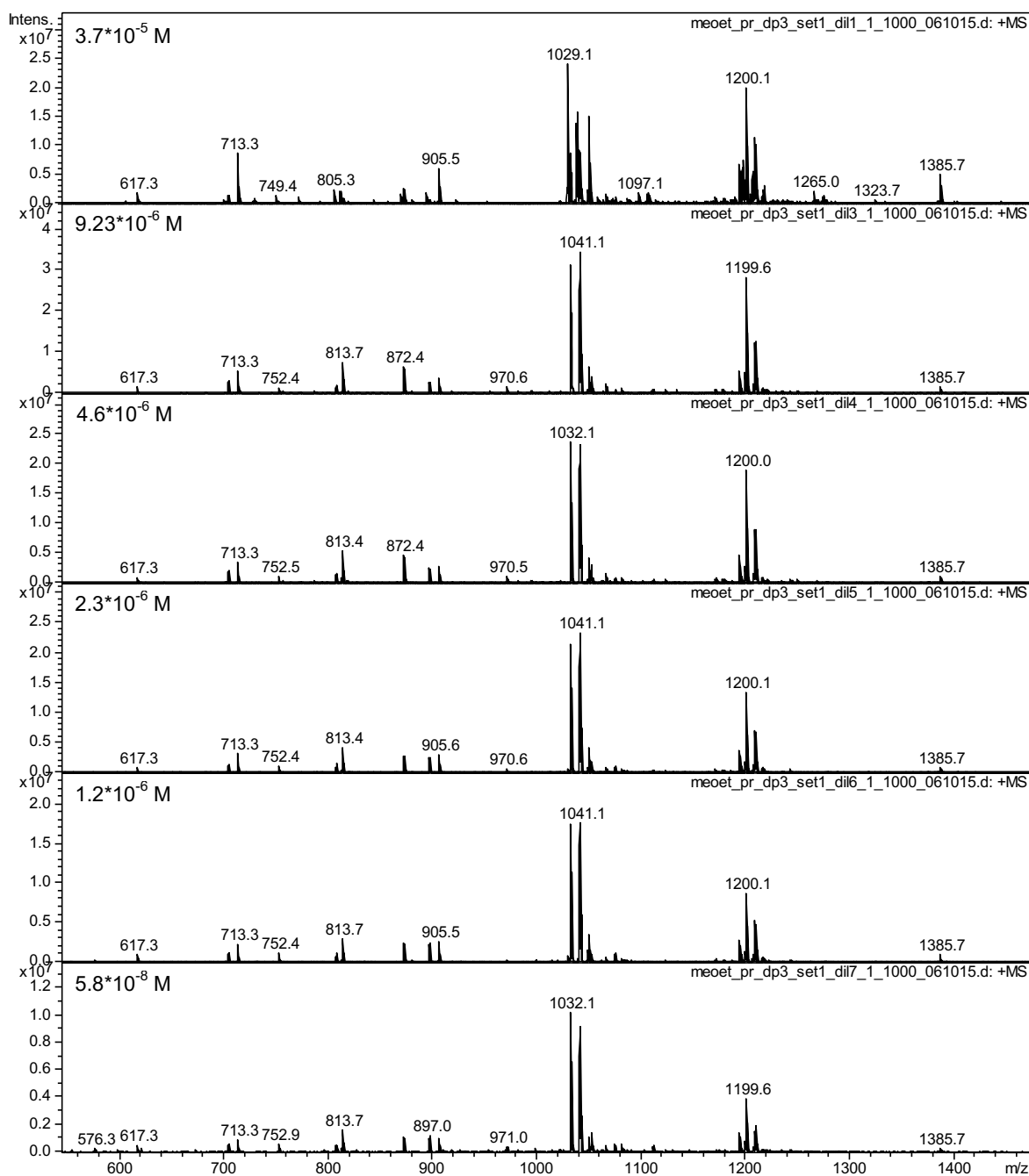
ESI mass spectra of Pr/Me (CM2 Table 7); To show the change of peaks with concentration, only the section up to DP 3 Pr is shown. 449.2, 653.3 and 857.5 are peaks from Me DP 2, DP 3 and DP 4 respectively, 617.3 and 905.5 are from DP 2 and DP 3 Pr. All the additional peaks seen in the first mass spectrum (1.5×10^{-4} M) are from doubly charged peaks from higher DPs (DP 5-7). With the decrease of concentration intensity of doubly charged peaks and background noise increases



ESI mass spectra of Pr/Et (CM1 Table 8); To show the change of peaks with concentration, only the section upto DP3 Pr is shown. 533.3 and 779.4 are peaks from Et DP2 and DP3 respectively, 617.3 and 905.5 are from DP2 and DP3 Pr. All the additional peaks seen in the first mass spectrum (2.2×10^{-4} M) are from doubly charged peaks from higher DPs (DP 5-7). With the decrease of concentration intensity of doubly charged peaks and background noise increases.

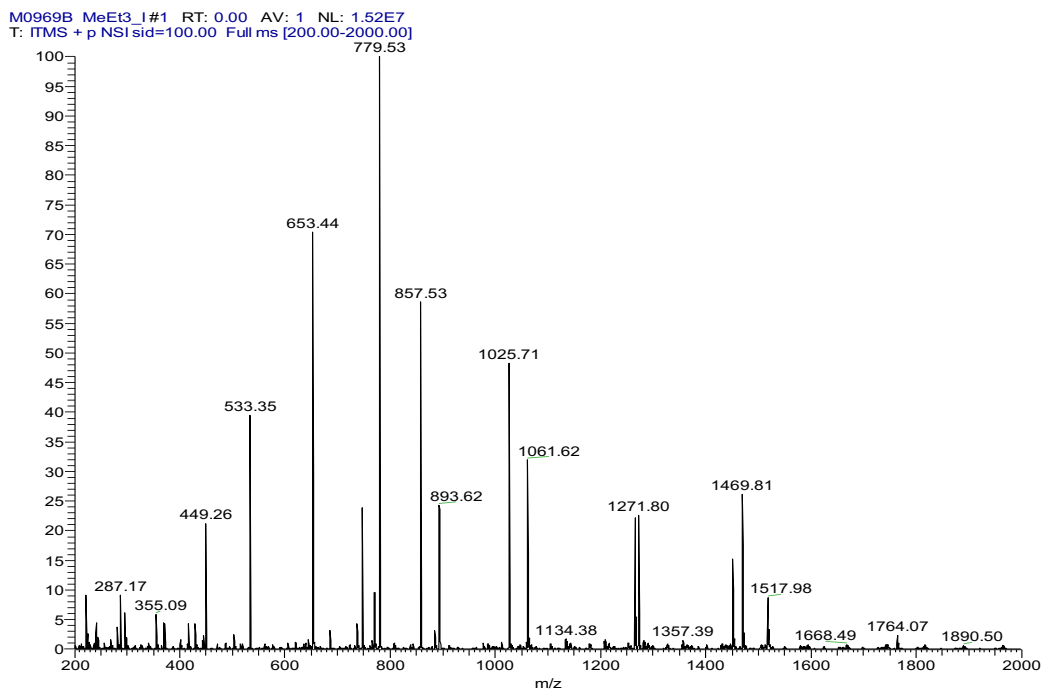


ESI mass spectra of MeOEt/Et (CM5 Table 10); To show the change of peaks with concentration, only the section upto DP3 MeOEt is shown for a full spectra see appendix. 533.3 and 779.4 are peaks from Et DP2 and DP3 respectively, 713.3 and 1049.5 are from DP2 and DP3 MeOEt. All the additional peaks seen in the first mass spectrum (8.5×10^{-5} M) are from doubly and triply charged peaks from higher DPs (DP 5-7). With the decrease of concentration intensity of doubly and triply charged peaks and background noise increases.

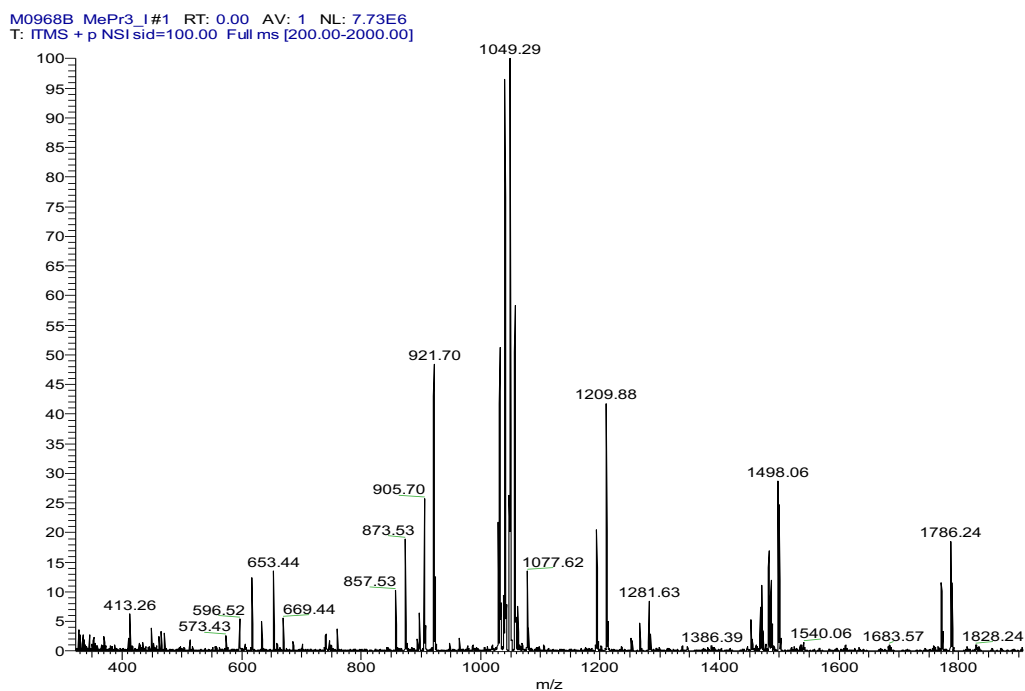


ESI mass spectra of MeOEt/Pr (CM2 Table 11); To show the change of peaks with concentration, only the section upto DP3 MeOEt is shown for a full spectra see appendix. 617.3 and 905.5 are from DP2 and DP3 Pr, 713.3 and 1049.5 are from DP2 and DP3 MeOEt. All the additional peaks seen in the first mass spectrum (8.5×10^{-5} M) are from doubly and triply charged peaks from higher DPs (DP 5-7). With the decrease of concentration intensity of doubly and triply charged peaks and background noise increases

9.7 Nano-ESI-IT mass spectrum of Alk/Me and MeOEt/Alk CM, measured in methanol in positive ion mode at a concentration of 10^{-6} M. Oligomers are seen as sodium adducts, in mixtures with Pr they are seen as both sodium and potassium adducts

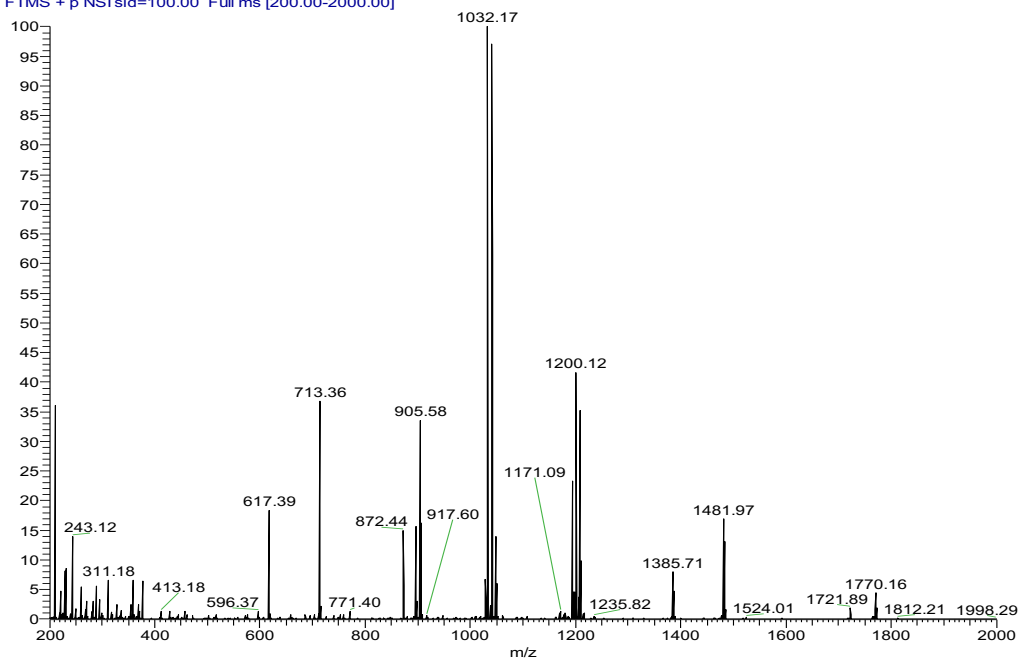


Et/Me CM 5, Table 5



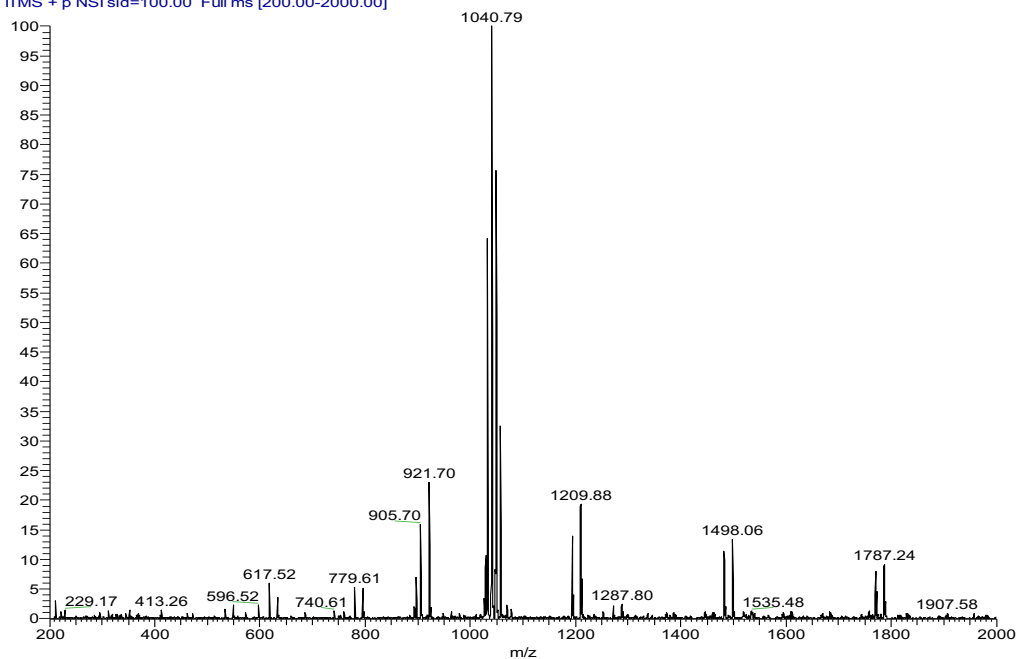
Pr/Me CM 2, Table 7

M0962B meoetpr2_1#1 RT: 0.01 AV: 1 NL: 4.42E7
T: FTMS + p NSI sid=100.00 Full ms [200.00-2000.00]



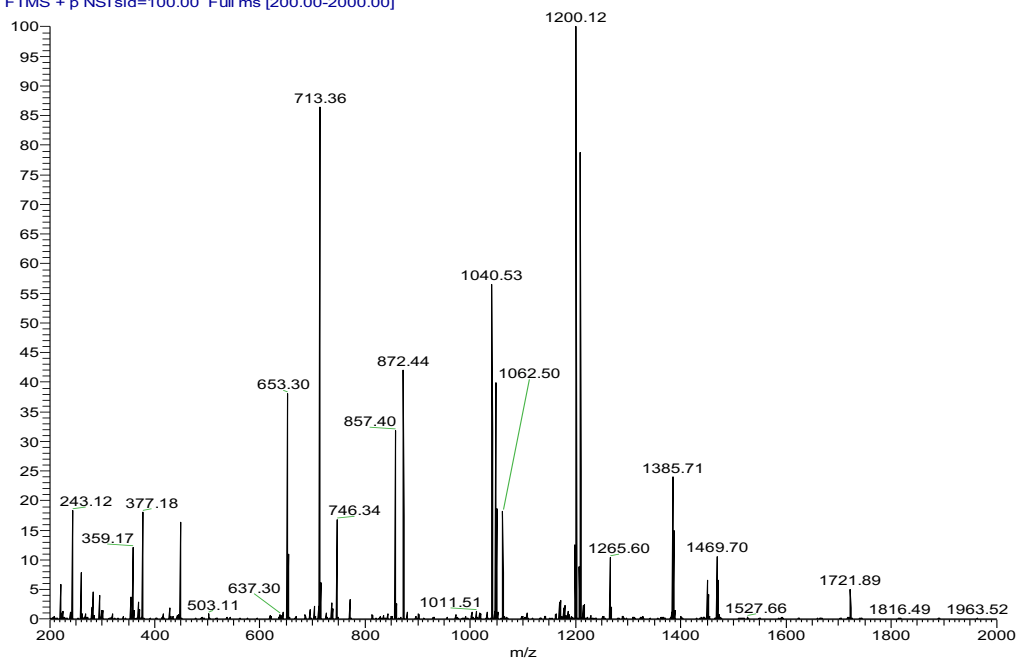
MeOEt/Pr CM 1, Table 11

M0966B EtPr2_1#1 RT: 0.00 AV: 1 NL: 6.44E6
T: FTMS + p NSI sid=100.00 Full ms [200.00-2000.00]



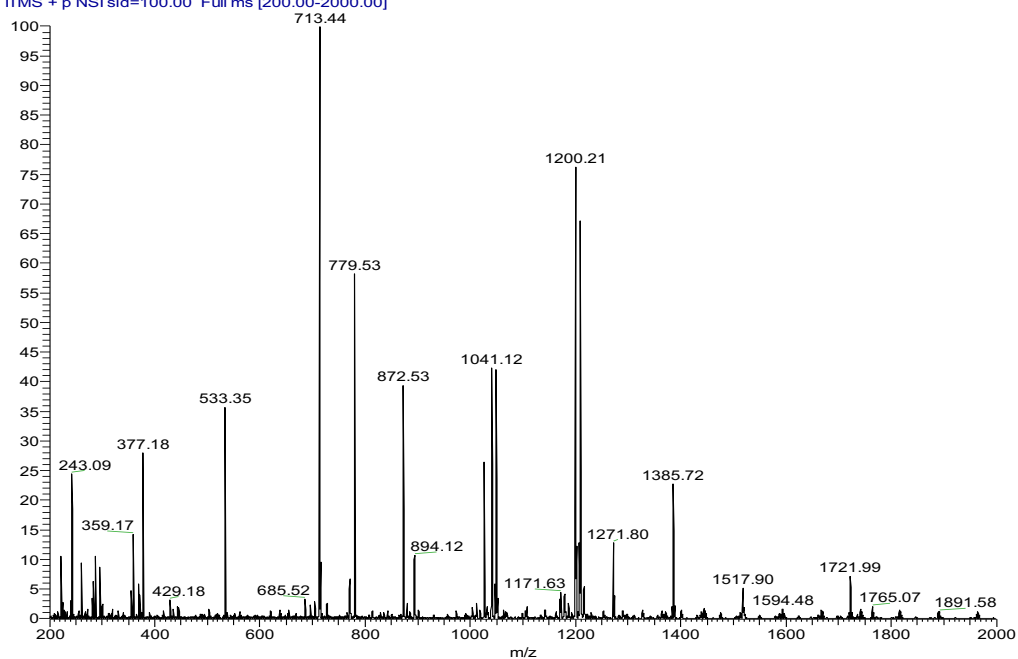
Pr/Et CM1, Table 8

M0964B meoetMe3_I#1 RT: 0.01 AV: 1 NL: 5.70E7
T: FTMS + p NSI sid=100.00 Full ms [200.00-2000.00]



MeOEt/Me CM 5, Table 9

M0965B meoetEt3_I#1 RT: 0.00 AV: 1 NL: 1.87E7
T: FTMS + p NSI sid=100.00 Full ms [200.00-2000.00]



MeOEt/Et

CM 5,

Table 10

Resume

Sheetal Gangula

Birthdate	13.08.1987
Birthplace	Ramchandrapuram, India
Marital status	Married
Nationality	India

Doctoral studies

Jul. 11-Feb. 16	University	Technische Universität Braunschweig
	Specialization	Naturwissenschaften
	Topic	<i>Relative ion intensities of O-alkyl -oligosaccharides in ESI-IT-MS: A quantitative evaluation</i>

Previous Studies

Jan.09-Aug.10	University	Governors State University, USA
	Specialization	Analytical Chemistry
	Degree	Master of Science

May.04-May.08	University	Osmania University, India
	Specialization	Bachelors in Pharmacy
	Degree	Bachelor of Pharmacy

School Studies

2002-2004	Intermediate studies (Gymnasium)
1997-2002	Higher school education
1992-1997	Primary school education